Retinal Diseases

2

Gensheng Wang, Peipei Xie, Jiayu Wang, and Hanyi Min

Retina is located at the innermost layer of the wall of the eyeball, which surrounds the vitreous together with the non-pigmented ciliary epithelium, suspensory ligament, and posterior capsular of the lens.

From the inside out, the retina consists of inner limiting membrane, neural fiber layer, ganglion cell layer, inner plexiform layer, inner nuclear layer, outer plexiform layer, outer nuclear layer, outer limiting membrane, and photoreceptors. The outer segment of photoreceptors is surrounded by the microvilli on top of the pigment epithelium. The pigment epithelium is connected by tight junction, which constitutes the inner barrier of the retina. Figure 2.1a, b show the biopsy section and schematic diagram of the retina.

The fovea is located in the center of the posterior retina, 3 mm lateral to the optic disc. The central of the fovea is the avascular foveola, which is the most sensitive part of visual acuity. The optic disc lies 3 mm medial to the macular. This pale pink/whitish area is 1.8 mm in diameter with a slightly raised rim. The central retinal vessels emerge at the center of the optic disc, pass over the rim, and radiate out to supply the retina.

The blood supply of the retina mainly comes from central retinal artery and its branches, which runs into the eye within the optic nerve and supplies a sector of the retina as in the superior temporal, superior nasal, inferior temporal, and inferior nasal area. Cilioretinal artery, which mainly supplies macular, can be occasionally seen in some eyes. Central retinal artery mainly supplies inner layers of the retina, i.e., the part inside of the outer nuclear layer. There are two main levels of capillary networks, which are spreading like a vast cobweb throughout the retina. The inner plexus is situated at the level of nerve fiber layer and the ganglion cell layer and the outer plexus at the level of inner nuclear cell (Fig. 2.2a). The capillary plexus between the nerve fiber layer and the inner nuclear layer is distributed three-dimensionally, just like a "hammock"(Fig. 2.2b). There is no anastomosis or short-cuts between the retinal arterioles and venules.

The most wide usage of stereo photography is in diabetic retinal study [1–5]. Since 1968, Airlie House Symposium established the first diabetic retinopathy classification system, stereo fundus photography had been a cornerstone of diabetic retinopathy assessment, and the stereo photography protocol and severity classifications were modified during the Diabetic Retinopathy Study and were later expanded in the Early Treatment Diabetic Retinopathy Study (ETDRS). Until now stereo, 30°, seven-field, 35-mm color slides remain the gold standard for clinically evaluating diabetic retinopathy and are widely used in the DR studies such as Diabetic Retinopathy Clinical Research Network studies, the Action to Control Cardiovascular Risk in Diabetes Eye Study, Epidemiology of Diabetes Interventions and Complications, and the Diabetes Control and Complications Trial. Telemedicine programs also include stereo photography.

It is generally assumed that depth perception helps in distinguishing subtle extraretinal neovascularization elevated above the plane of the retina from intraretinal microvascular abnormalities (IRMAs) [6]. This discrimination is important on the ETDRS severity scale. Stereopsis may also aid in detecting new vessels elsewhere (NVE), new vessels on the disc (NVD), and vitreous fibrosis and hemorrhages. Confusing these advanced abnormalities with other lesions could result in missed opportunities for timely intervention to prevent vision loss. Correct classification of the diabetic retinopathy severity level is also essential in clinical and epidemiology studies in which diabetic retinopathy progression is observed. It is also believed that stereo photography's

G. Wang
Department of Ophthalmology, Handan Eye Hospital, Handan, Hebei, P.R. China

P. Xie
Department of Ophthalmology, The People's Liberation Army No. 152 Hospital, Pingdingshan, Henan Province, P.R. China

J. Wang
Department of Ophthalmology, Wangjing Hospital, Beijing, P.R. China

H. Min (✉)
Department of Ophthalmology, Peking Union Medical College Hospital and Chinese Academy of Medical Science, Beijing, P.R. China

H. Min (ed.), *Stereo Atlas of Vitreoretinal Diseases*, https://doi.org/10.1007/978-981-13-8399-1_2

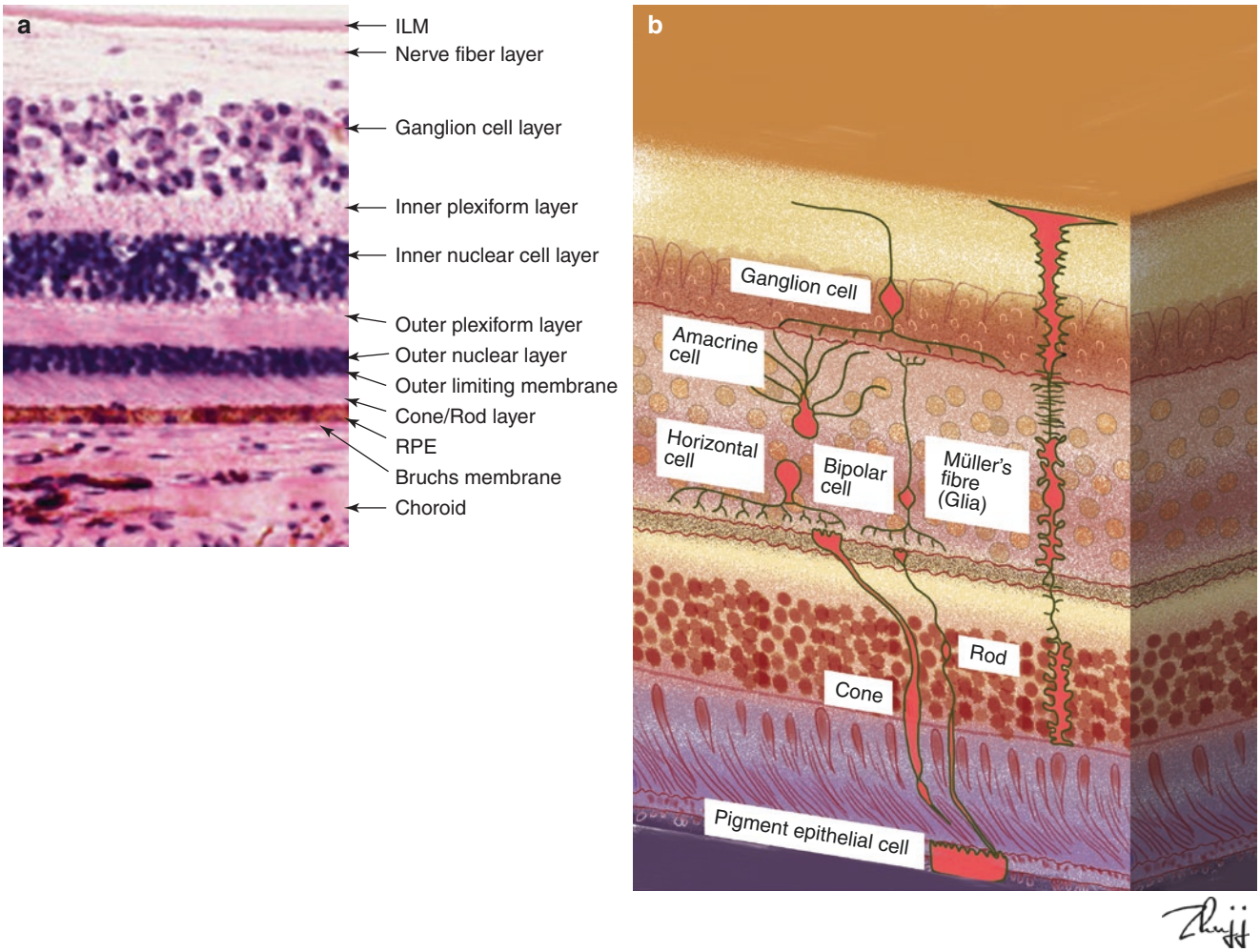

Fig. 2.1 Schematic diagram of retina. (**a**) Biopsy section of the retina. (**b**) Schematic diagram of retina layers

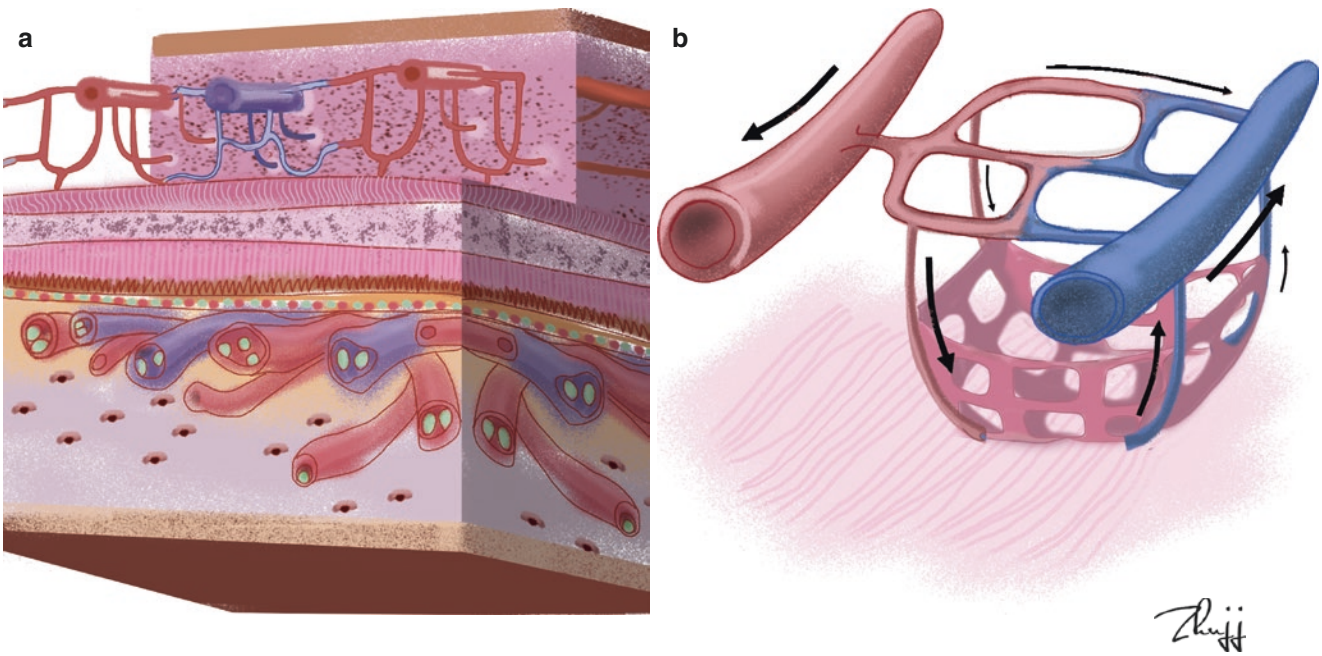

Fig. 2.2 Schematic diagram of retinal vessels. (**a**) Schematic diagram of retinal vessels. (**b**) Framework of retinal arteries and veins, which looks like a hammock

illusion of depth is useful for assessing the severity of diabetic macular edema. Detailed classification of macular edema is dependent on identifying and measuring retinal thickening on 90D/78D microscopy or stereo pairs.

Due to the improvement of digital camera and the burdens of stereo photography to photographers and the patients, many studies has forgone stereo photography, such as the Liverpool Diabetes Eye Study, the UK Prospective Diabetes Study et al. [4, 7, 8]. But until 2010, Li HK had reported monoscopic photography was equal to the reliability of stereo photography for full ETDRS DR severity scale grading and a stereo effect may not be critical for accurate classification of ETDRS diabetic retinopathy severity when using current technology and an optimized framework for fundus photography acquisition and reviewing [5].

Besides the colorful stereoscopic photography, FFA also can be captured in stereo [9]. This facilitates the interpretation of stereo FA by visually separating retinal and choroidal circulation. Both of them can deeply explain and differentiate the exact location and mechanism of the diseases. Though not always necessary, well-resolved stereo images can aid in the interpretation of angiogram with, for instance, choroidal neovascularization associated with age-related macular degeneration.

Comparing with OCT images with cross-section scan, SS-OCT, or even en-face OCT, stereoscopic photography takes advantages such as wider field, freely selected angles, dynamic observation, and more vivid discrimination.

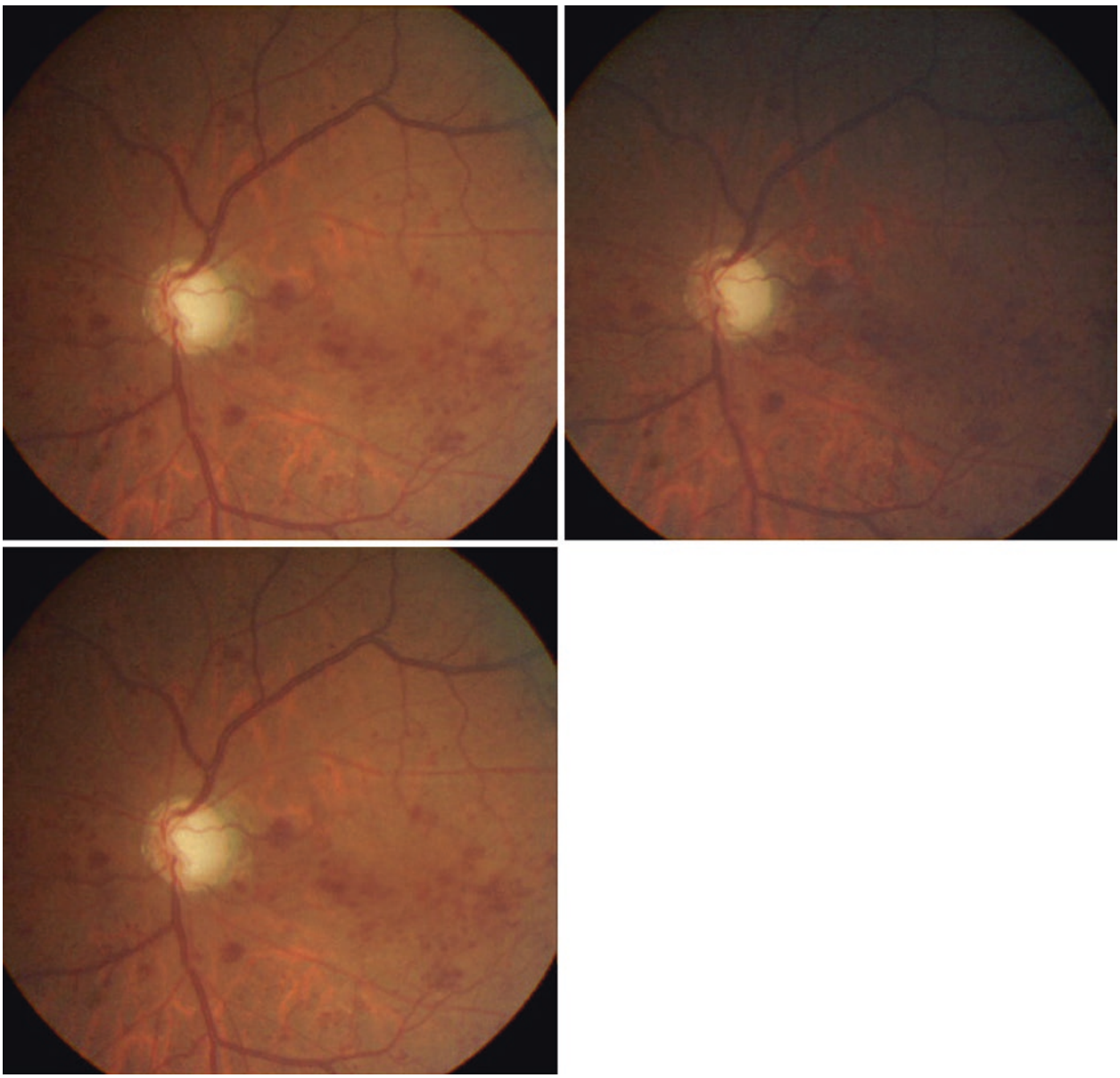

Fig. 2.3 Retinal vein occlusion
I. The cup of the optic disc is deepening
II. Retinal arteries became narrow and straight
III. Retinal veins became tortuous and wider, *A*/*V* ratio = 1/2 to 1/3
IV. Multiple retinal hemorrhages

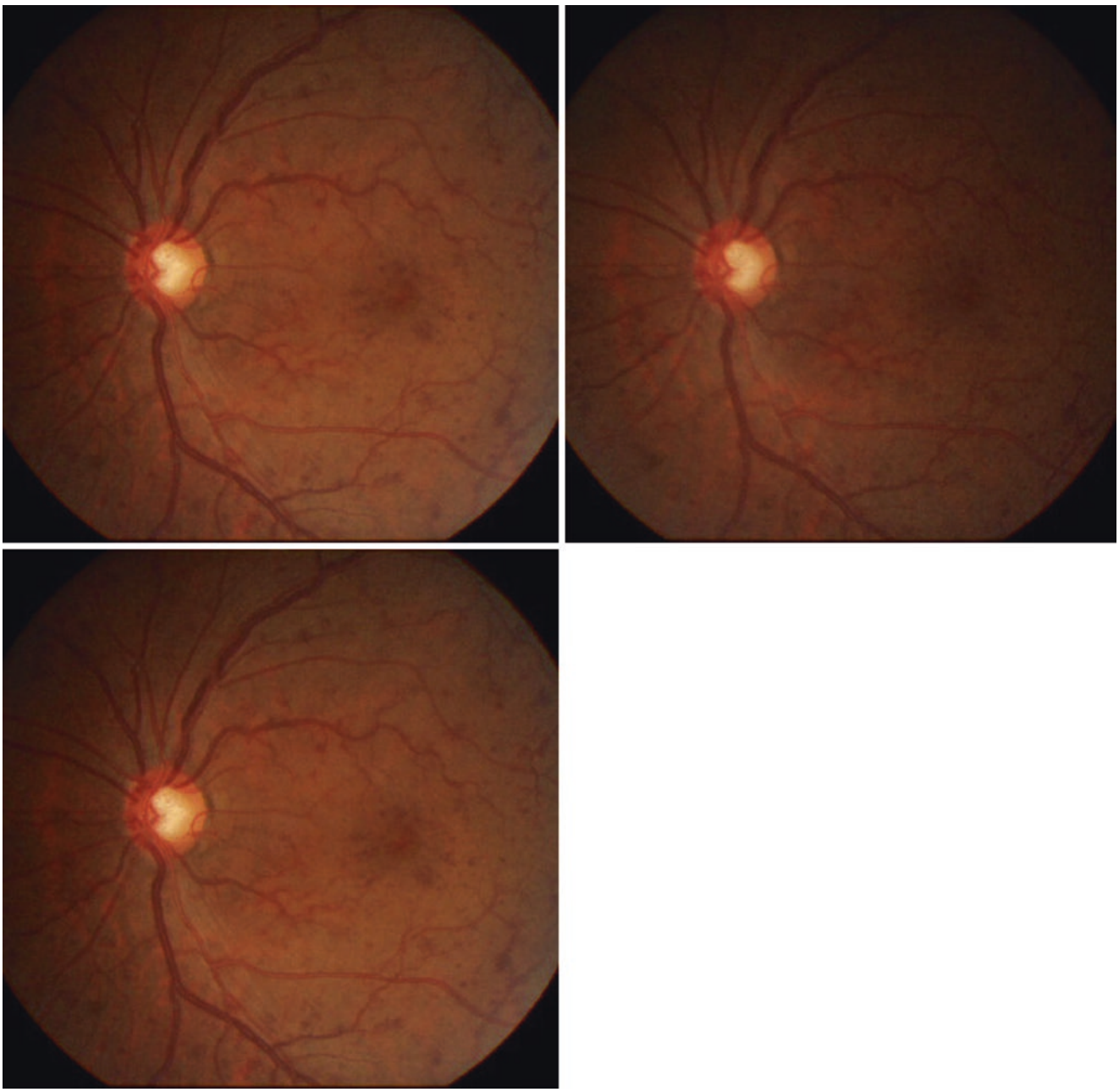

Fig. 2.4 Retinal vein occlusion
I. Retinal arteries became narrow and straight
II. Retinal veins became tortuous and wider, *A*/*V* ratio = 1/2
III. Arteriovenous nicking, the Gunn sign
IV. The retinal artery deflected the retinal vein and changed the course of the vein, the Salus sign
V. Multiple retinal hemorrhages

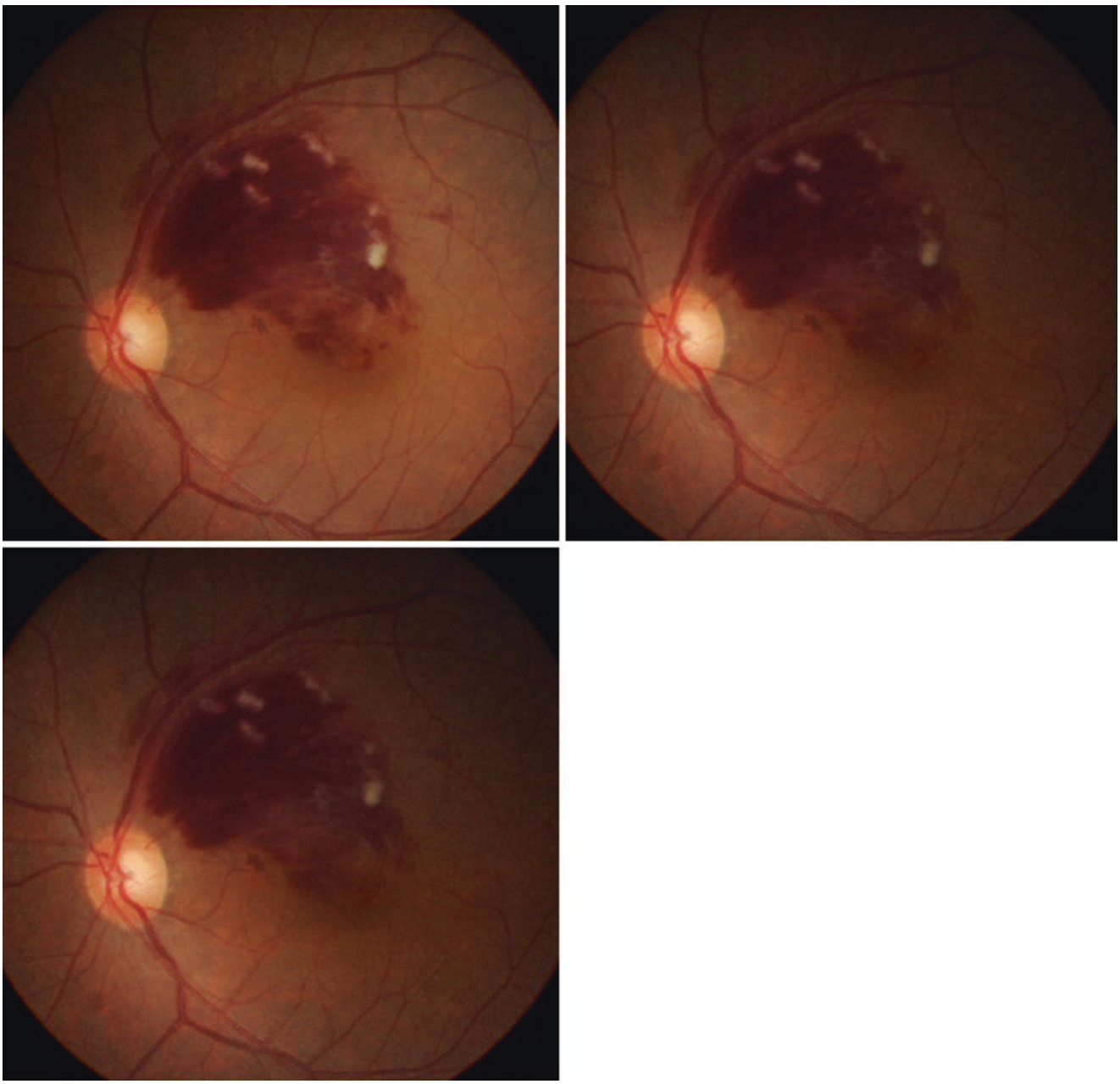

Fig. 2.5 Branch retinal vein occlusion
I. Superficial retinal hemorrhage
II. Superficial retinal exudates
III. Deep retinal exudates
IV. Macular edema
V. Dilated retinal vein

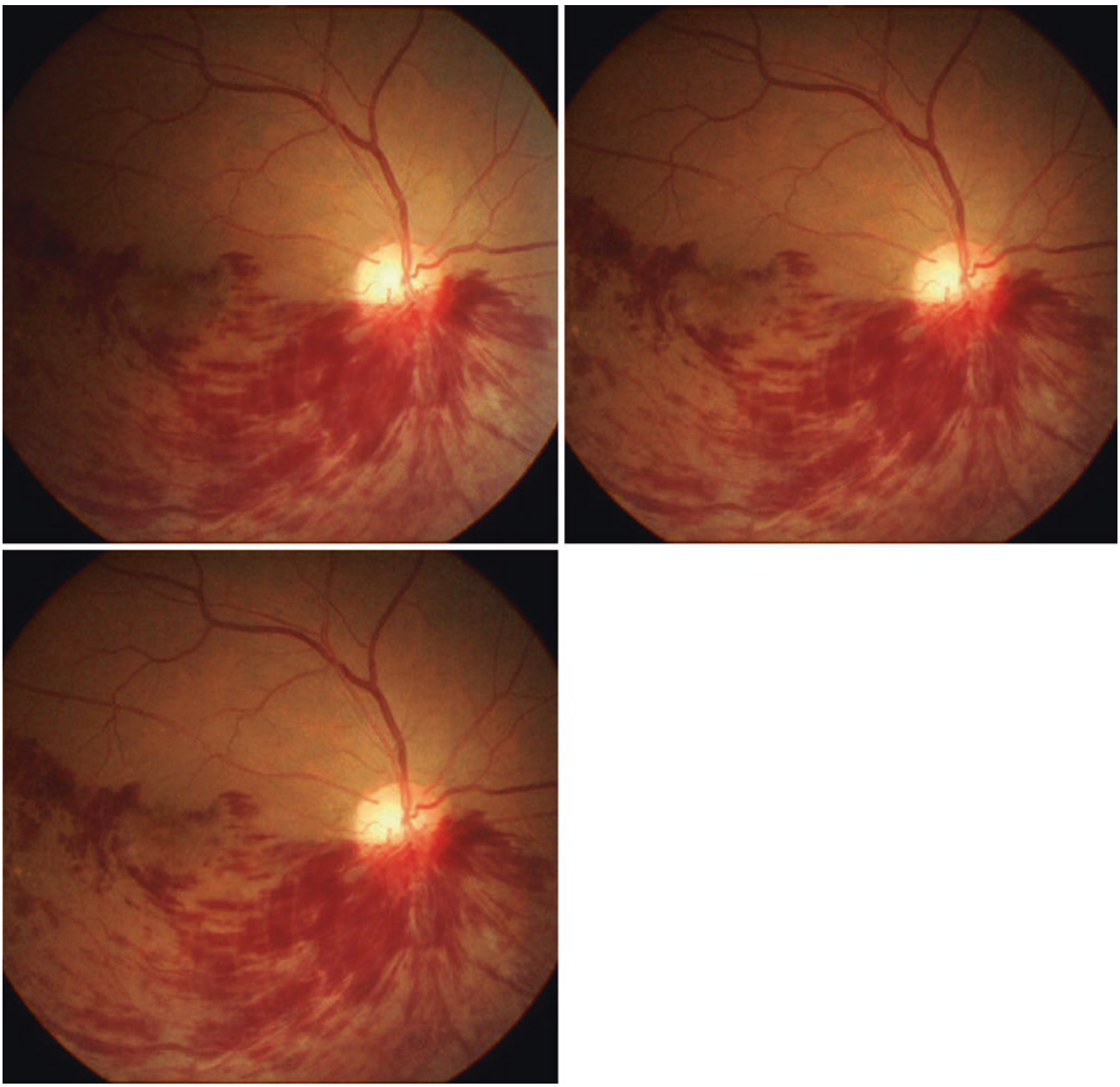

Fig. 2.6 Inferior hemi central retinal vein occlusion
I. Highly elevated retina in the inferior part, with flame-shaped retinal hemorrhage
II. Mild macular edema
III. Dilated retinal vein
IV. Flame-shaped retinal hemorrhage, less elevated than region I

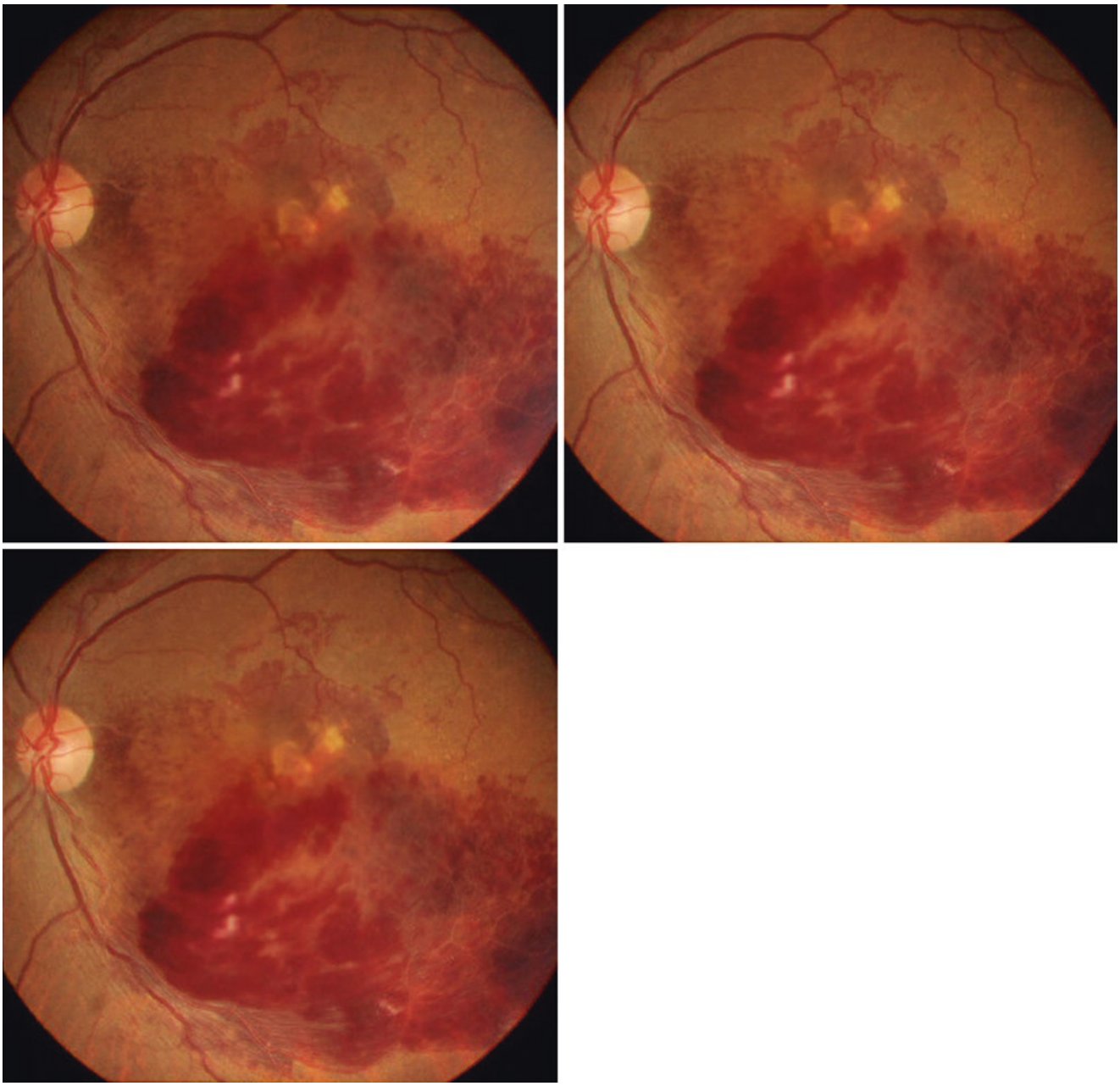

Fig. 2.7 Branch retinal vein occlusion
I. Superficial retinal hemorrhage
II. Retinal exudates
III. Ghost vessel in the distal part of the temporal inferior branch retinal vein
IV. Deep retinal exudates

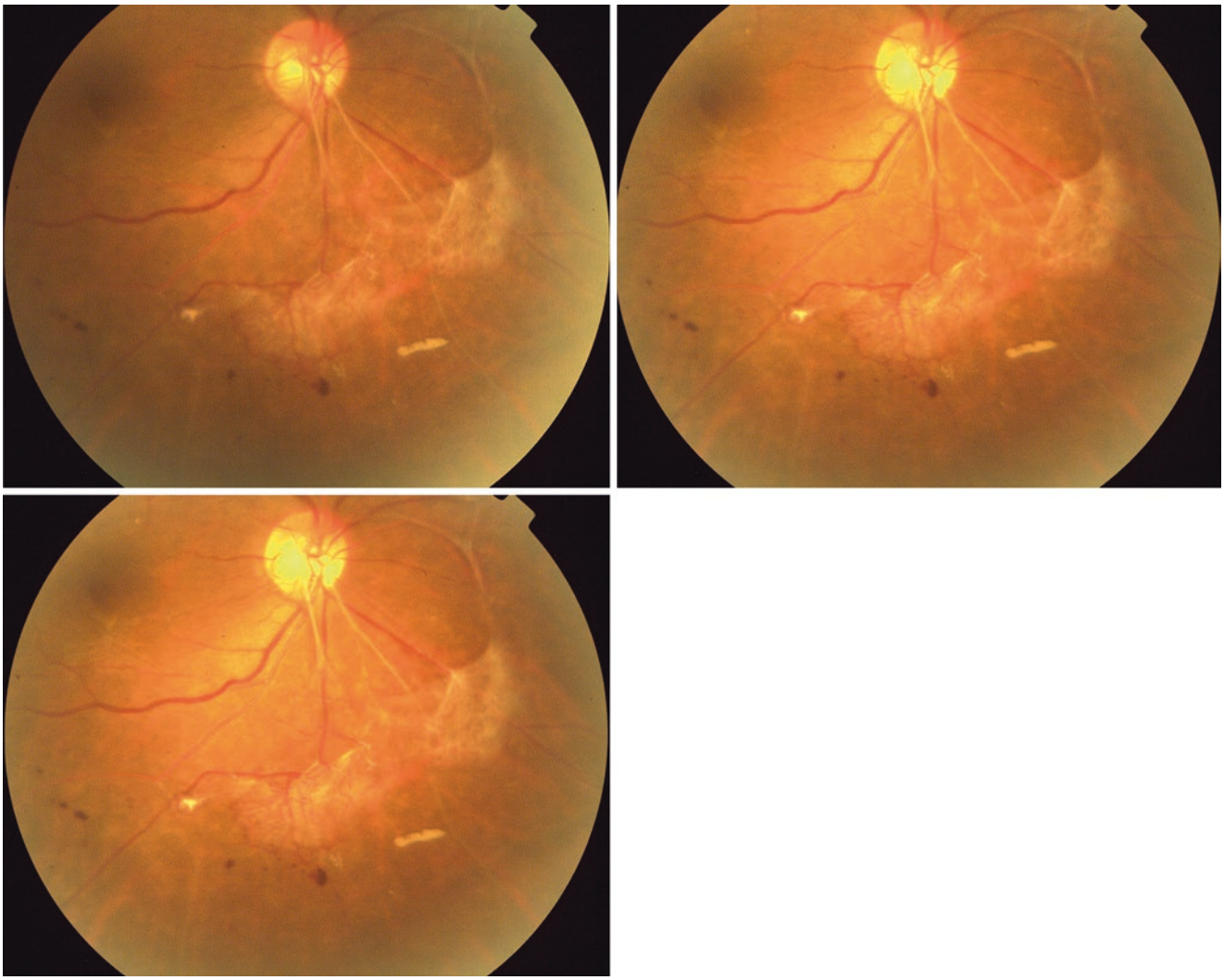

Fig. 2.8 Old branch retinal vein occlusion
I. Ghost vessel of retinal neovascularization, extended as a webbed membrane
II. Retinal artery looks like a white line and extended to the peripheral retina
III. Webbed membrane with thin underlying retina, suspected localized retinal detachment
IV. Retinal artery looks like a silver wire
V. Regressive neovascularization in the peripheral retina

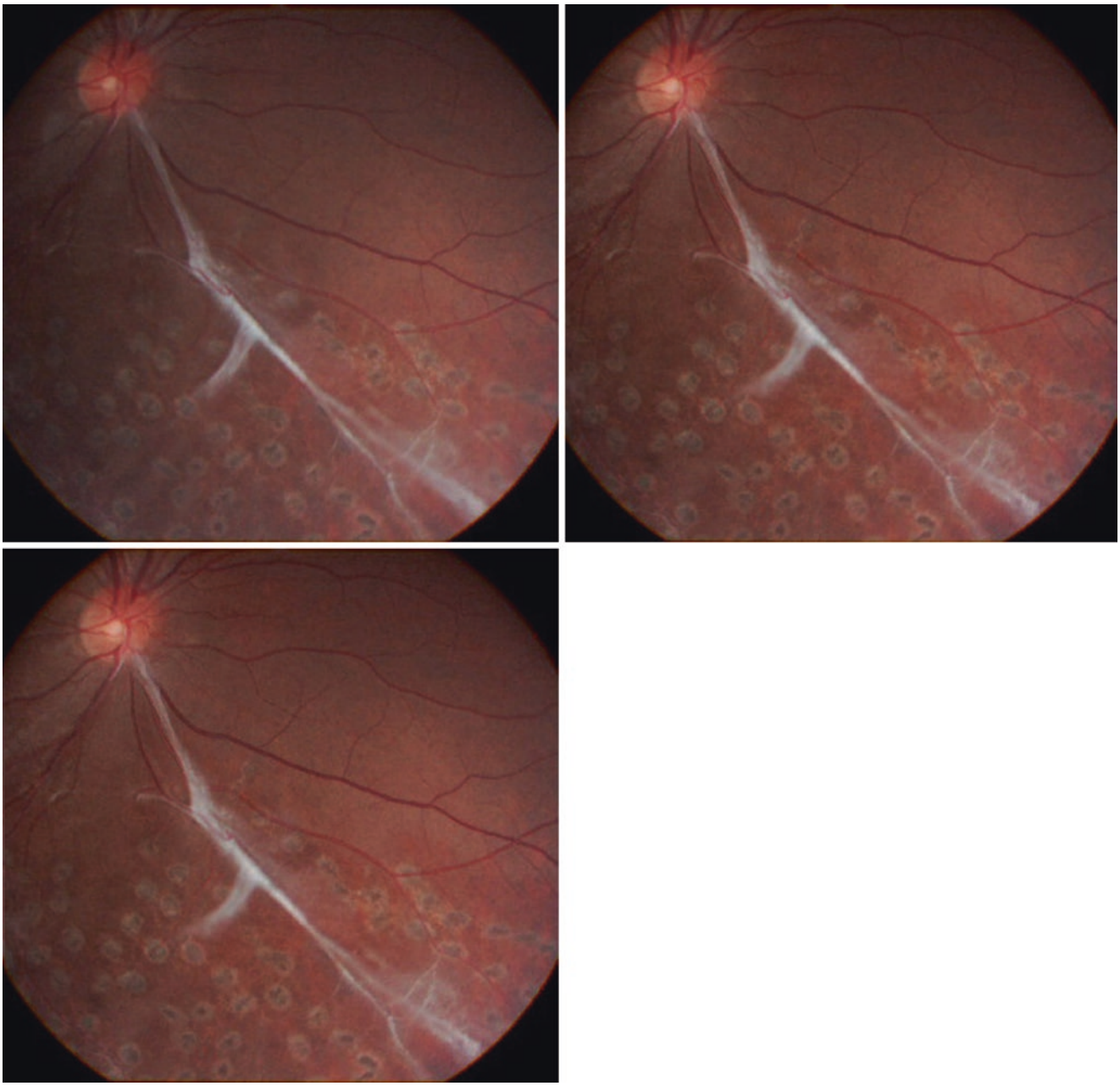

Fig. 2.9 Old branch retinal vein occlusion
I. The fibrotic membrane originated from the optic disc extended to the peripheral retina as like a tree branch
II. Inferior temporal branch was distorted by the membrane
III. Ghost vessel in the distal part of the retinal vein
IV. Extension of membrane
V. Laser spot

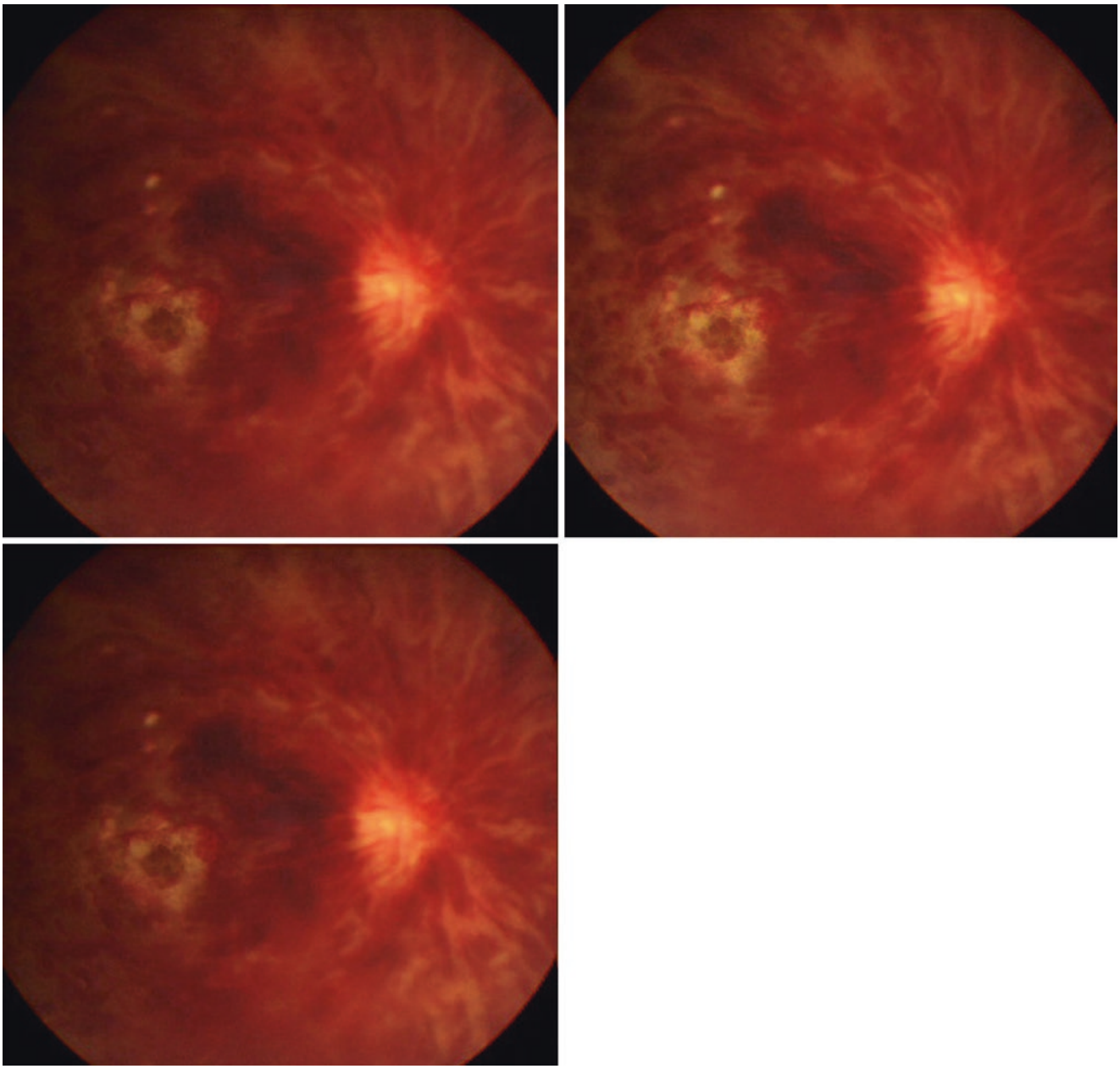

Fig. 2.10 Central retinal vein occlusion
I. Retinal hemorrhage around the optic disc
II. Macular edema (most elevated part)
III. Macular edema (the second layer)
IV. Deep retinal hemorrhage

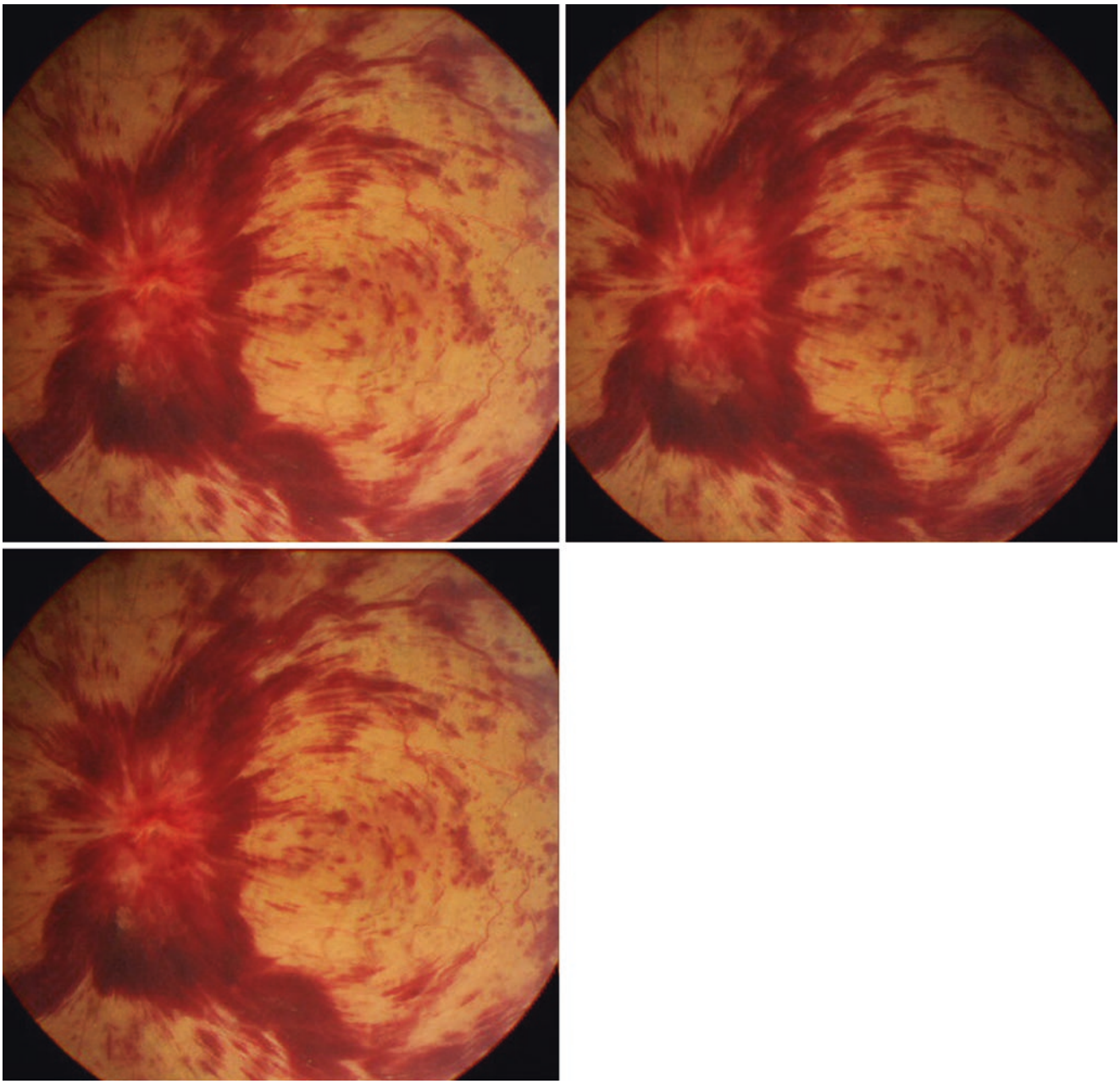

Fig. 2.11 Central retinal vein occlusion
I. Severe optic disc edema, with massive hemorrhage
II. Macular edema
III. Intermediate retinal exudates
IV. The retinal artery looks like a silver wire
V. Engorged retinal vein and narrowing of adjacent artery

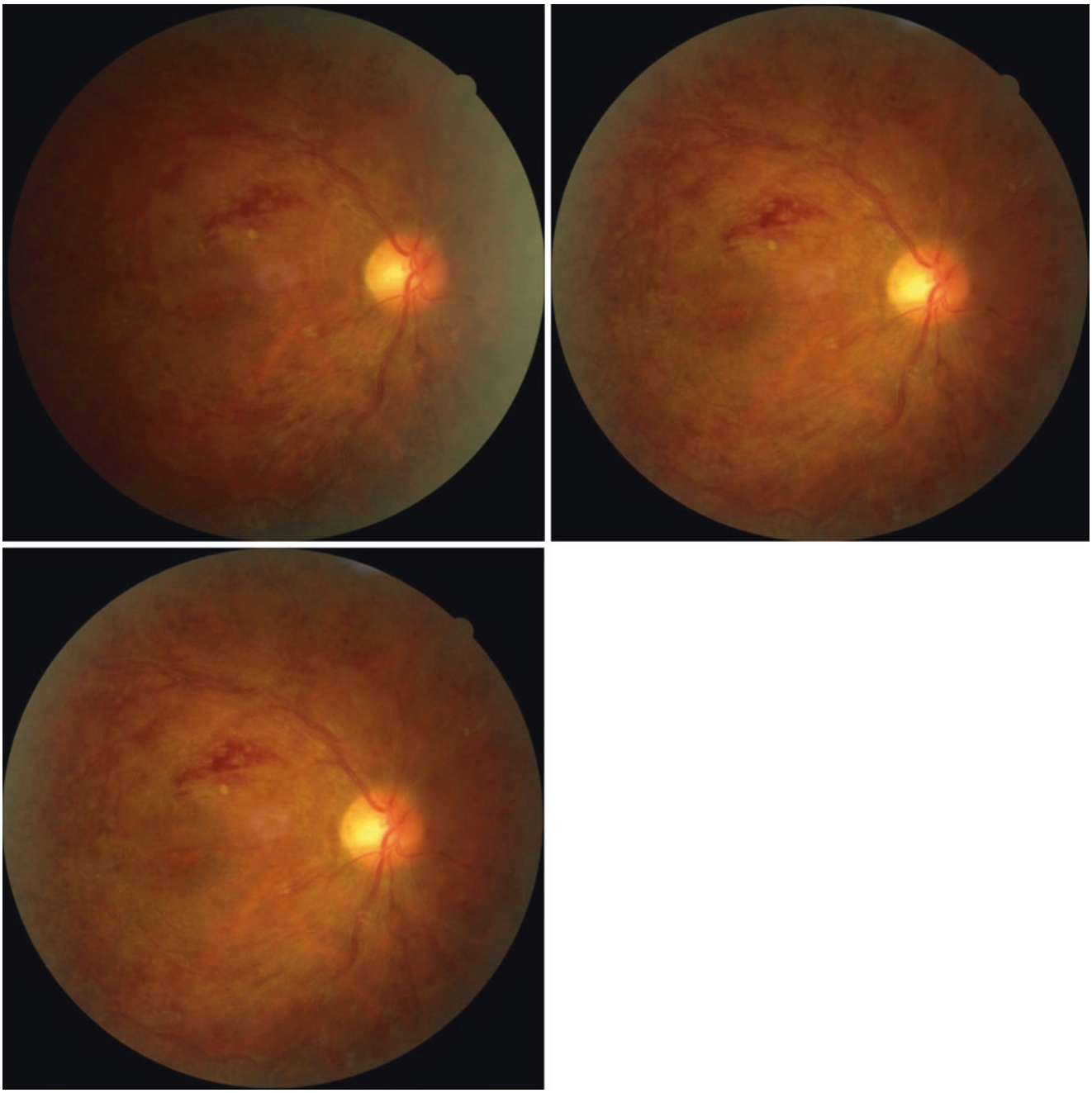

Fig. 2.12 Central retinal vein occlusion
I. Superficial retinal hemorrhage
II. Retinal exudates
III. Arteriovenous crossing change
IV. Macular edema

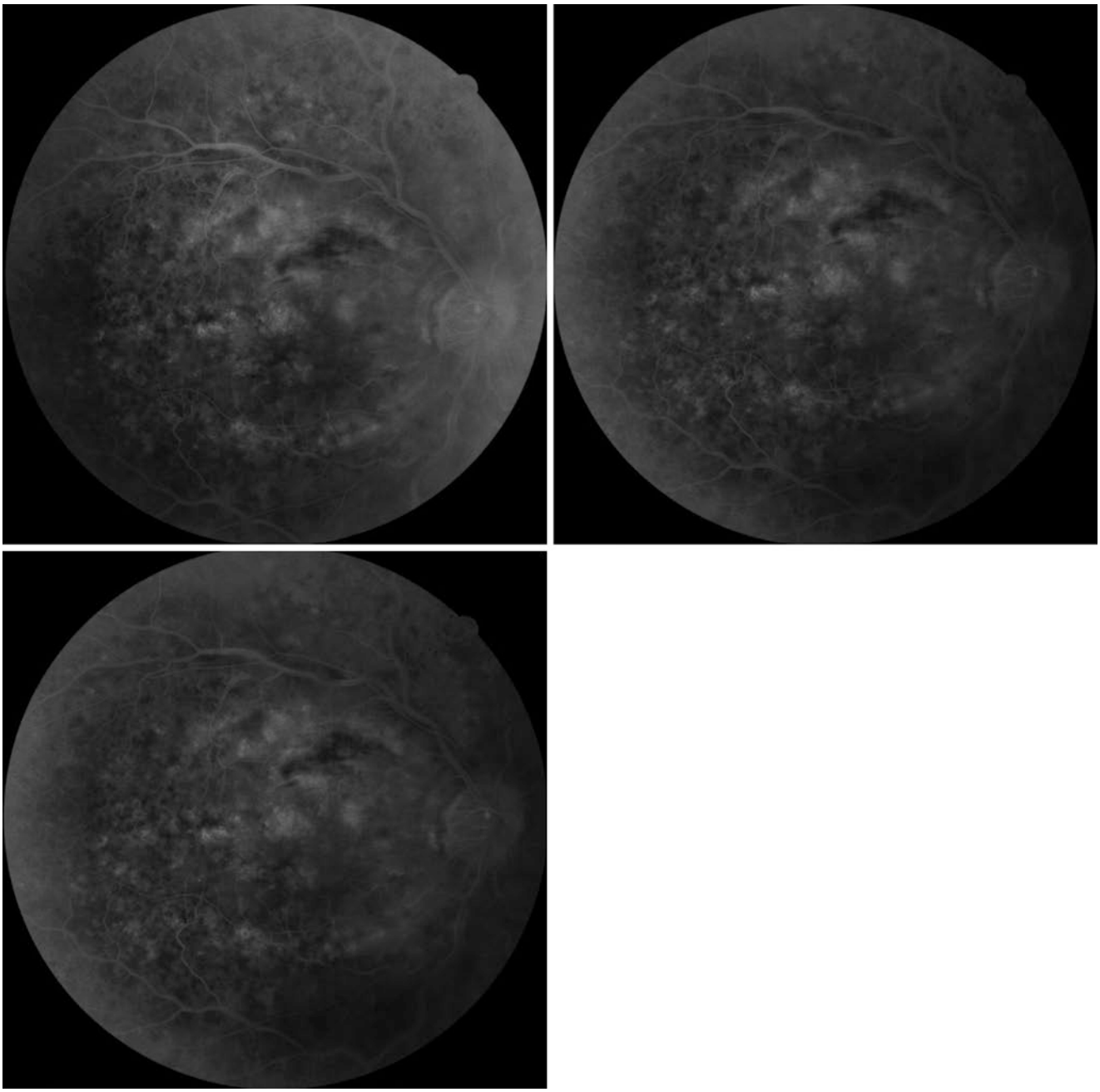

Fig. 2.13 Fluorescein fundus angiography of central retinal vein occlusion
I. Cystoid macular edema
II. The apex of the edema
III. Vessels pushed up by edema
IV. Blocked fluorescence by hemorrhage

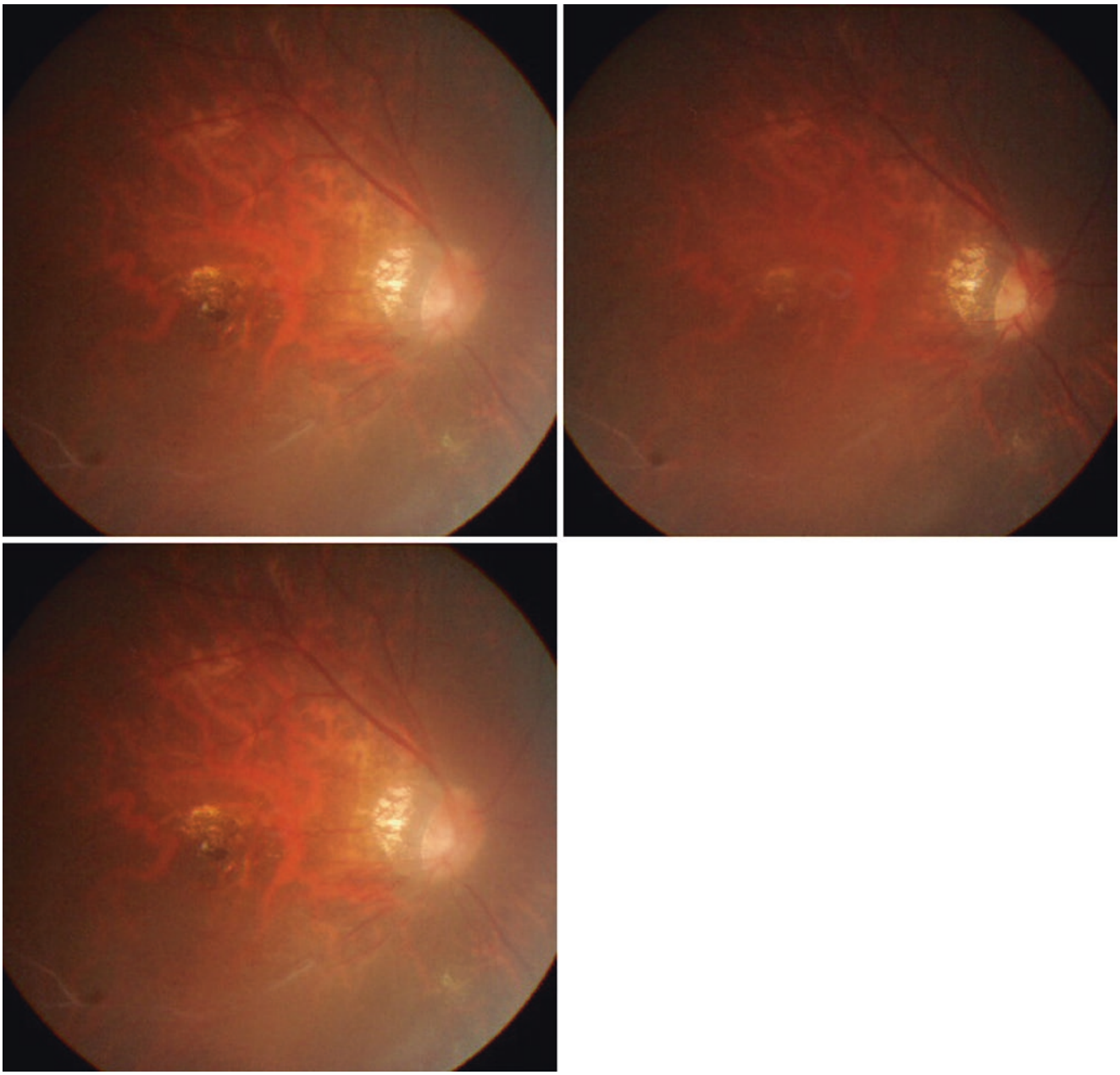

Fig. 2.14 High myopia with old branch retinal vein occlusion
I. Weiss ring
II. Ghost vessel in the temporal inferior retinal vein branch
III. Fuchs spot
IV. Atrophy of retinal pigment epithelium and exposure of sclera
V. Large choroidal vessels

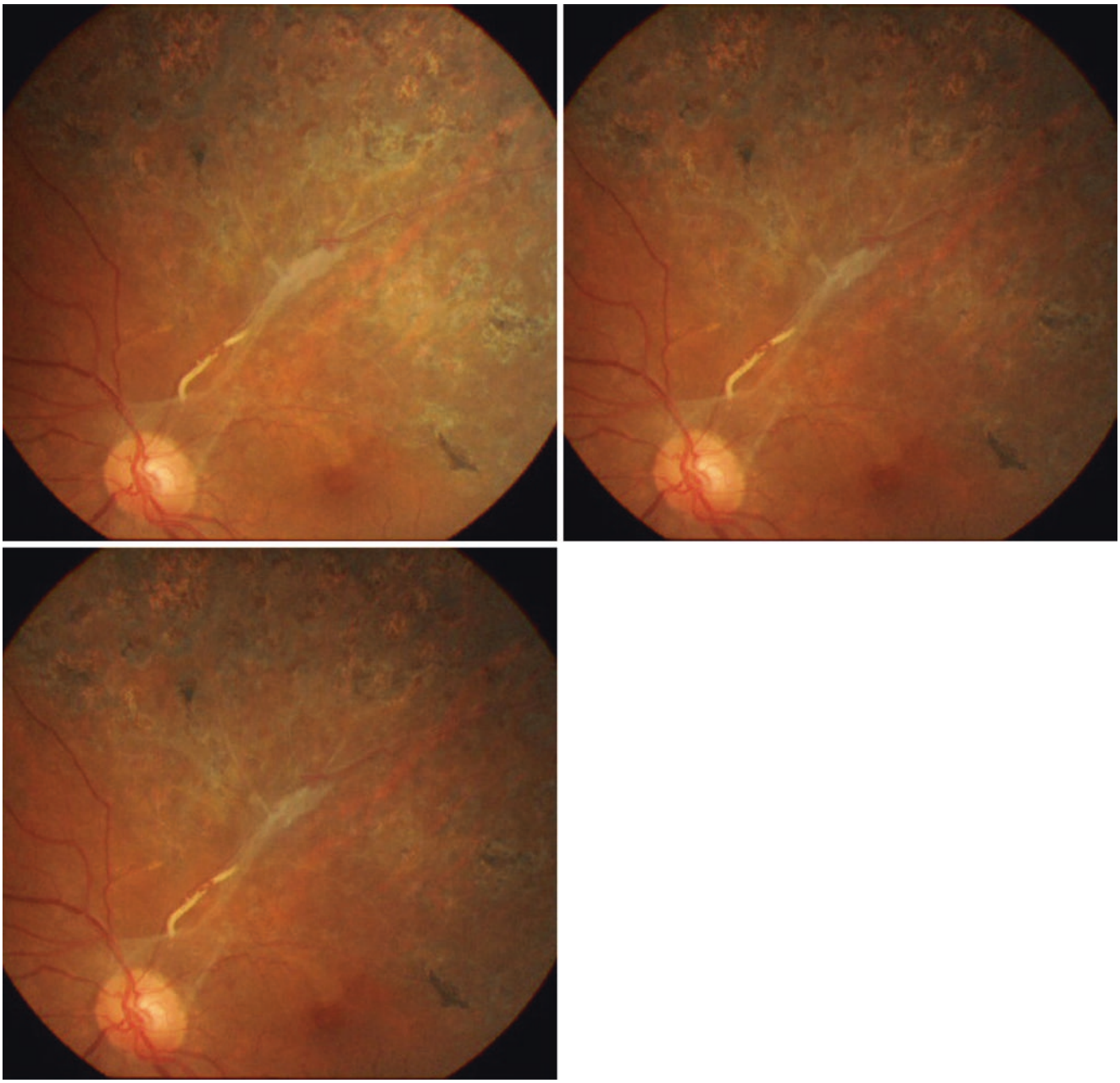

Fig. 2.15 Chronic branch retinal vein occlusion after laser treatment
I. Proliferative membrane extended from the optic disc to peripheral retina
II. Venous loop sprouted to the vitreous cavity
III. Ghost vessel of retinal vein
IV. Atrophic retinal areas
V. Retinal pigment proliferation

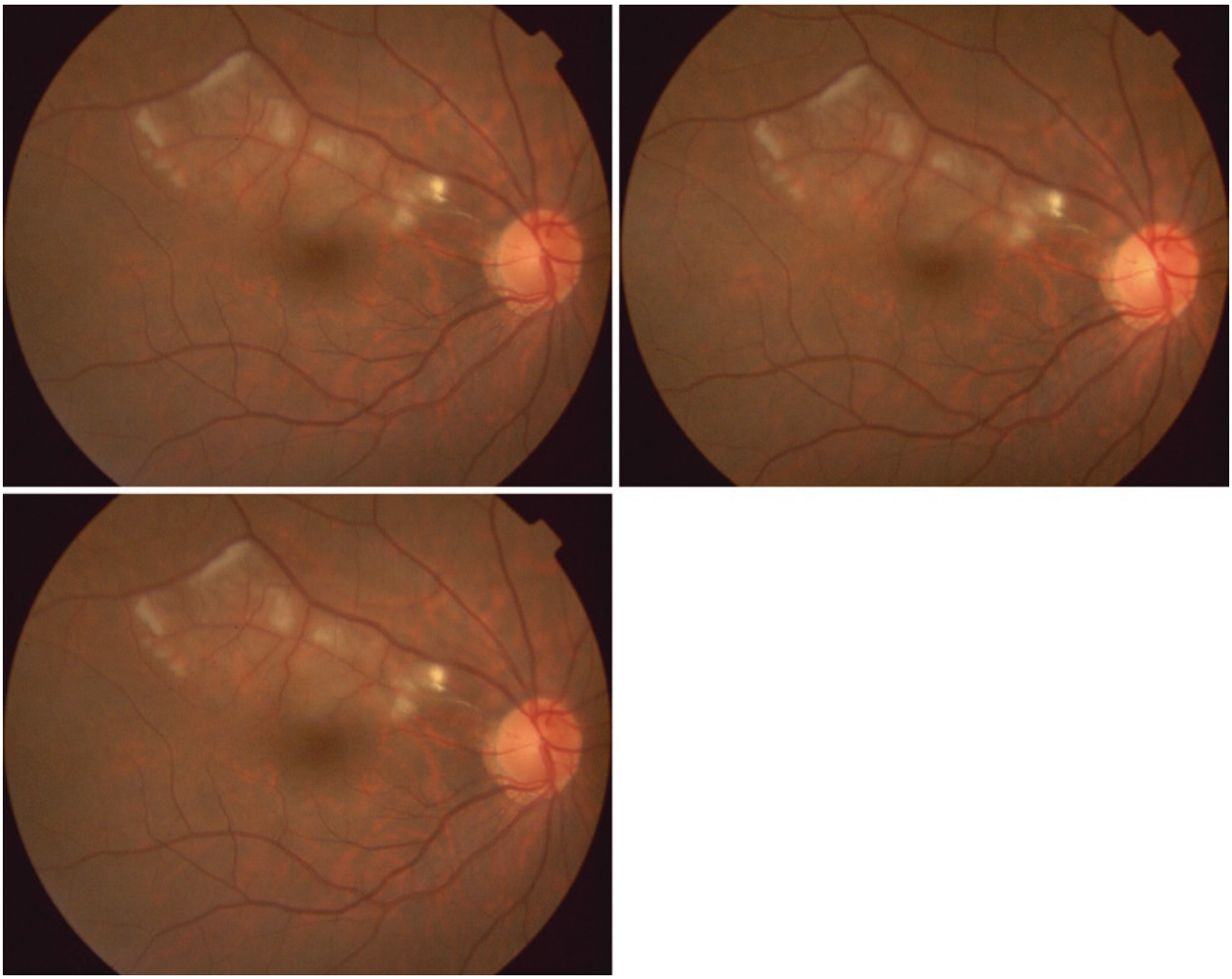

Fig. 2.16 Branch retinal artery occlusion
I. Occlusive spot of retinal artery
II. Pale zone corresponding to the occlusive artery
III. Partial involvement of macula

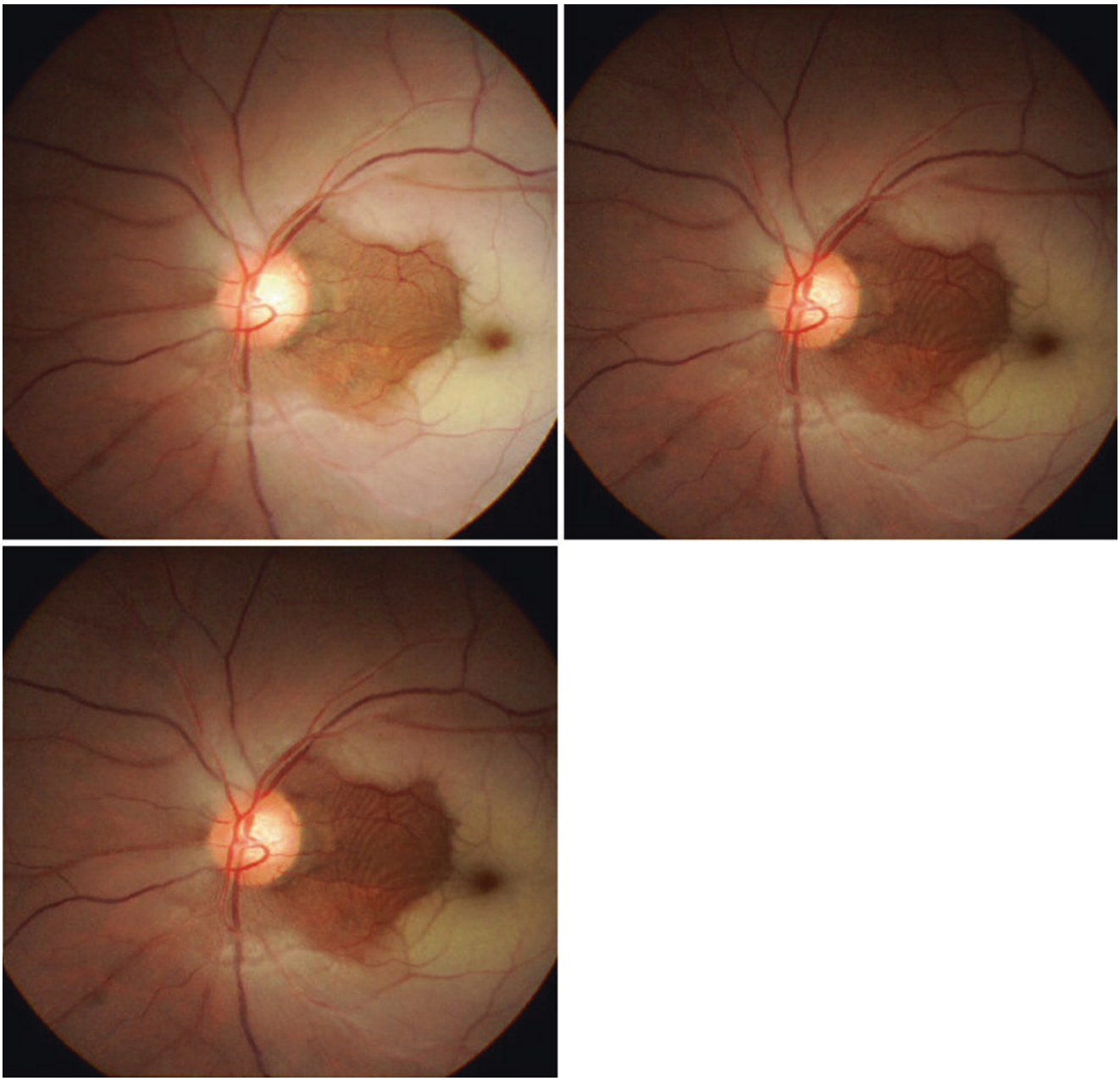

Fig. 2.17 Central retinal artery occlusion
I. Ligulate sparing of retinal area
II. Two suspected cilioretinal artery
III. Grey-whitish retinal area
IV. Cherry-red spot
V. Segmentation of the blood column in the arterioles

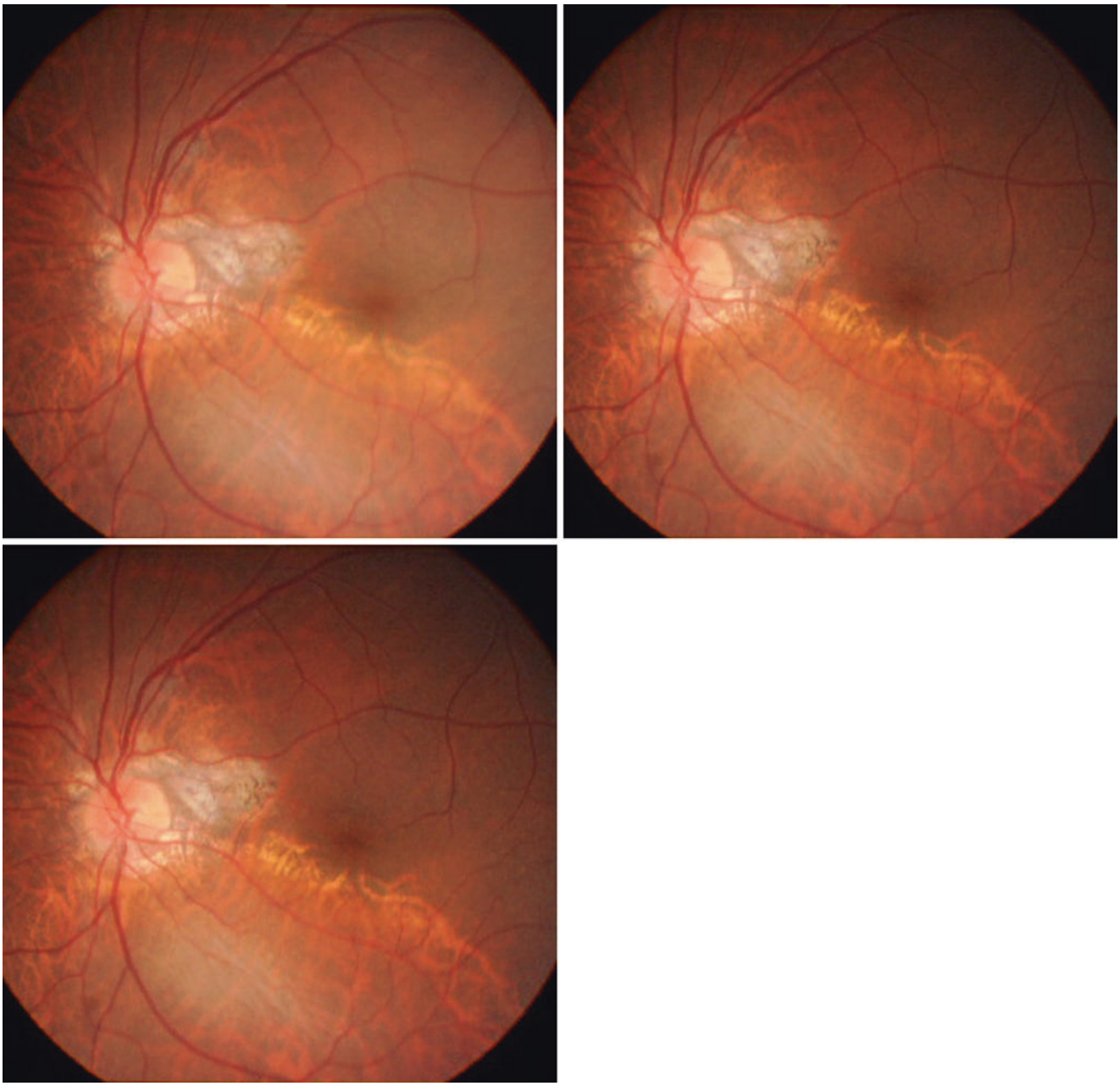

Fig. 2.18 Branch choroidal artery occlusion
I. Choroidal atrophy of the choroidal artery occluded area
II. The retina was mildly depressed

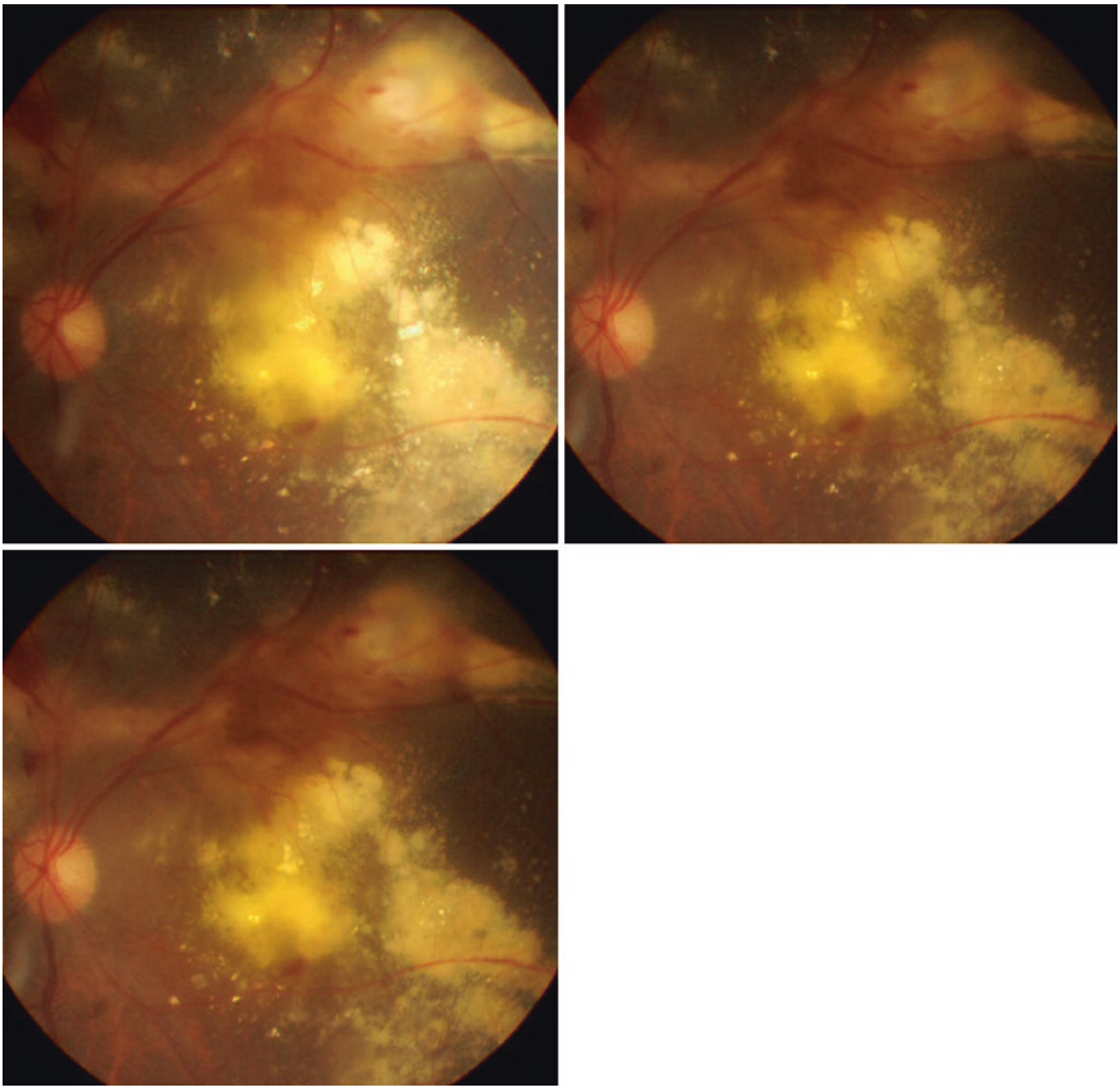

Fig. 2.19 Coats disease
I. Superficial retinal hemorrhage
II. Cholesterol crystal
III. Suspending retinal vessels
IV. Intermediate retinal exudates
V. Dilated retinal vessels

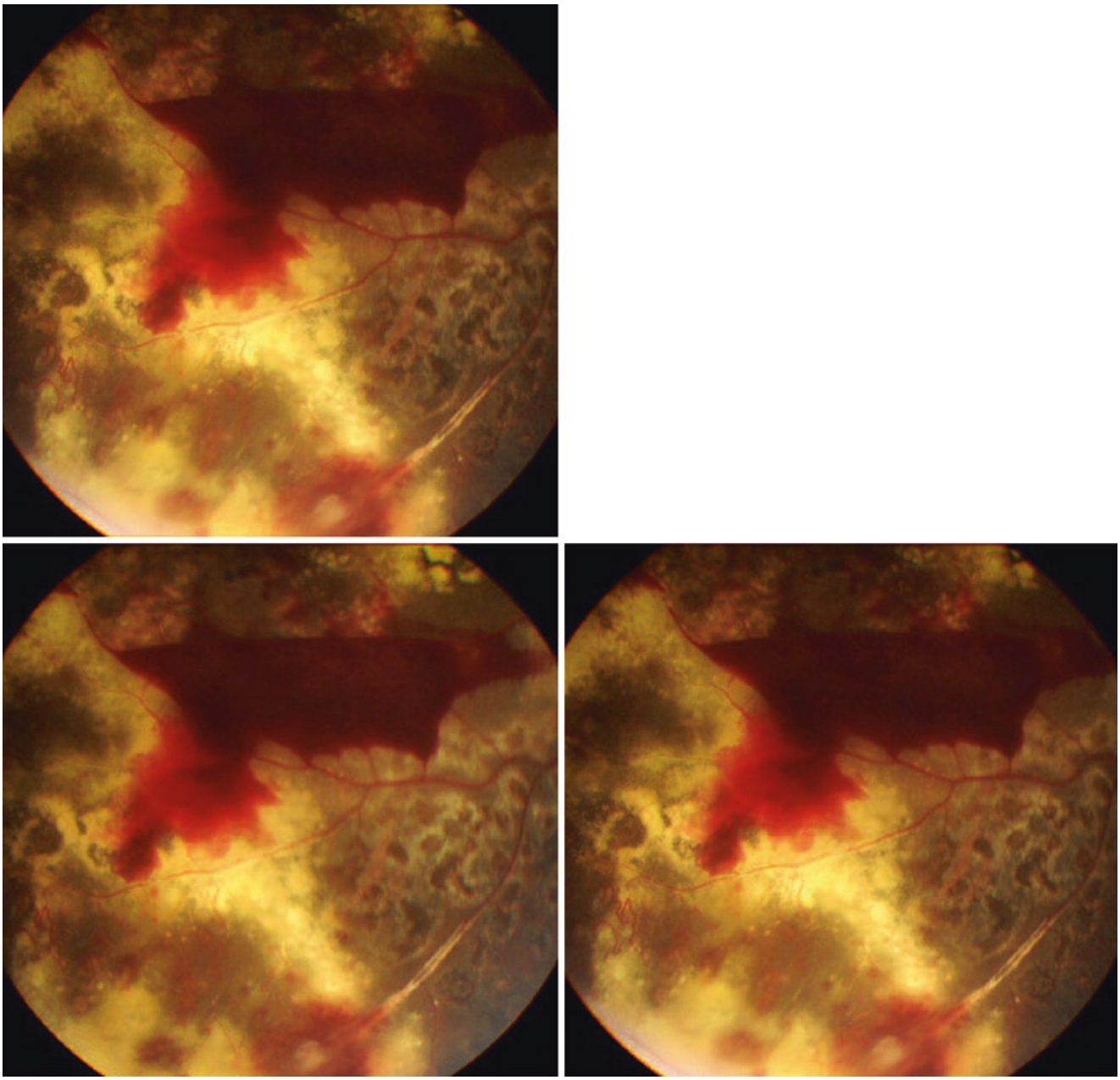

Fig. 2.20 Coats disease after laser treatment
I. Pre-retinal hemorrhage
II. Superficial retinal hemorrhage
III. Abnormal dilated vessels and yellow-white exudates
IV. Suspending vessels with white sheath
V. Laser spots and atrophic retinal area

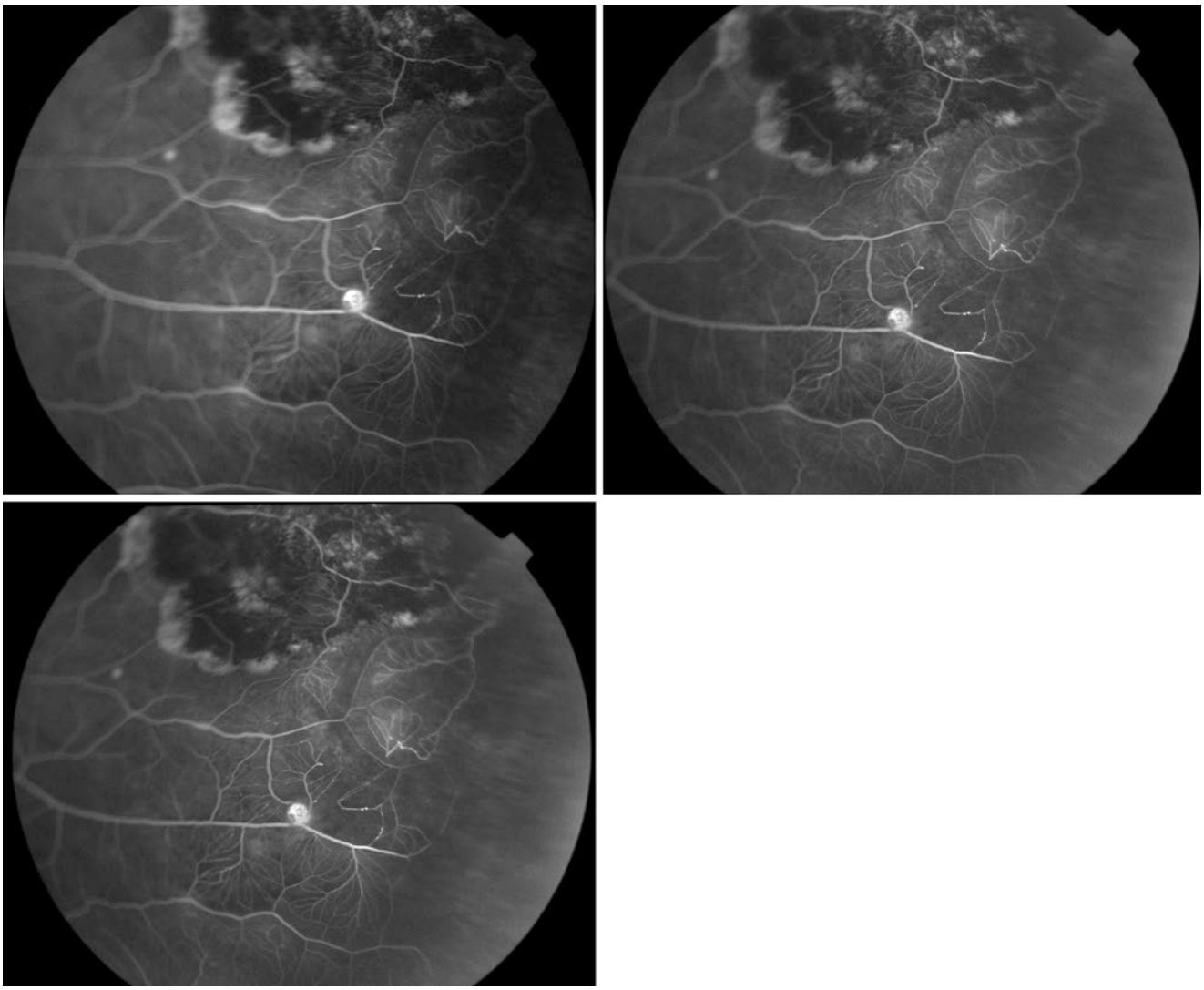

Fig. 2.21 Coat disease after laser treatment
I. Dilated superficial retinal vessel
II. Dilated deep retinal vessel
III. The end of the vessel was dilated and leaked fluorescein, which was near the base of the lesion
IV. The area of laser, where the retina was atrophied

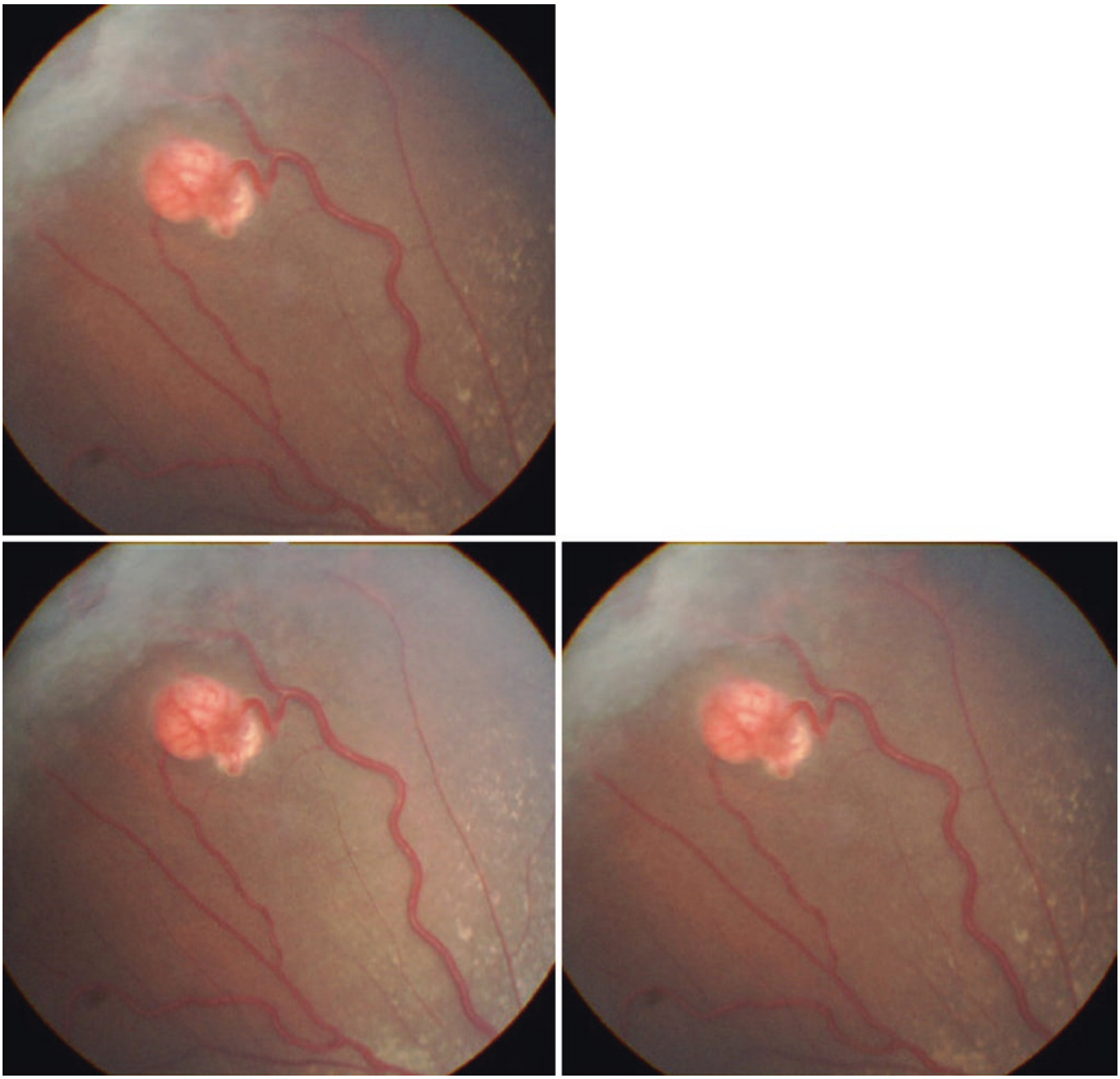

Fig. 2.22 Von-Hippel retinal capillary hemangiomatosis
I. Hemangioma
II. Dilated feeder artery
III. Draining vein
IV. Deep exudates
V. Old vitreous hemorrhages

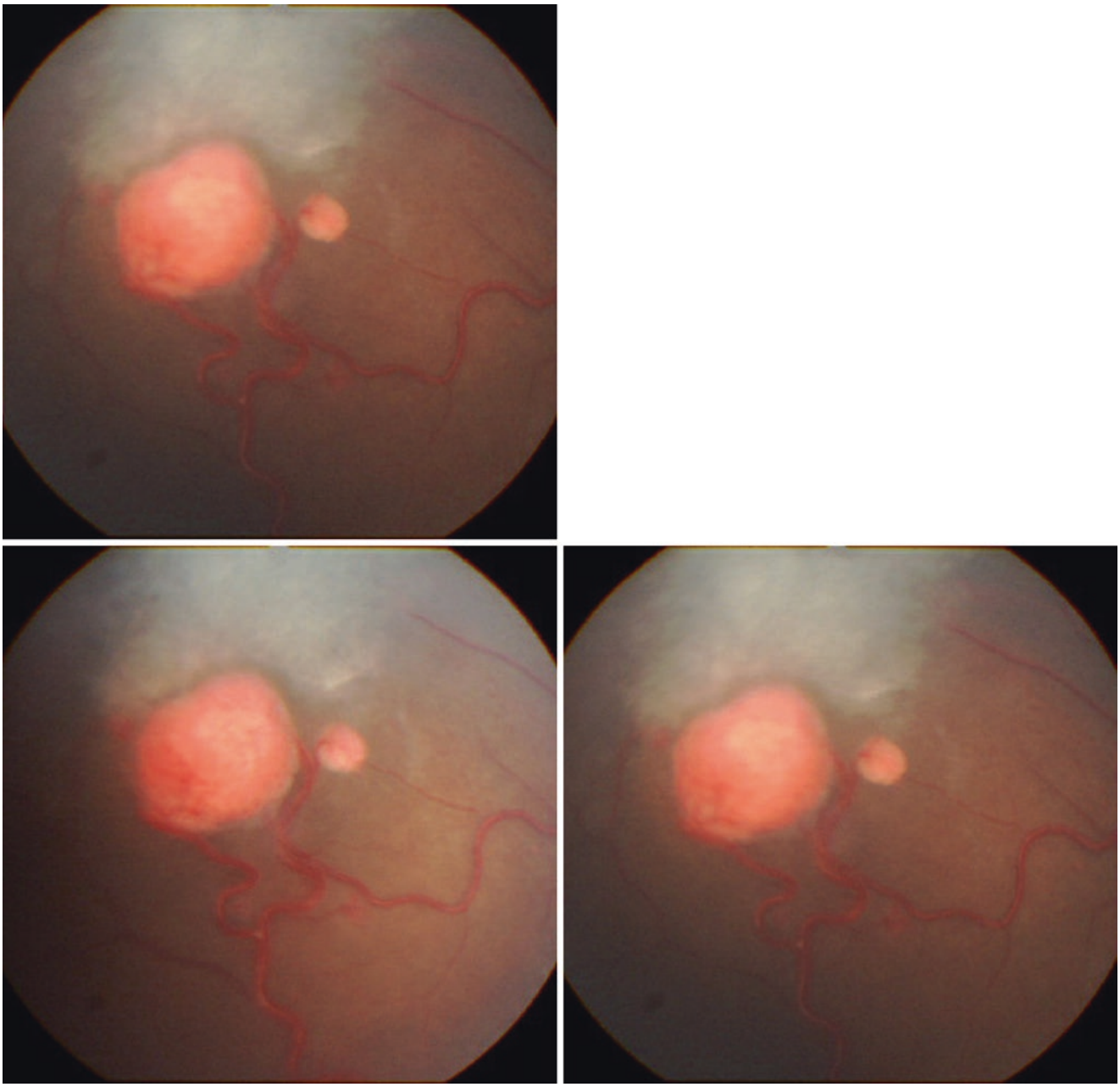

Fig. 2.23 Von-Hippel retinal capillary hemangiomatosis
I+II. Two capillary hemangiomas
III. Draining vein
IV. Peripheral vitreous opacities

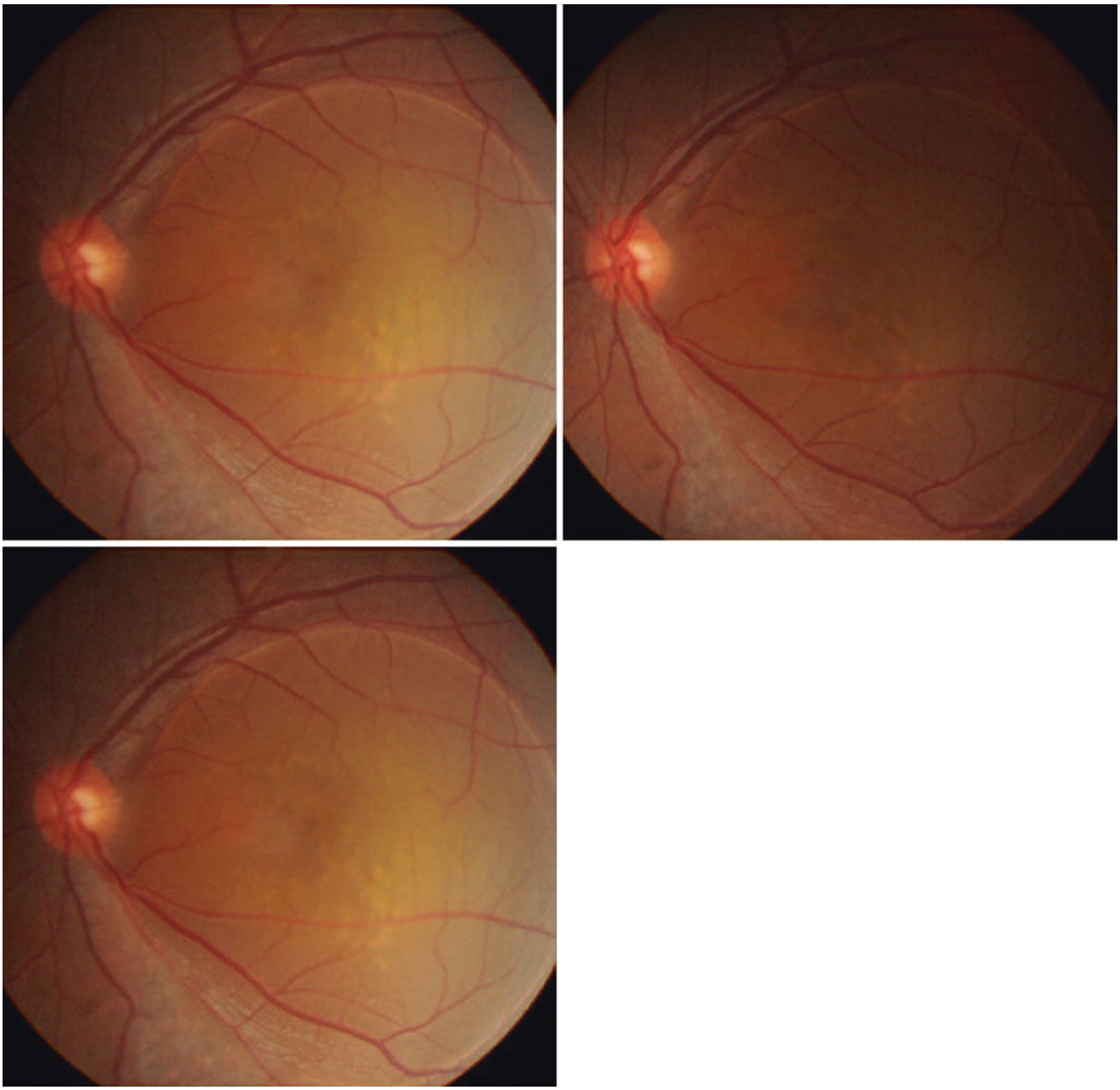

Fig. 2.24 Retinal pigment epithelium detachment
I. Apex of detachment
II. Intermediate retinal exudates
III. Boundary of detachment

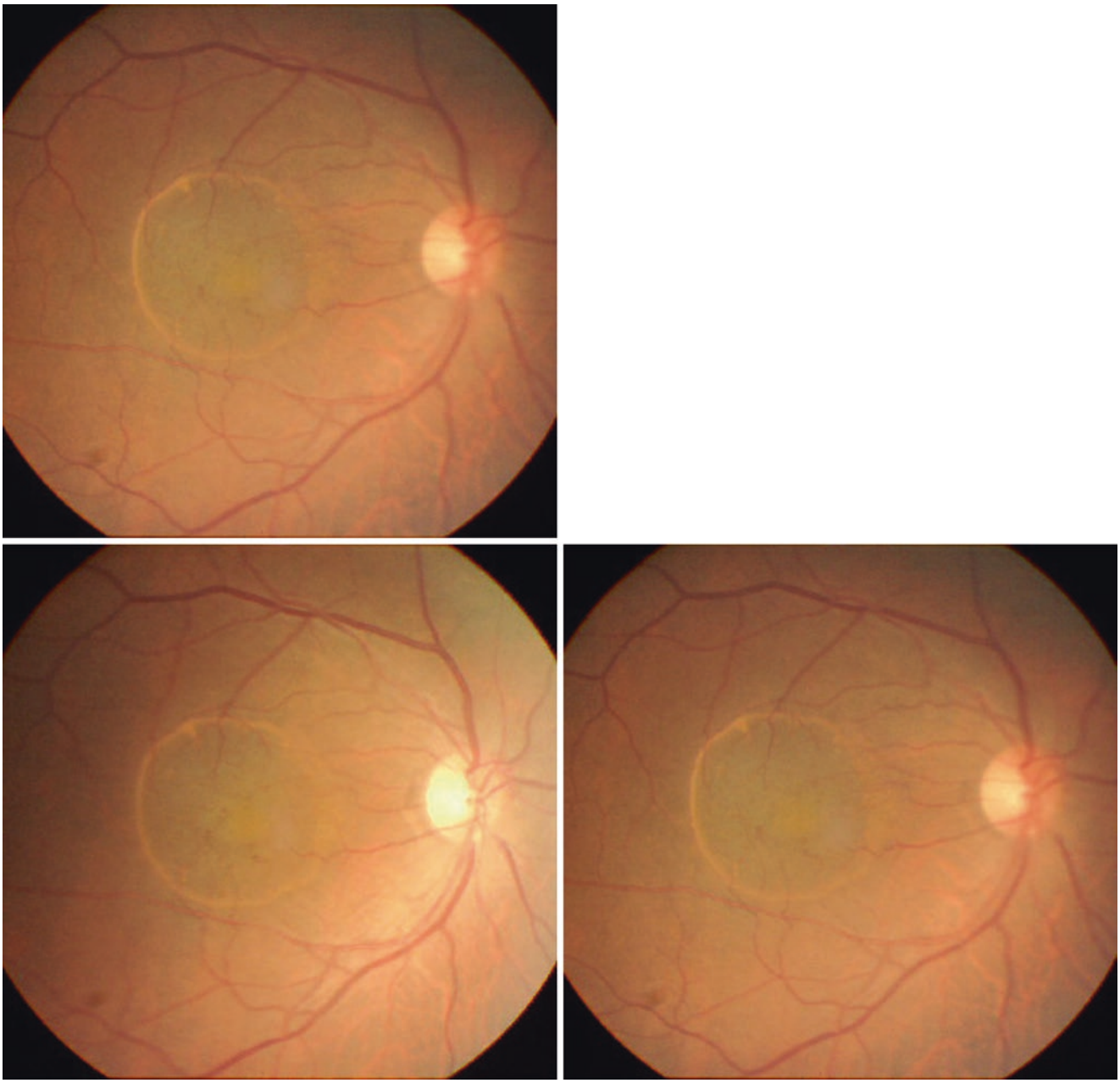

Fig. 2.25 Sensory retinal detachment in the posterior pole
I. Highly elevated sensory retinal detachment of the posterior pole
II. Yellow-white lipid exudates in the margin of detached retina

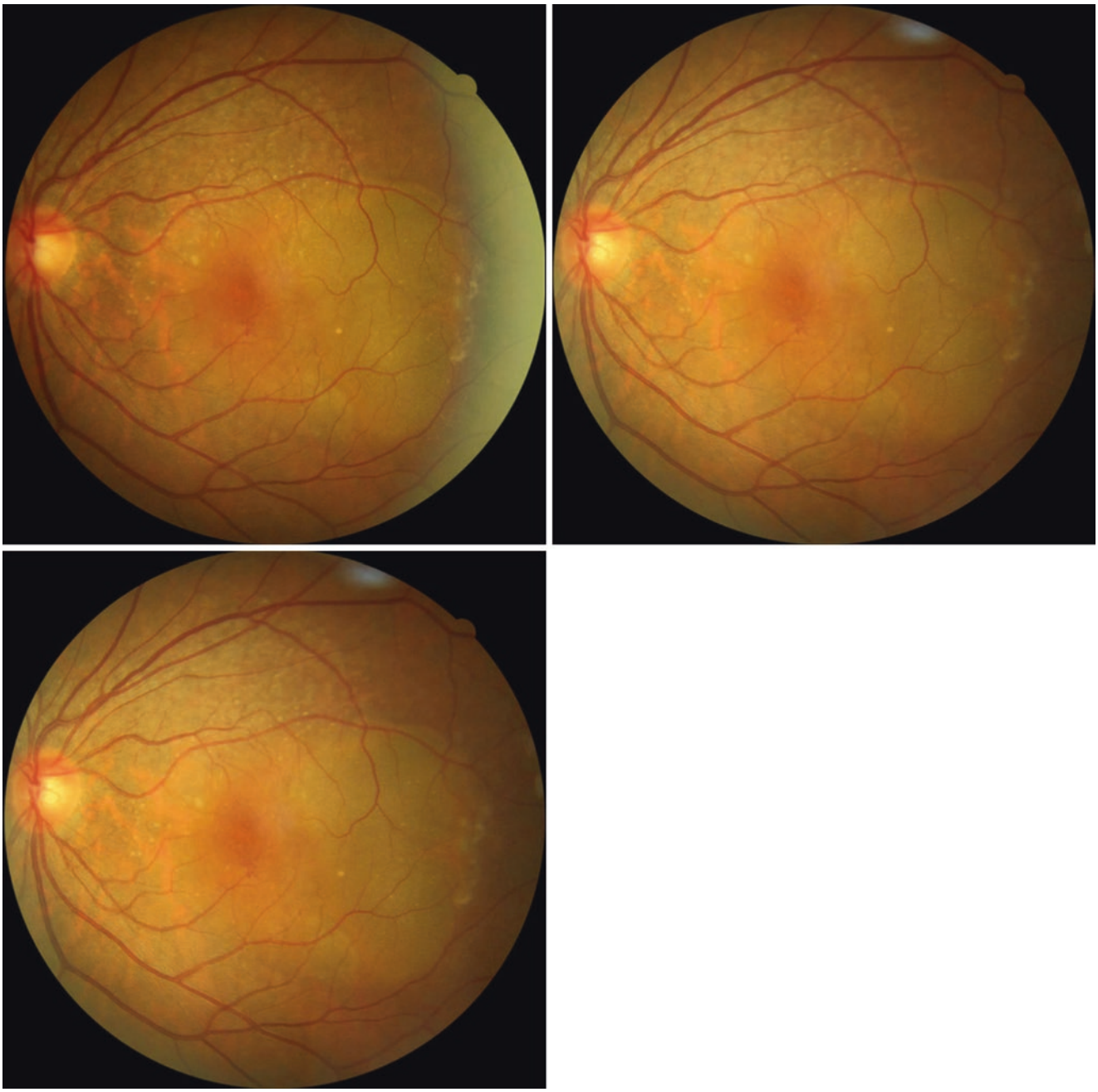

Fig. 2.26 Sensory retinal detachment with pigment epithelium detachment
I. Area of pigment epithelium detachment
II. Area of sensory retinal detachment
III+IV. Intermediate retinal exudates

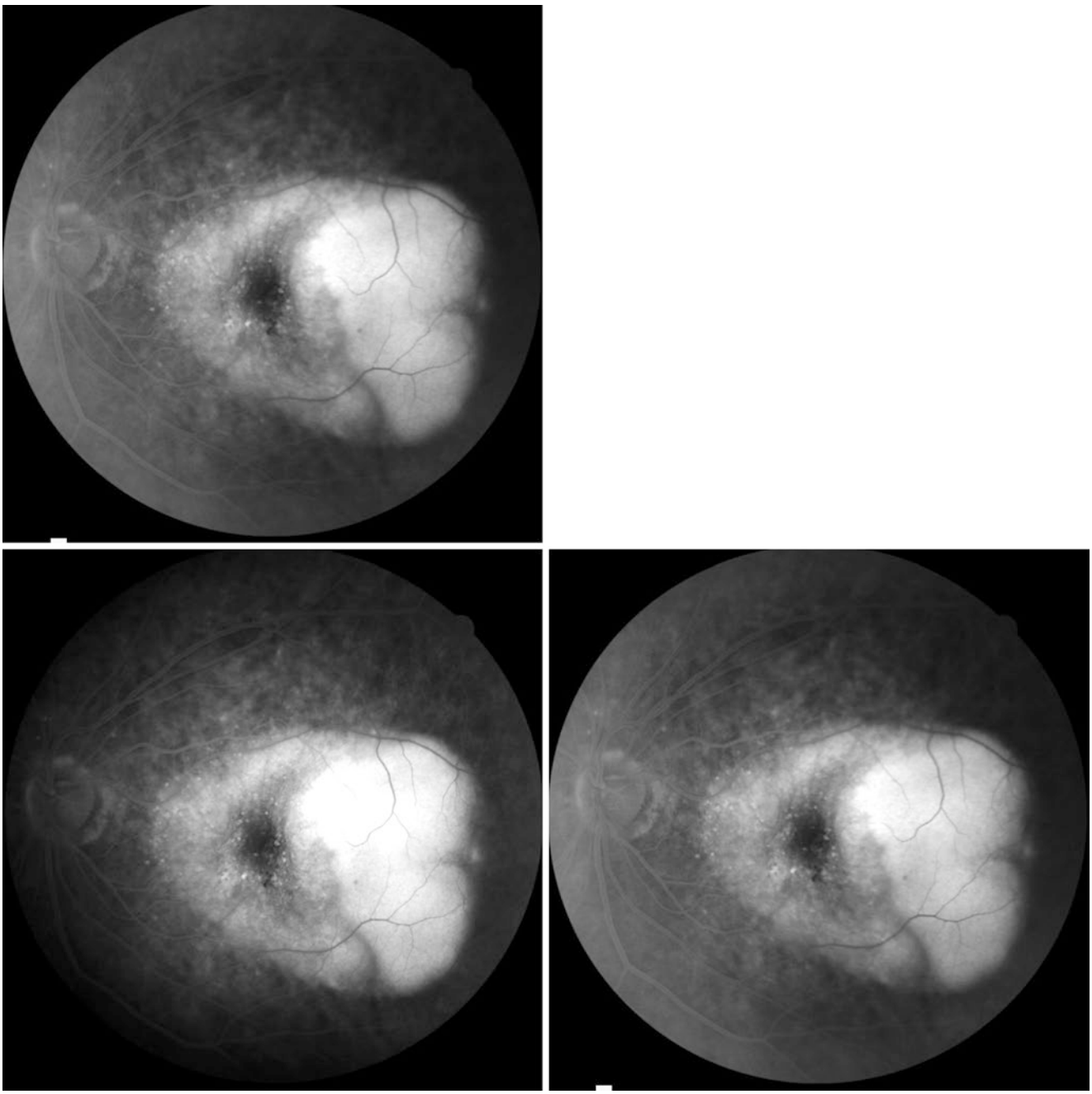

Fig. 2.26 (continued)

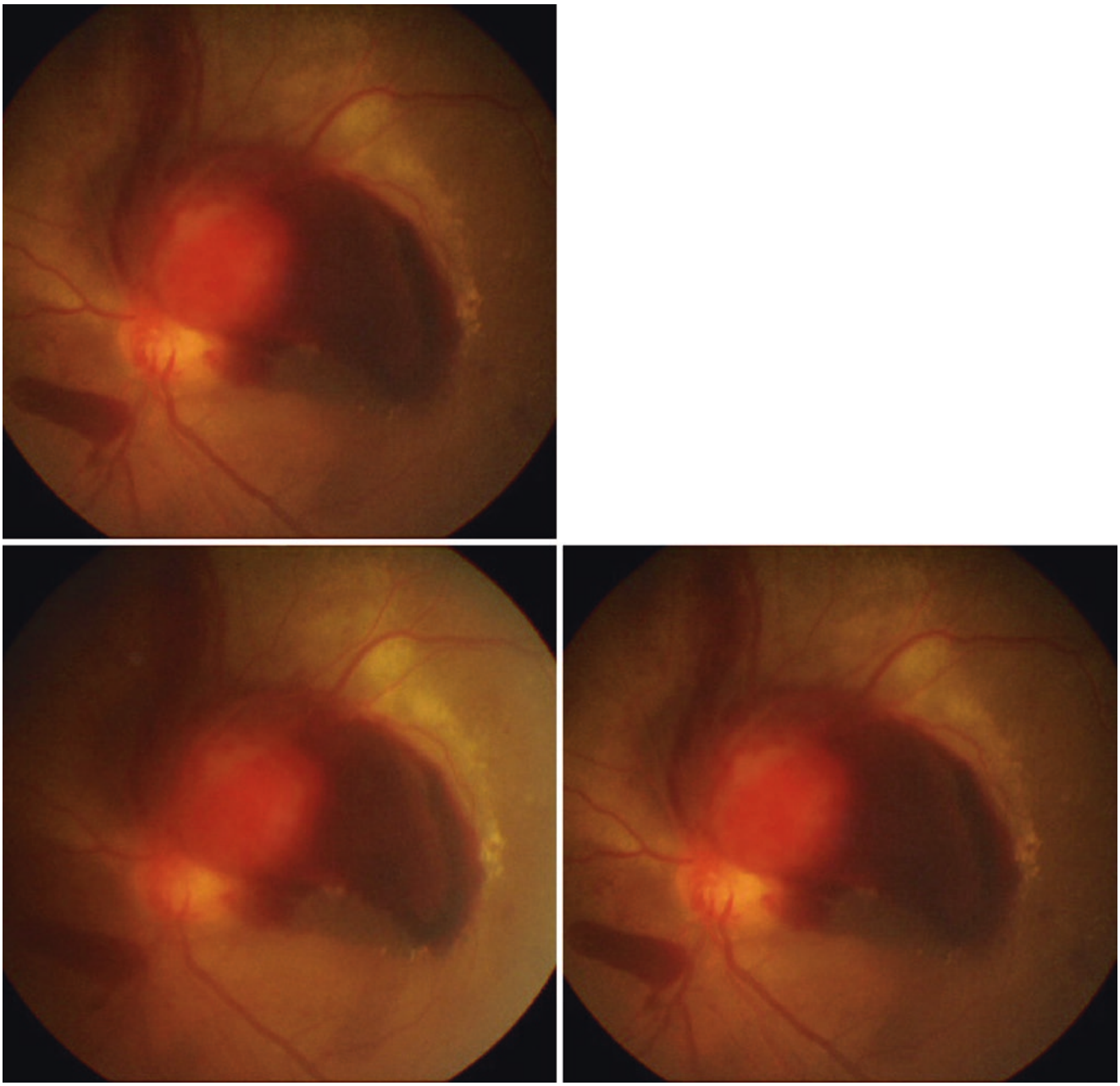

Fig. 2.27 Retinal macroaneurysm near the optic disc
I. Retinal macroaneurysm near the optic disc
II. Superficial retinal hemorrhage
III. Deep retinal hemorrhage
IV. Sub-RPE hemorrhage
V. Intermediate retinal hard exudates
VI. Vitreous hemorrhage

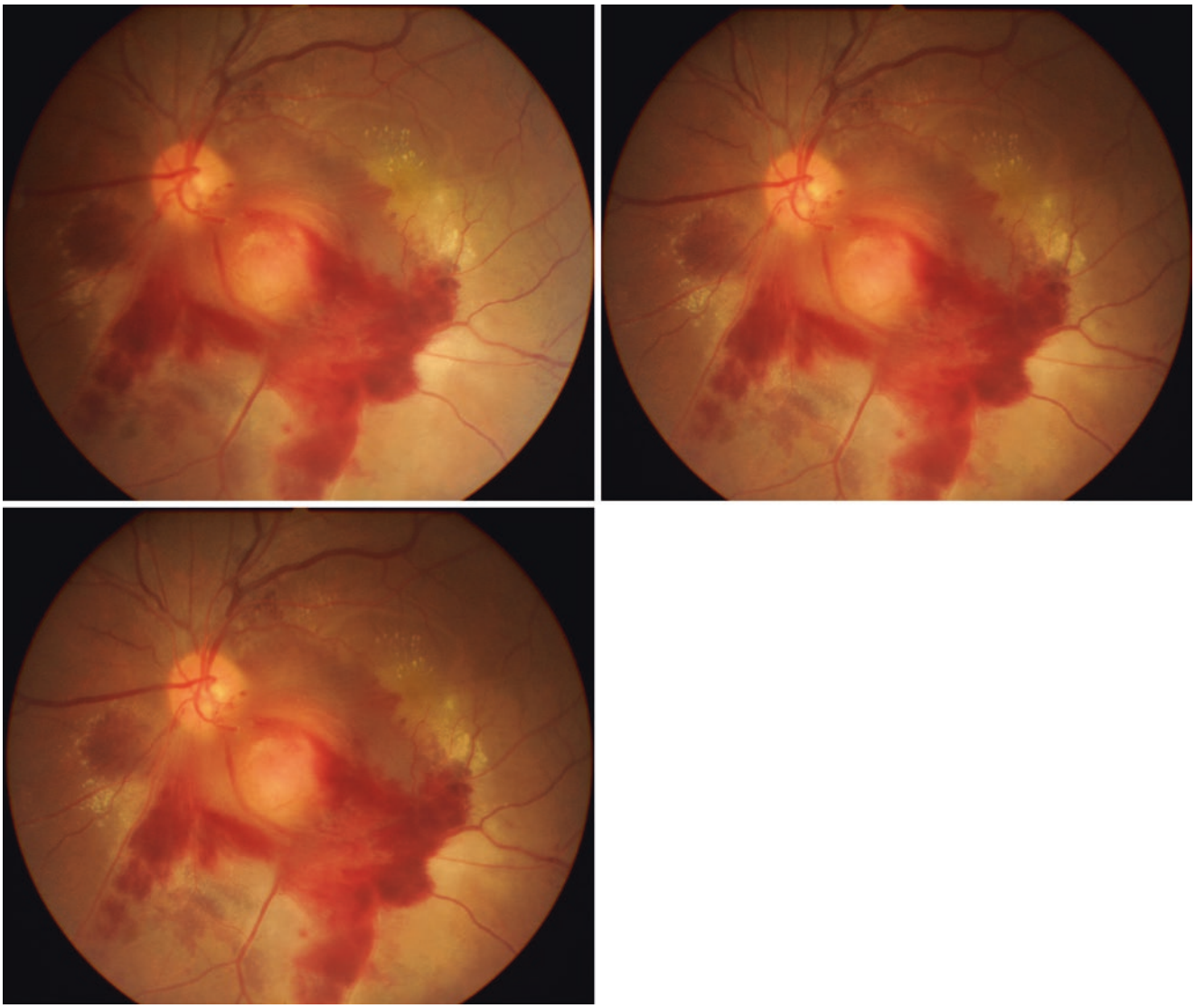

Fig. 2.28 Retinal macroaneurysm
I. Suspected area of the aneurysm
II. Superficial retinal hemorrhage
III. Subretinal hemorrhage and arterioles on the top
IV. Superficial retinal hemorrhage
V. Deep retinal exudates
VI Retinal epithelium detachment

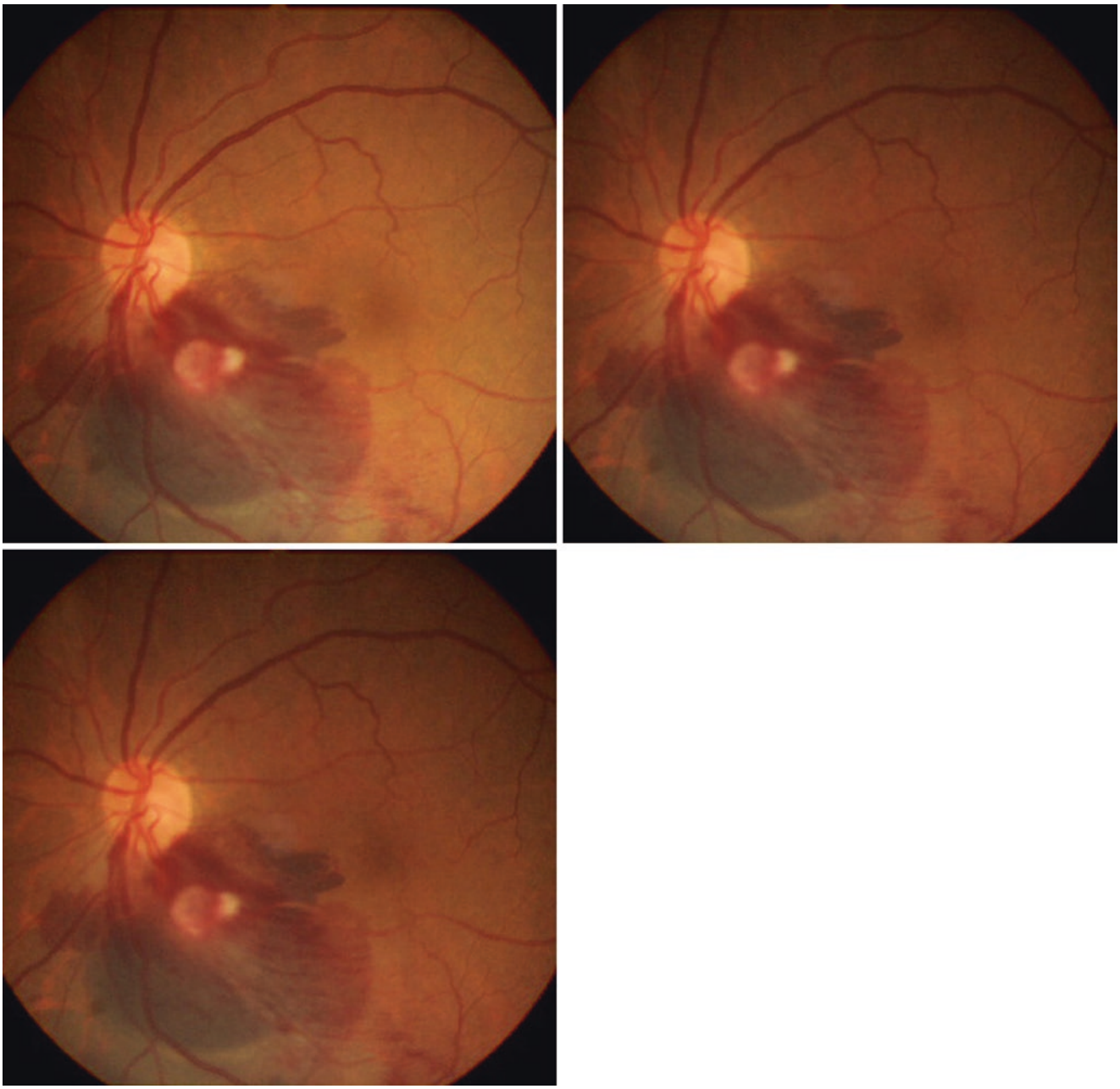

Fig. 2.29 Retinal macroaneurysm near the optic disc
I. Retinal macroaneurysm near the optic disc
II. Superficial retinal hemorrhage
III. Deep retinal hemorrhage
IV. Sub-RPE hemorrhage

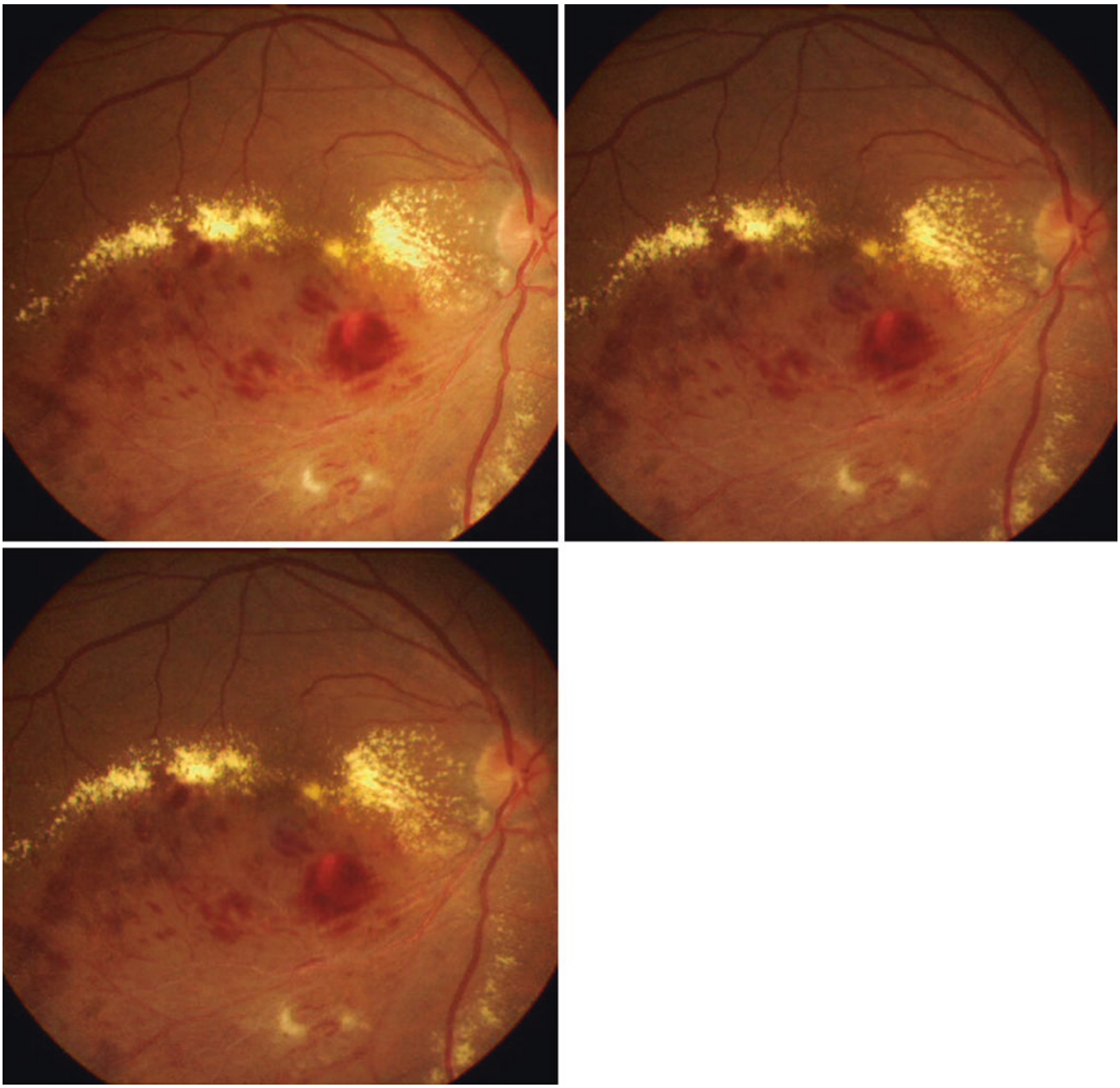

Fig. 2.30 Retinal macroaneurysm
I. Suspected area of the retinal aneurysm
II. Narrowing retinal artery and ghost vessel in the distal part
III. Superficial retinal hemorrhage
IV. Suspected retinal neovascularization
V. Intermediate retinal hard exudates
VI. Dilated retinal vein

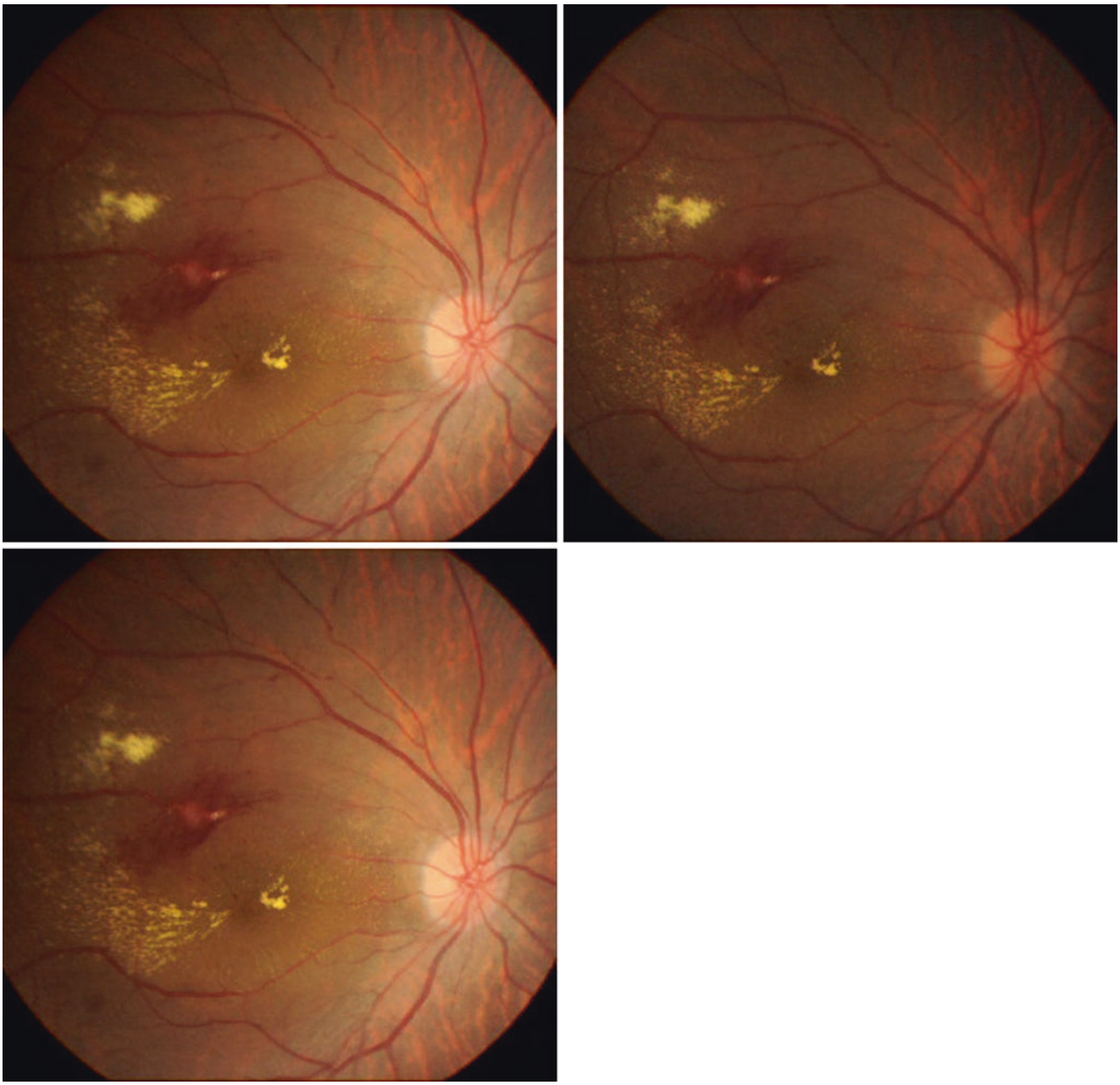

Fig. 2.31 Retinal macroaneurysm
I. Suspected area of the aneurysm
II. Narrowing retinal artery and dilating distal dilating part
III. Macular edema
IV. Intermediate retinal exudates
V. Deep retinal exudates

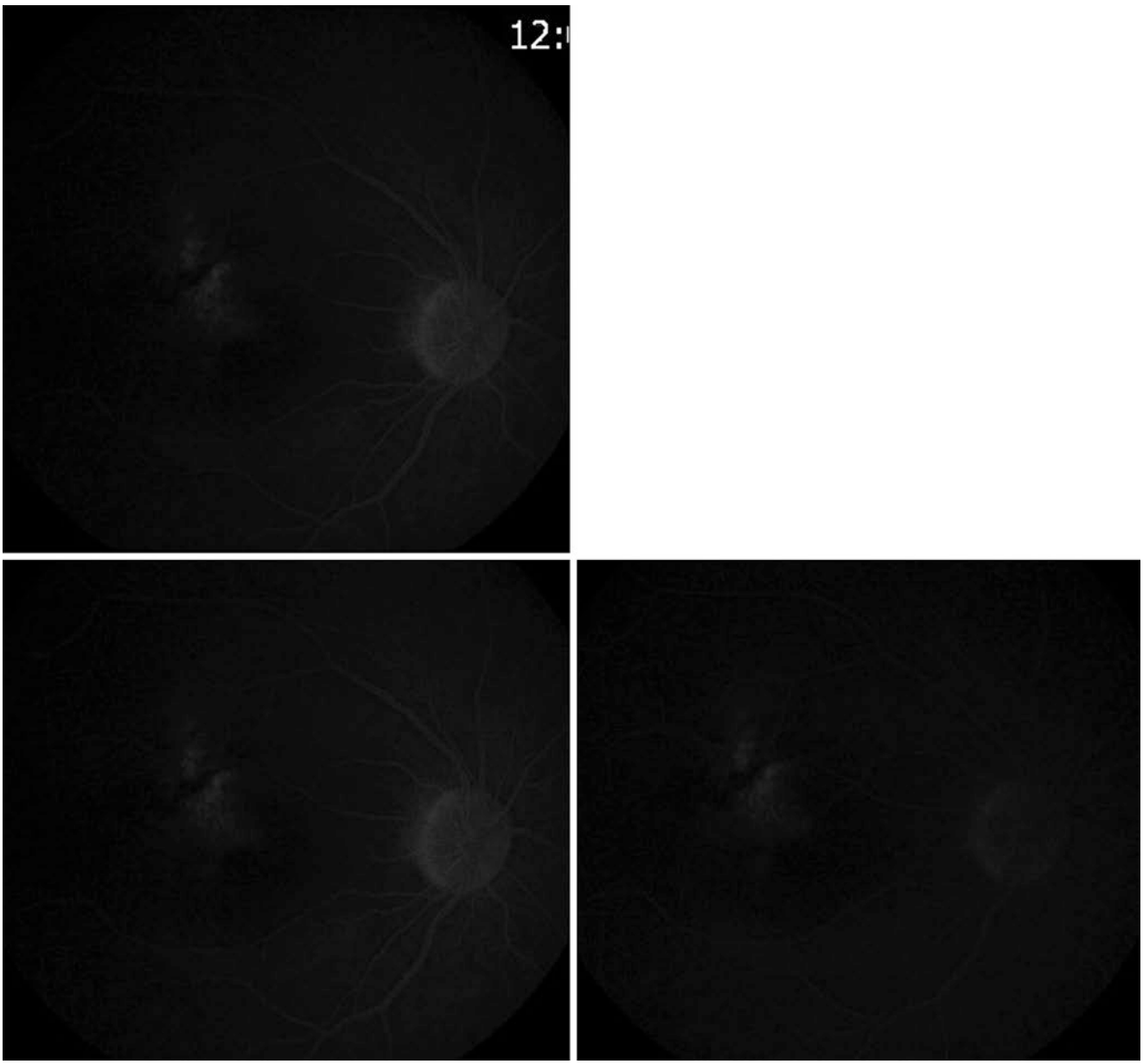

Fig. 2. 31 (continued)

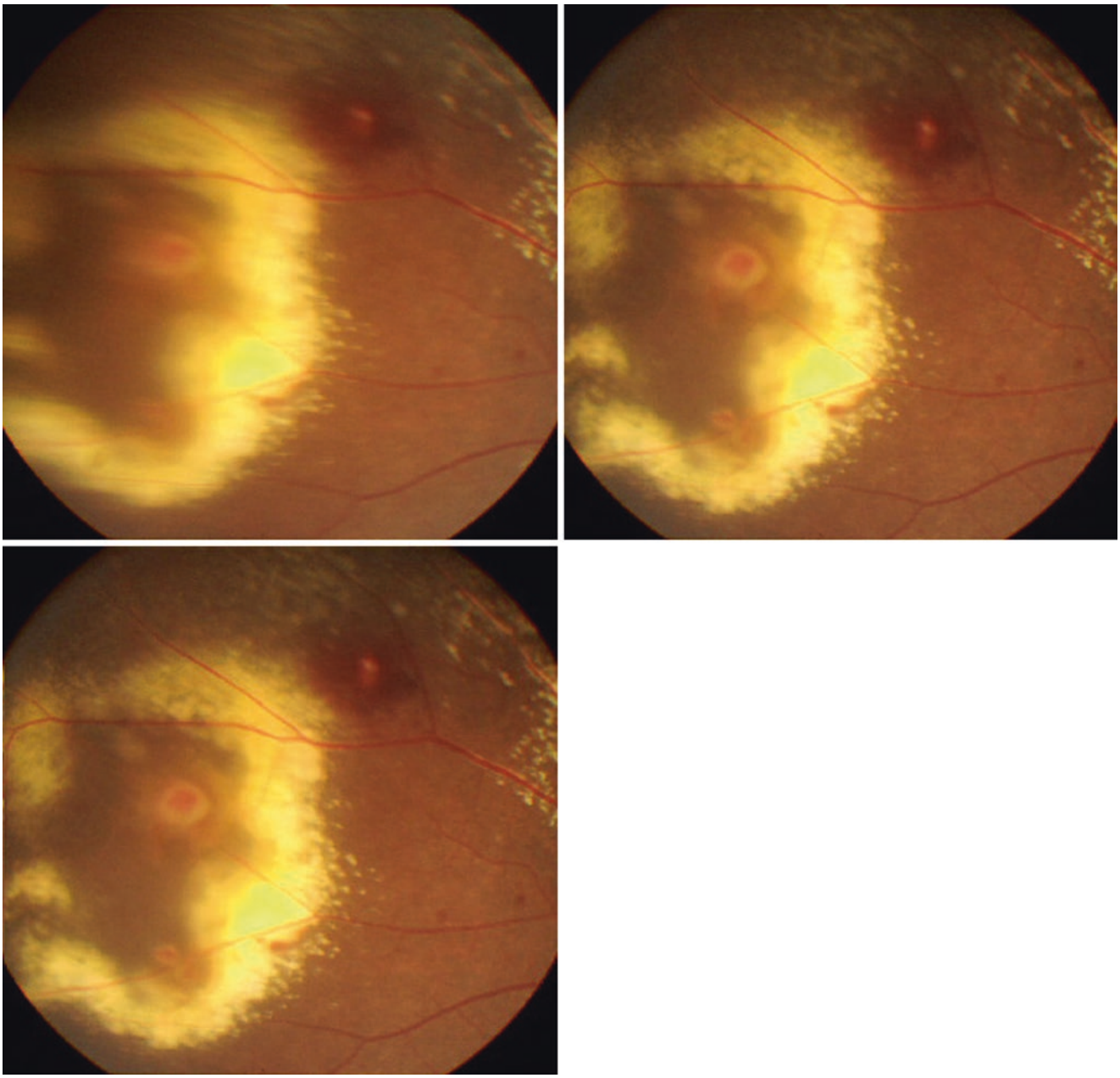

Fig. 2.32 Multiple retinal macroaneurysms
I. Superficial retinal macroaneurysm
II. Deep retinal macroaneurysm
III. Intermediate retinal annular exudates
IV. Retinal artery
V. Retinal vein

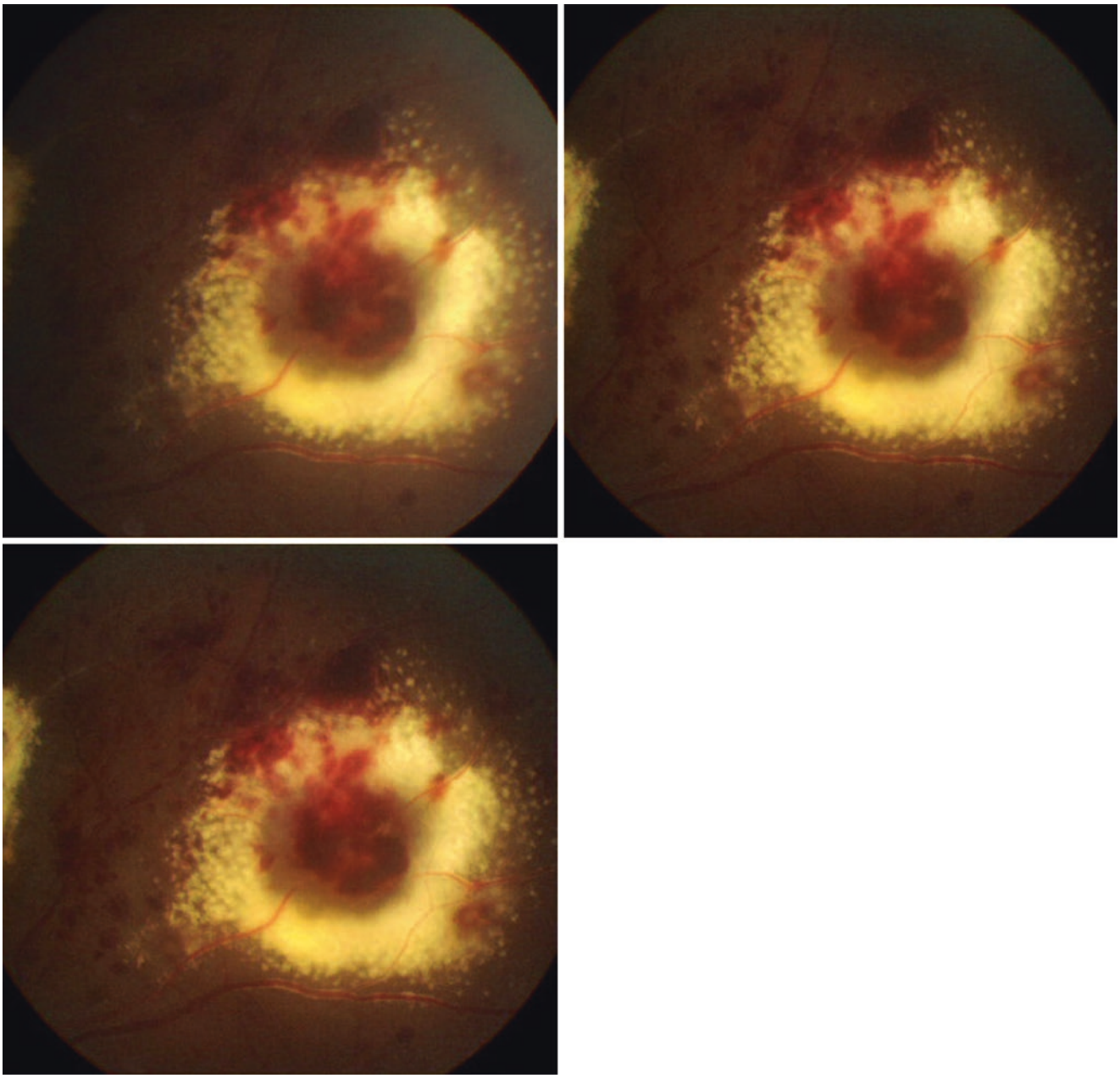

Fig. 2.33 Retinal macroaneurysm
I. Superficial retinal hemorrhage
II. Suspected area of the aneurysm
III. Intermediate retinal annular exudates
IV. retinal artery
V. Dilated retinal vein and white sheath

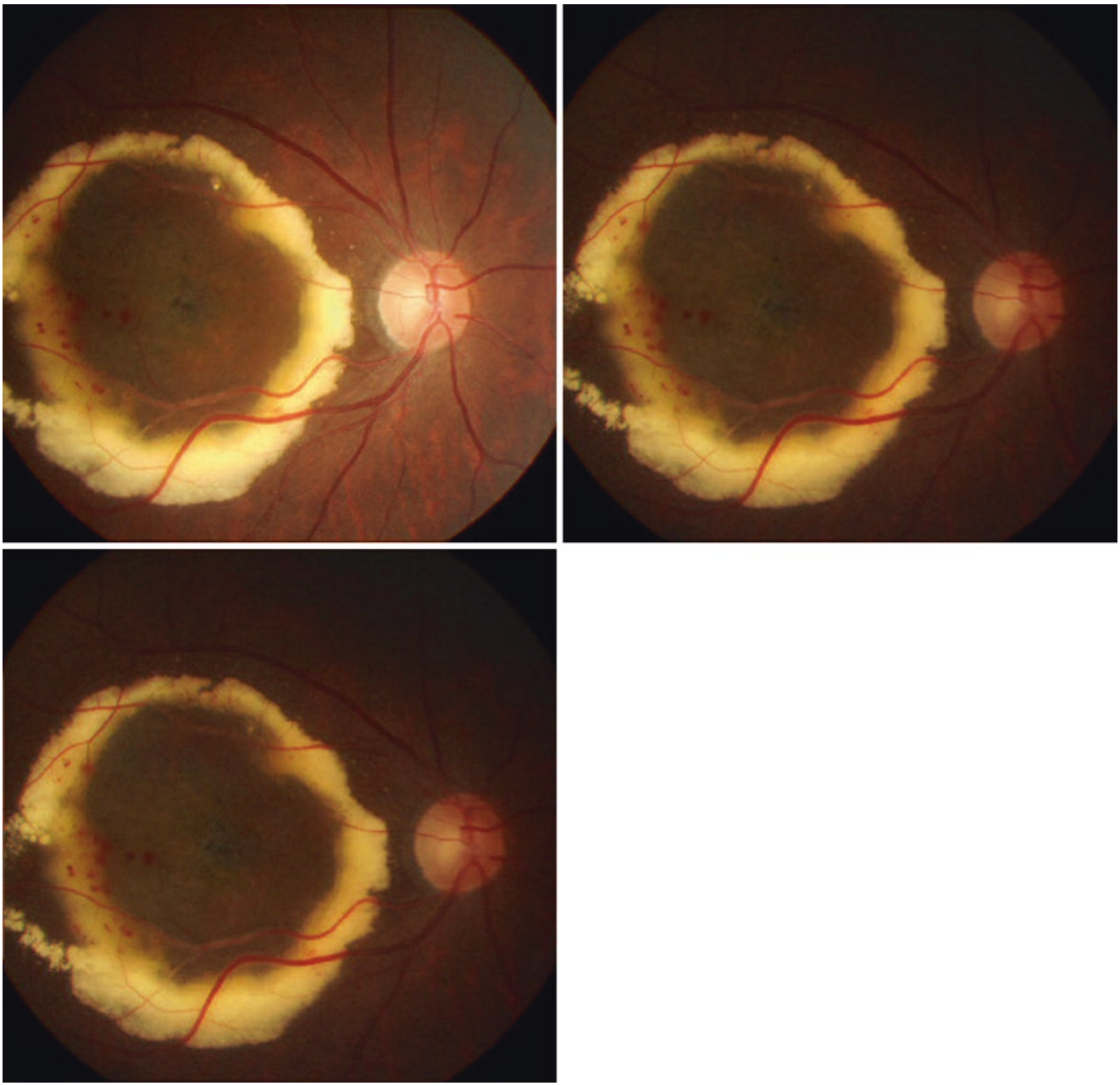

Fig. 2.34 Subretinal annular exudates in the posterior pole
I. Highly elevated sensory retinal detachment in the posterior pole
II. Superficial retinal hemorrhage
III. Subretinal hard exudates
IV. Sclerosis of deep retinal vessels like a cradle
V. Sclerosis of superficial retinal vessels with white sheath

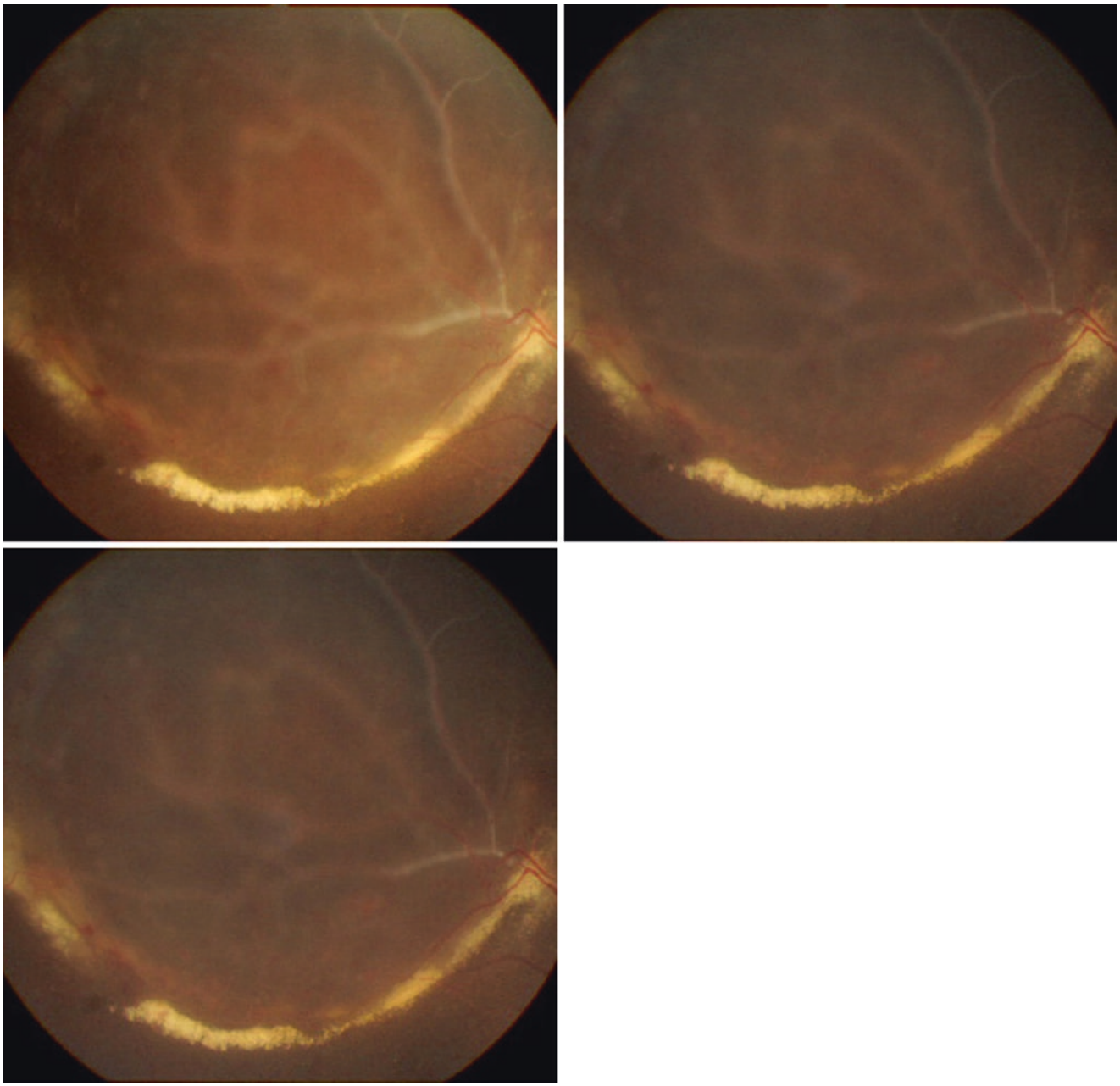

Fig. 2.35 Retinal macroaneurysm
I. The elevated retina elevated like a dome
II. The area with abnormal retinal artery, suspected retinal macroaneurysm
III. Ghost vessel of the retinal vein in the detached retina
IV. Deep retinal exudates

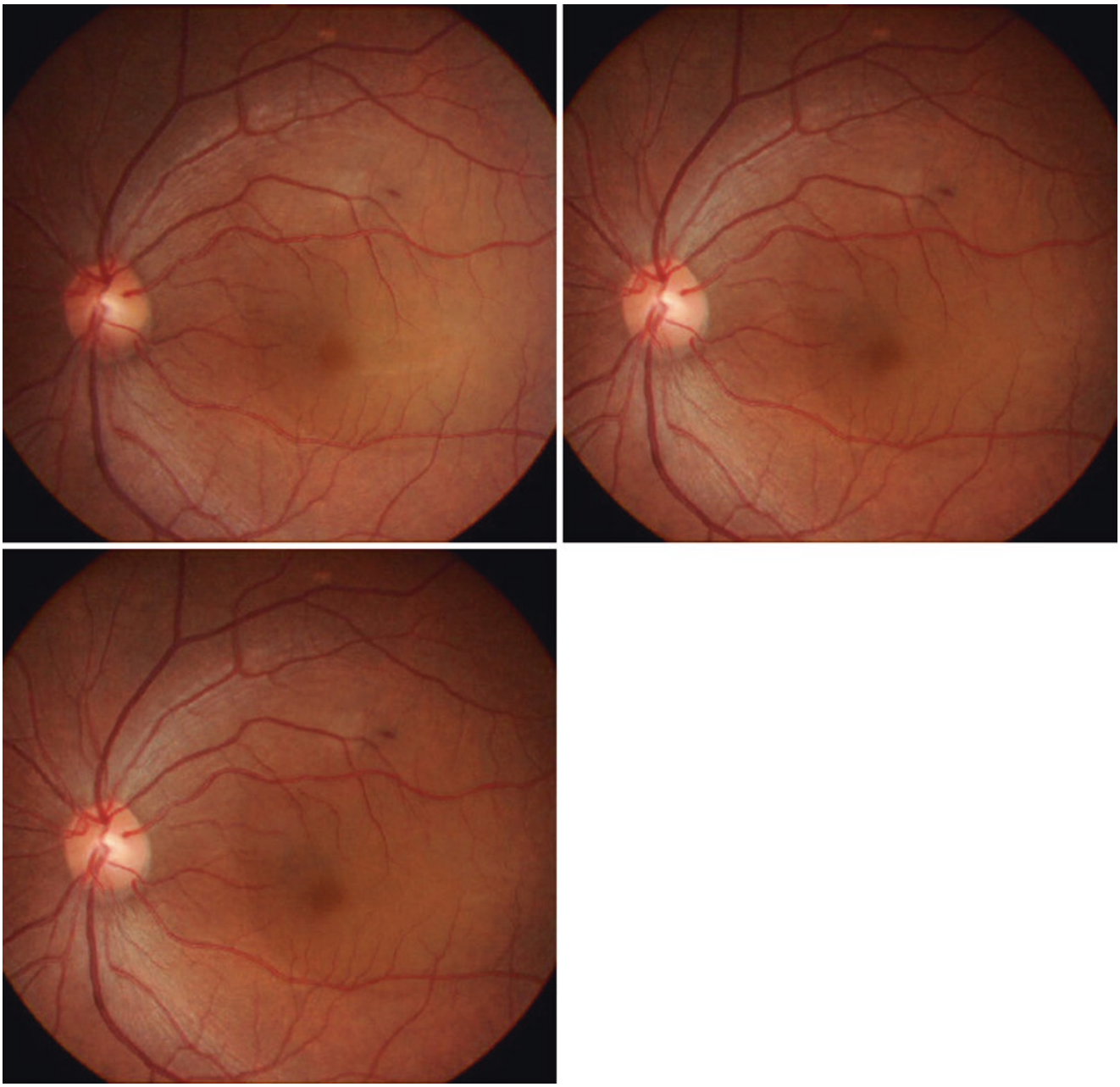

Fig. 2.36 Retinal macroaneurysm
I. The depressed area of retinal macroaneurysm after laser treatment
II. Sensory retinal detachment of macula
III. Apex of elevated retina

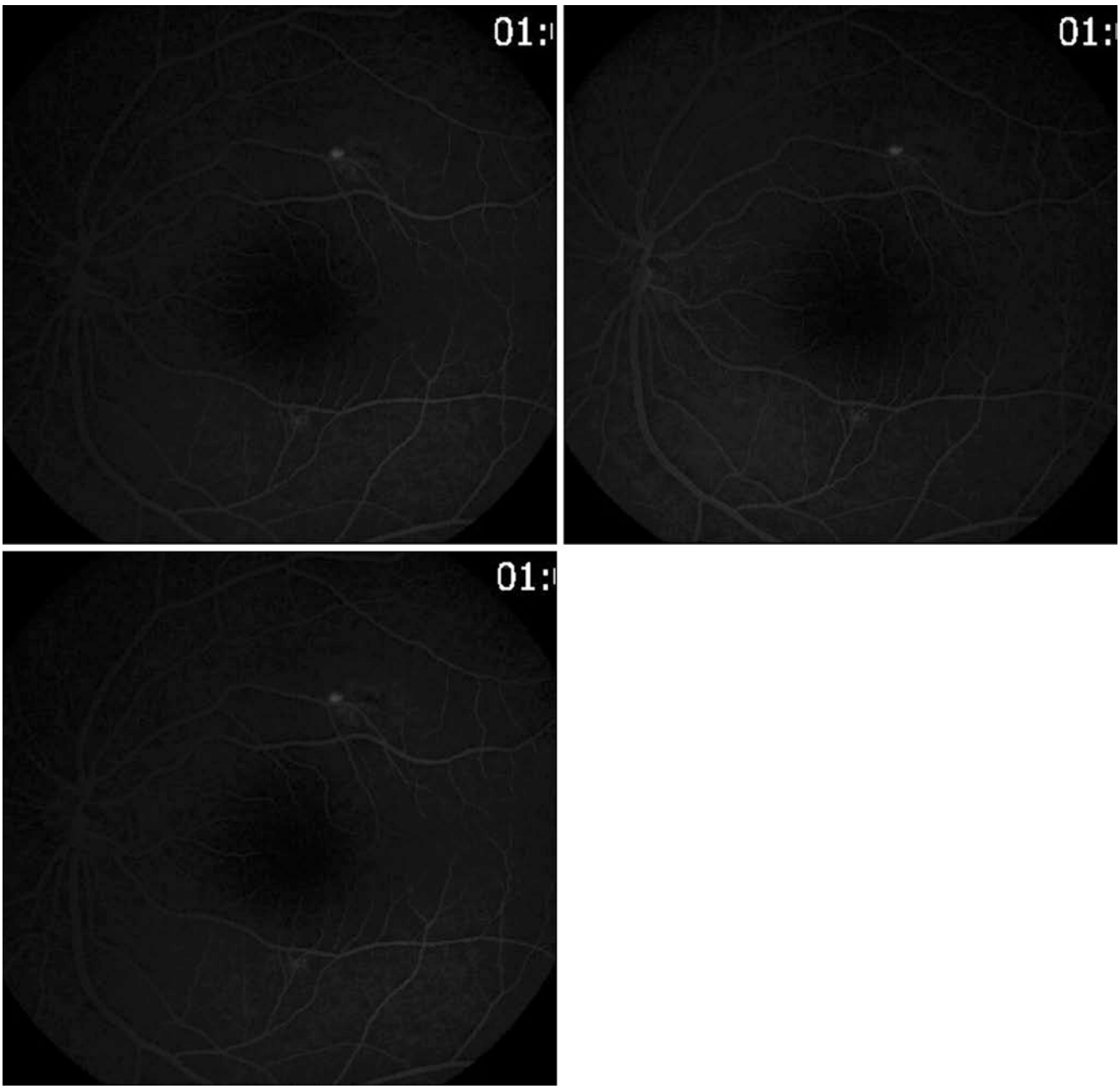

Fig. 2. 36 (continued)

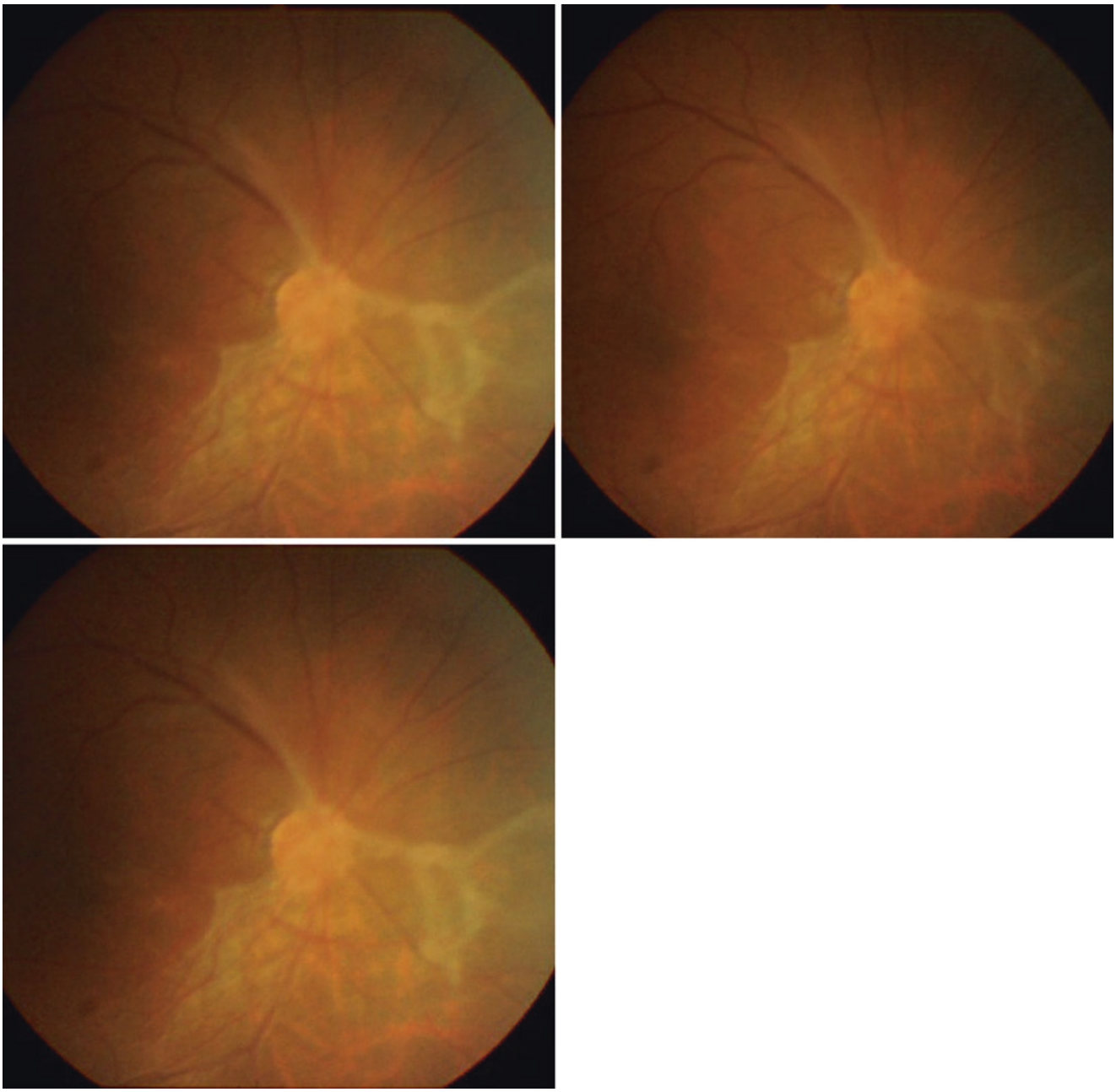

Fig. 2.37 Epiretinal membrane
I. Fibrotic membrane originated from the optic disc
II. Superior temporal membrane
III. Inferior nasal membrane
IV. Inferior temporal membrane and tractional retinal detachment
V. Fresh vitreous hemorrhage like an arc

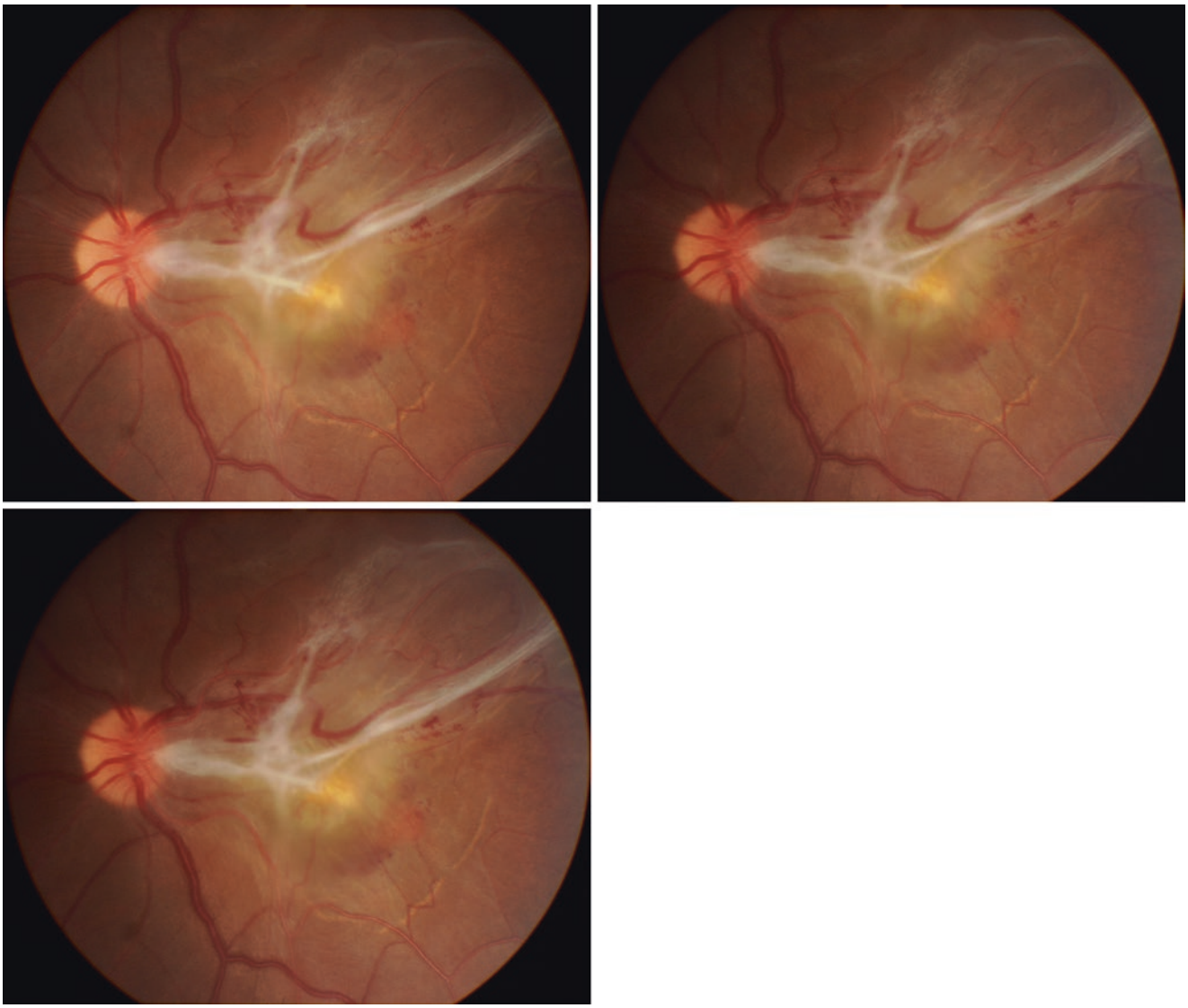

Fig. 2.38 Epiretinal membrane in the posterior pole
I. White fibrotic membrane originated from the optic disc
II. Tractional macular dislocation
III. Oxygonal shape of Superior temporal branch of the retinal vein in the elevated retina showed and tractional retinal detachment
IV. Subretinal membrane

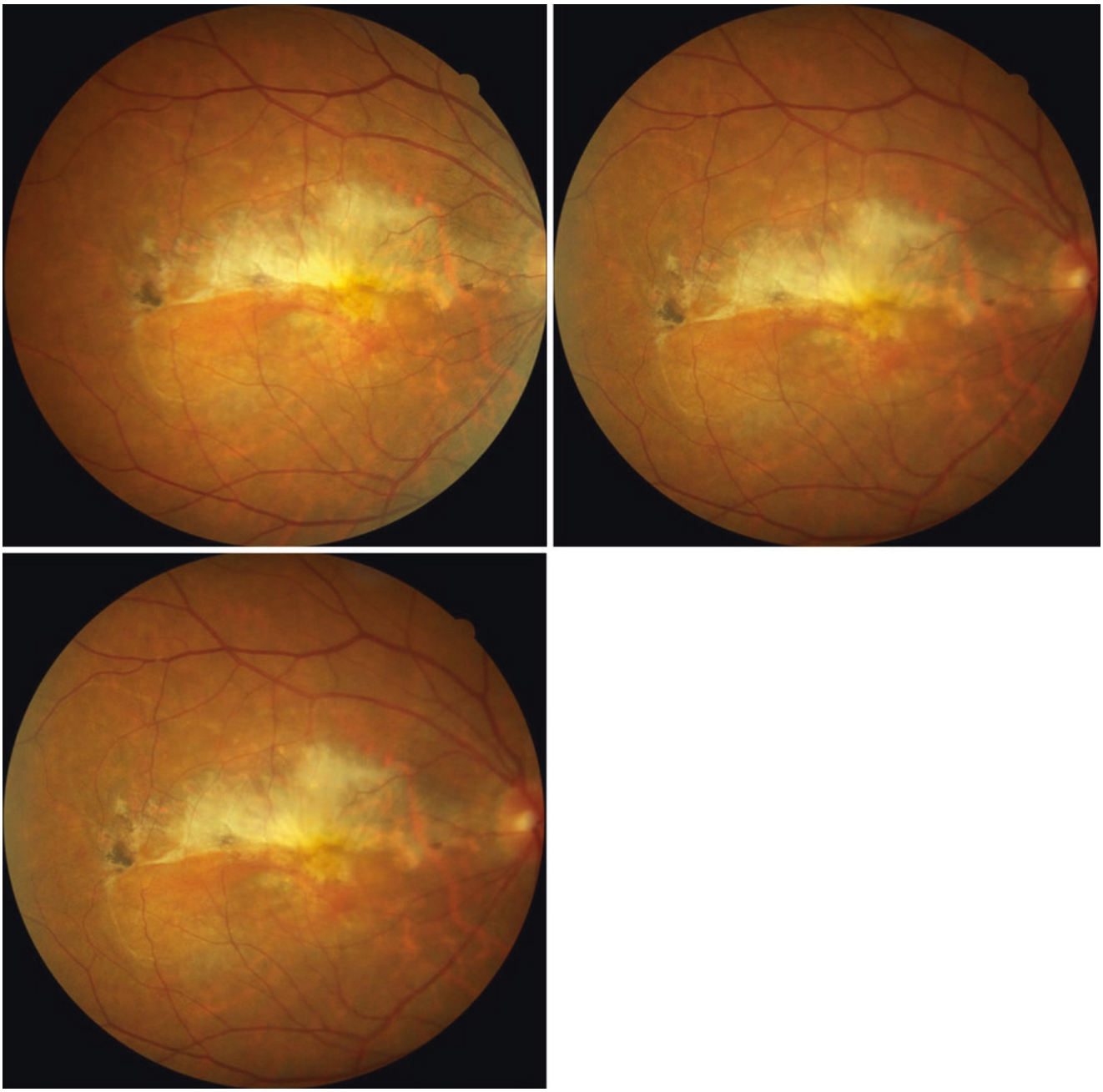

Fig. 2.39 Subretinal membrane
I. Shallow retinal detachment in the macula area
II. Subretinal membrane
III. Pigmentation

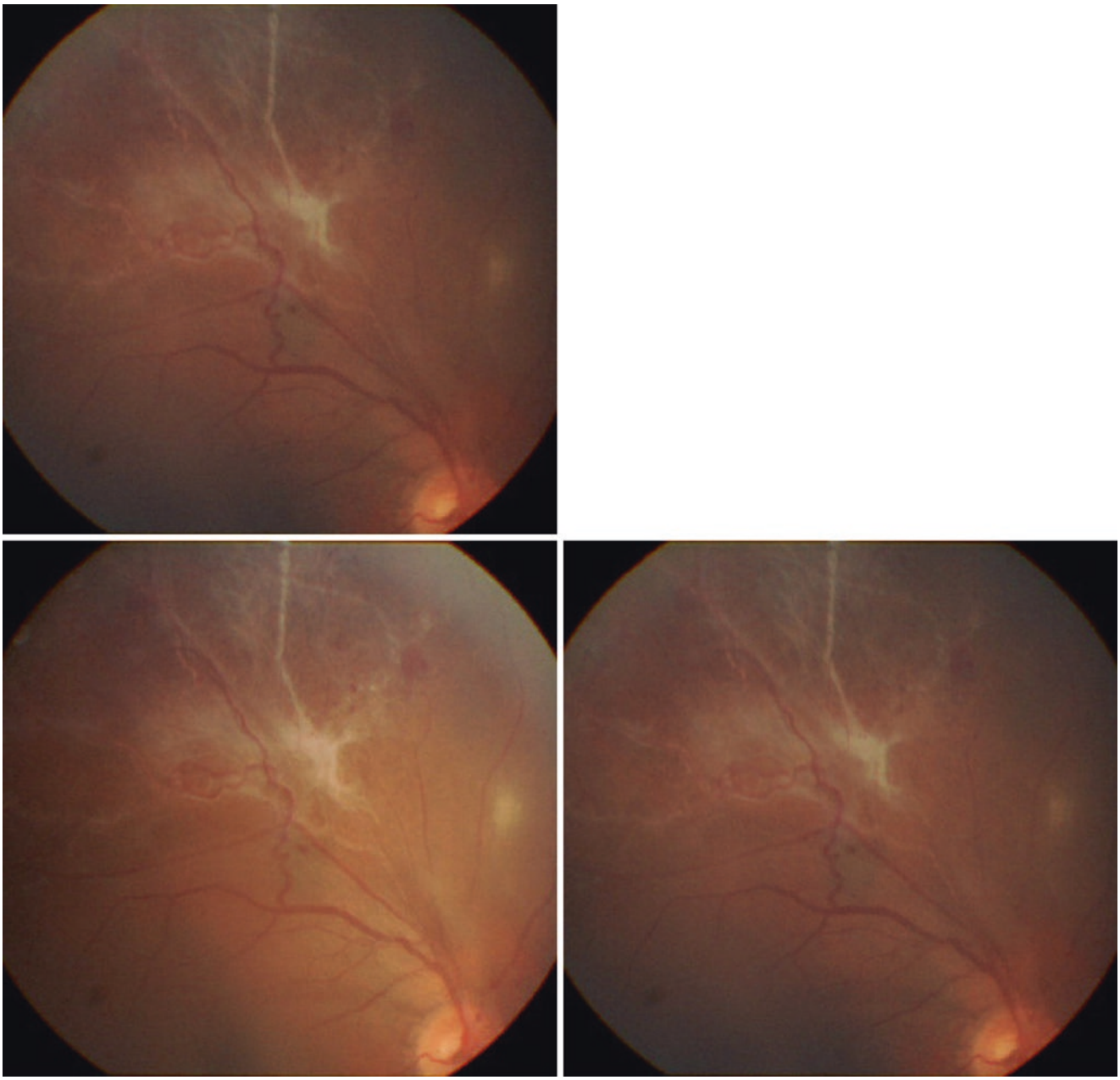

Fig. 2.40 Subretinal fibrous membrane
I. Subretinal fibrous streak superior to the optic disc
II. Ghost vessel in the retinal vein
III. Ghost vessel in the retinal artery
IV. Neovascularization bud near the retinal vein
V. The retinal vein was distorted like a loop

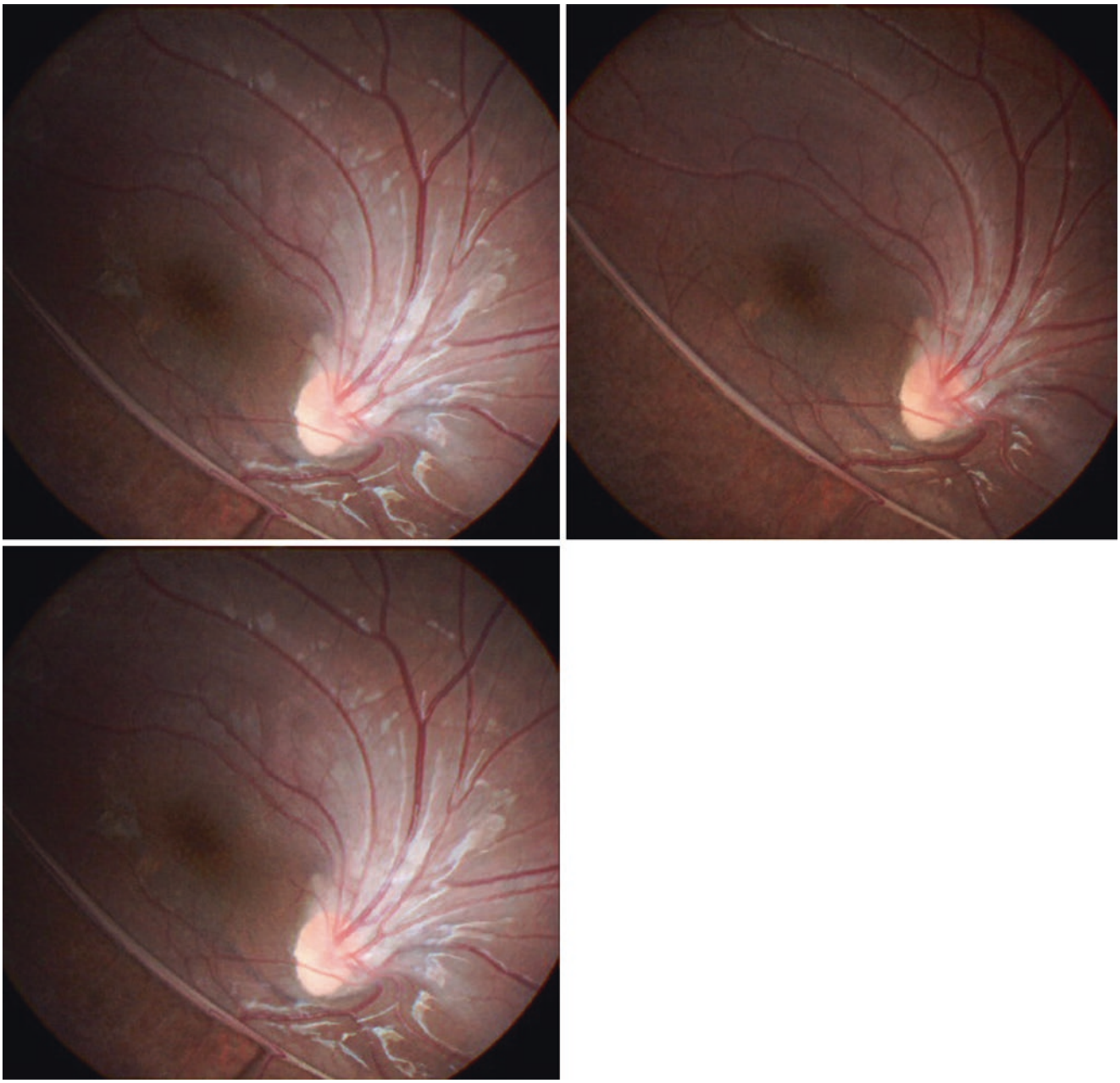

Fig. 2.41 Curly retinal edge
I. The inferior temporal edge of the retina was curly into the vitreous cavity
II. The impending retinal vein and its shadow
III. Exposed choroid

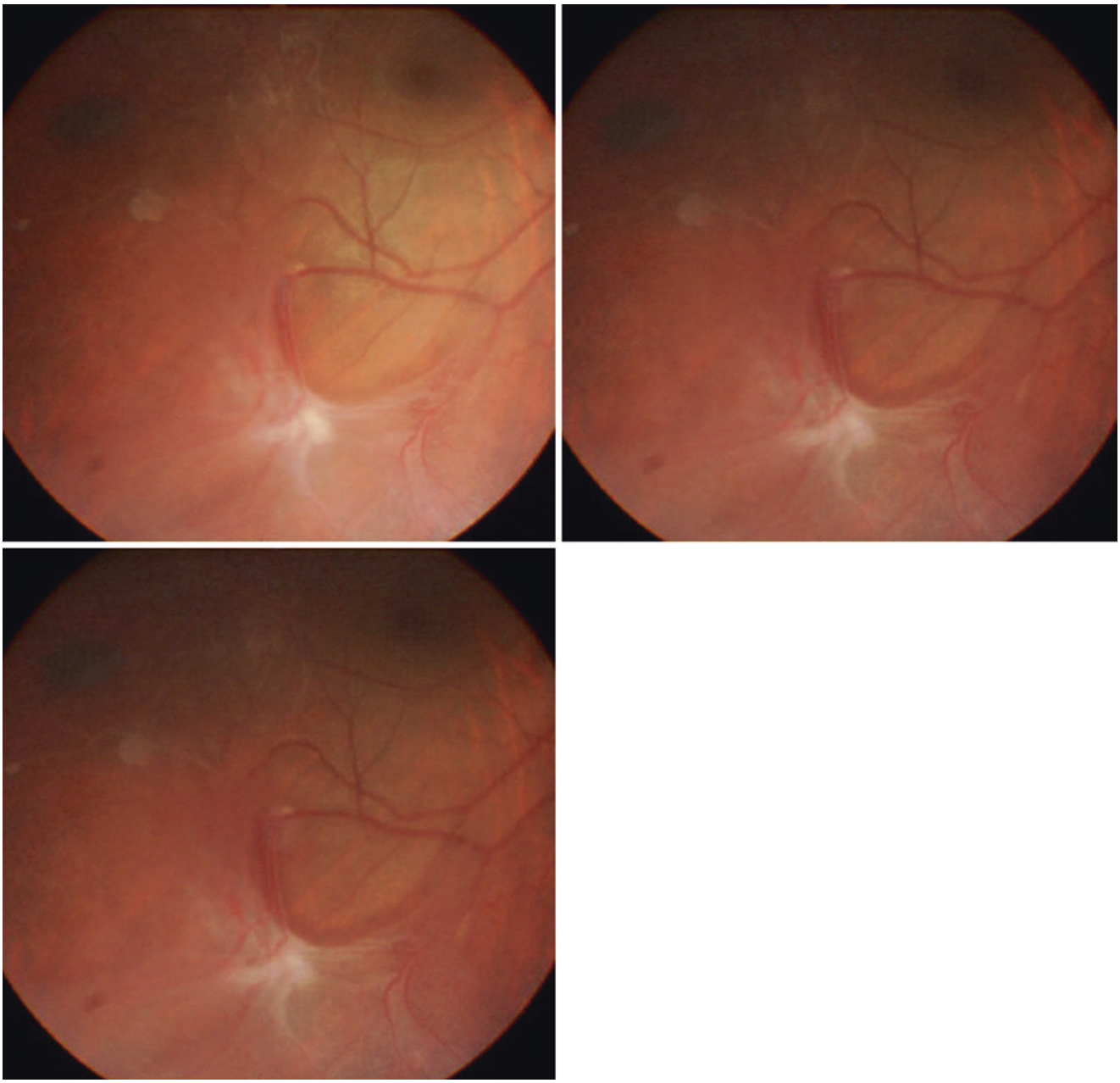

Fig. 2.42 Tractional retinal detachment
I. The retinal neovascularization extended into the vitreous cavity
II. Vitreous fibrous membrane
III. Retinal detachment in the peripheral retina
IV. Ghost vessel of the retinal vein
V. Retinal arterial sclerosis with white sheath

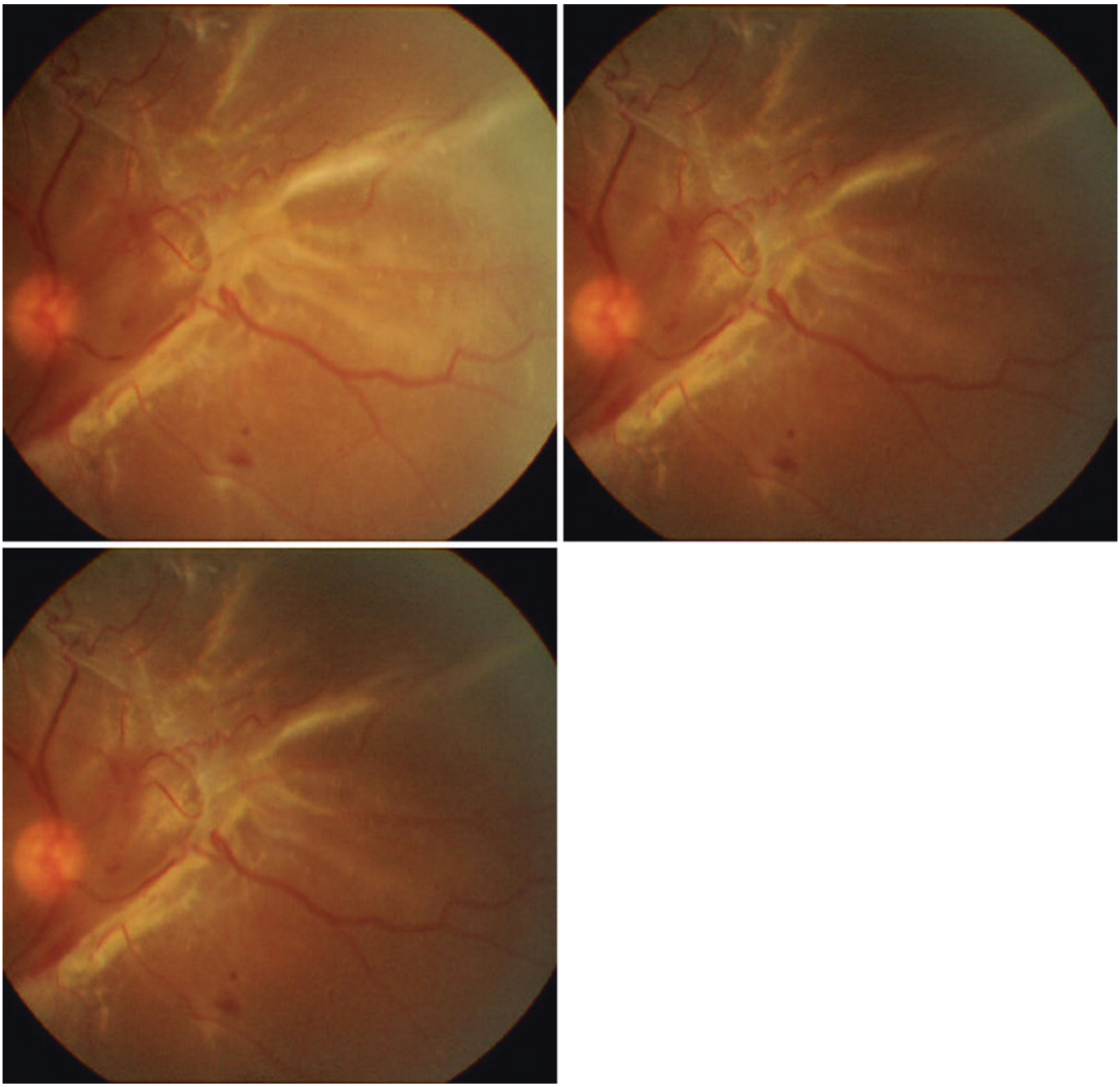

Fig. 2.43 Tractional retinal detachment
I. Vitreous hemorrhage
II. Vitreous proliferative membrane
III. Subretinal proliferative streak
IV. Estimated area of proliferative membrane

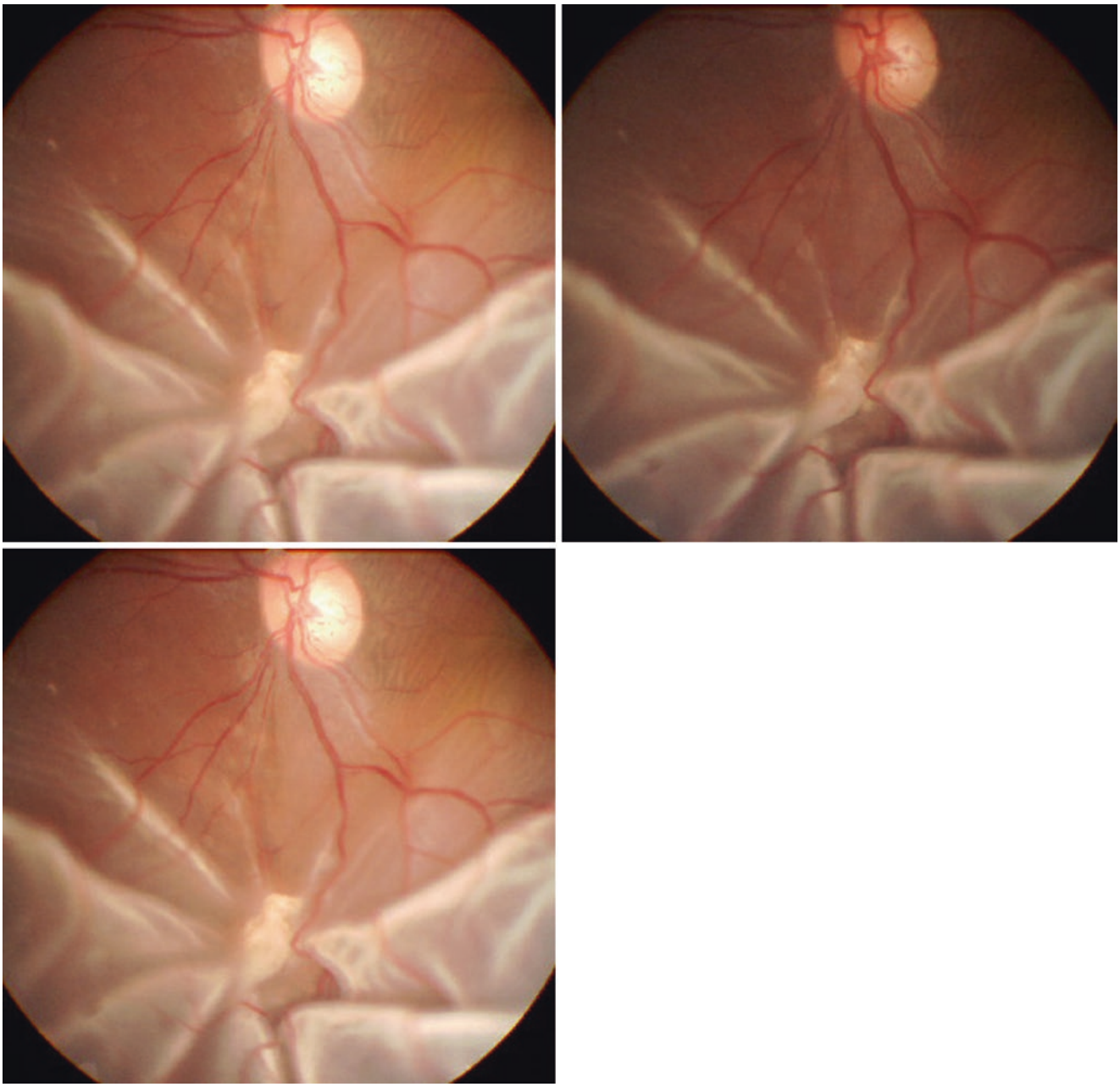

Fig. 2.44 Stellate retinal fold and retinal detachment
I. Stellate retinal fold in the lowest part of retinal adhesive area
II. Retinal detachment
III. Tractional retinal dislocation
IV. Subretinal membrane

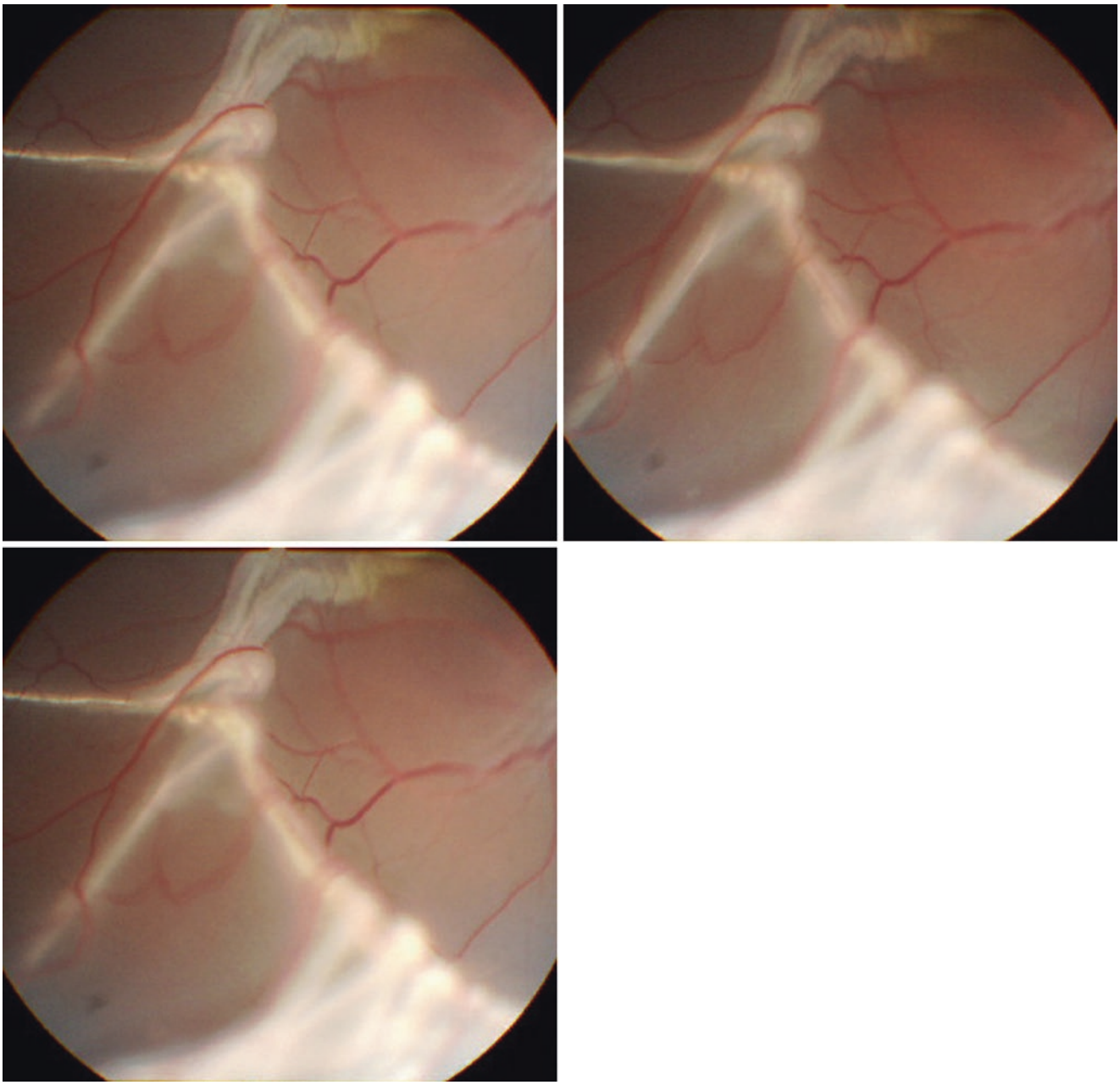

Fig. 2.45 Tractional retinal detachment
I. Subretinal streak like a clothesline pole
II. Retinal detachment

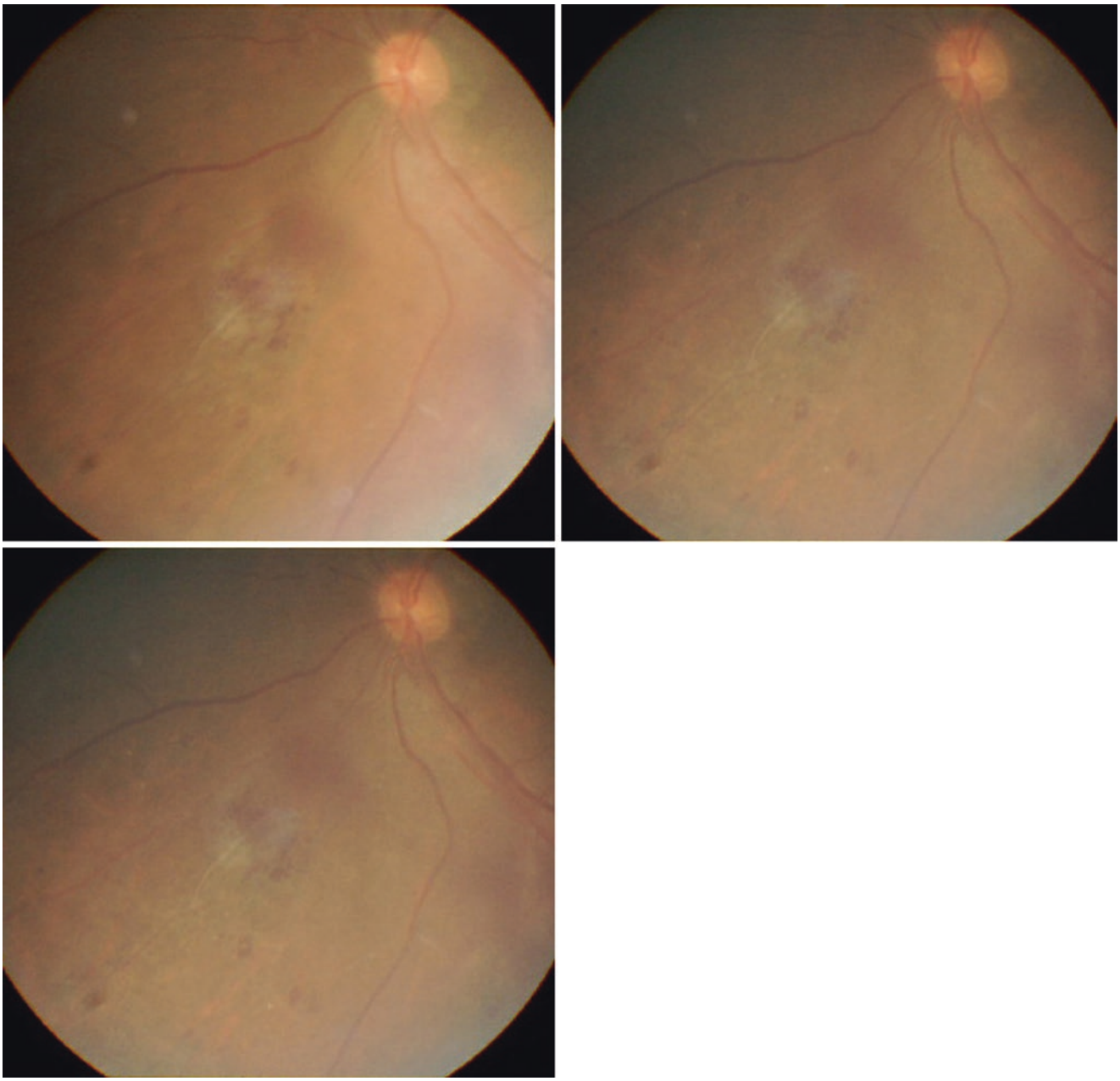

Fig. 2.46 Retinal detachment
I. Discontinuous blood flow in inferior nasal branch of retinal artery and ghost vessel in the distal part
II. Subretinal exudates and hemorrhage
III. Exudative retinal detachment

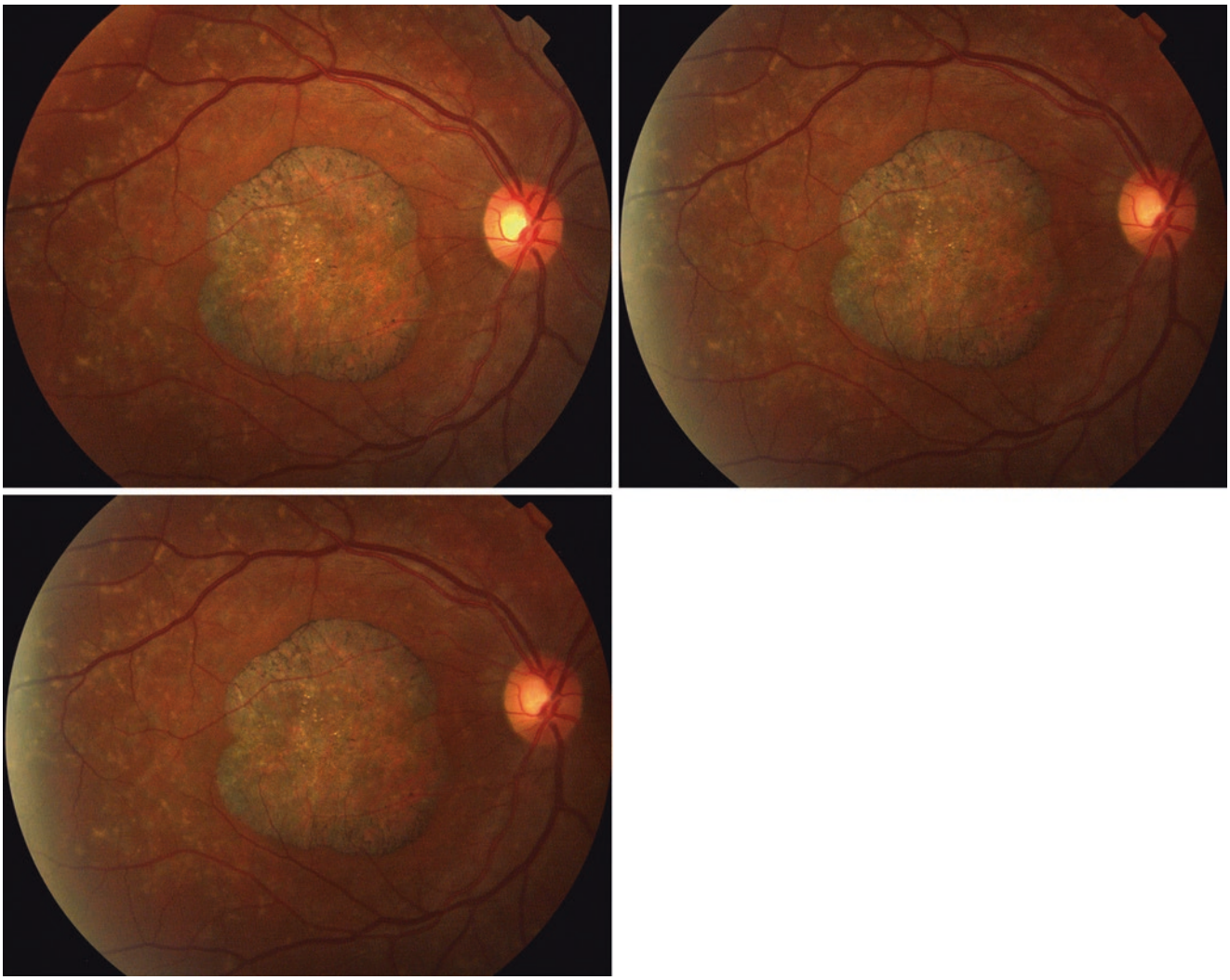

Fig. 2.47 Stargardt disease
I. Boundary of the lesion, irregular with pigmentation
II. Retinal and choroidal atrophy in the lesion like a basin
III. Retinal vessels that passed through the lesion went attenuated

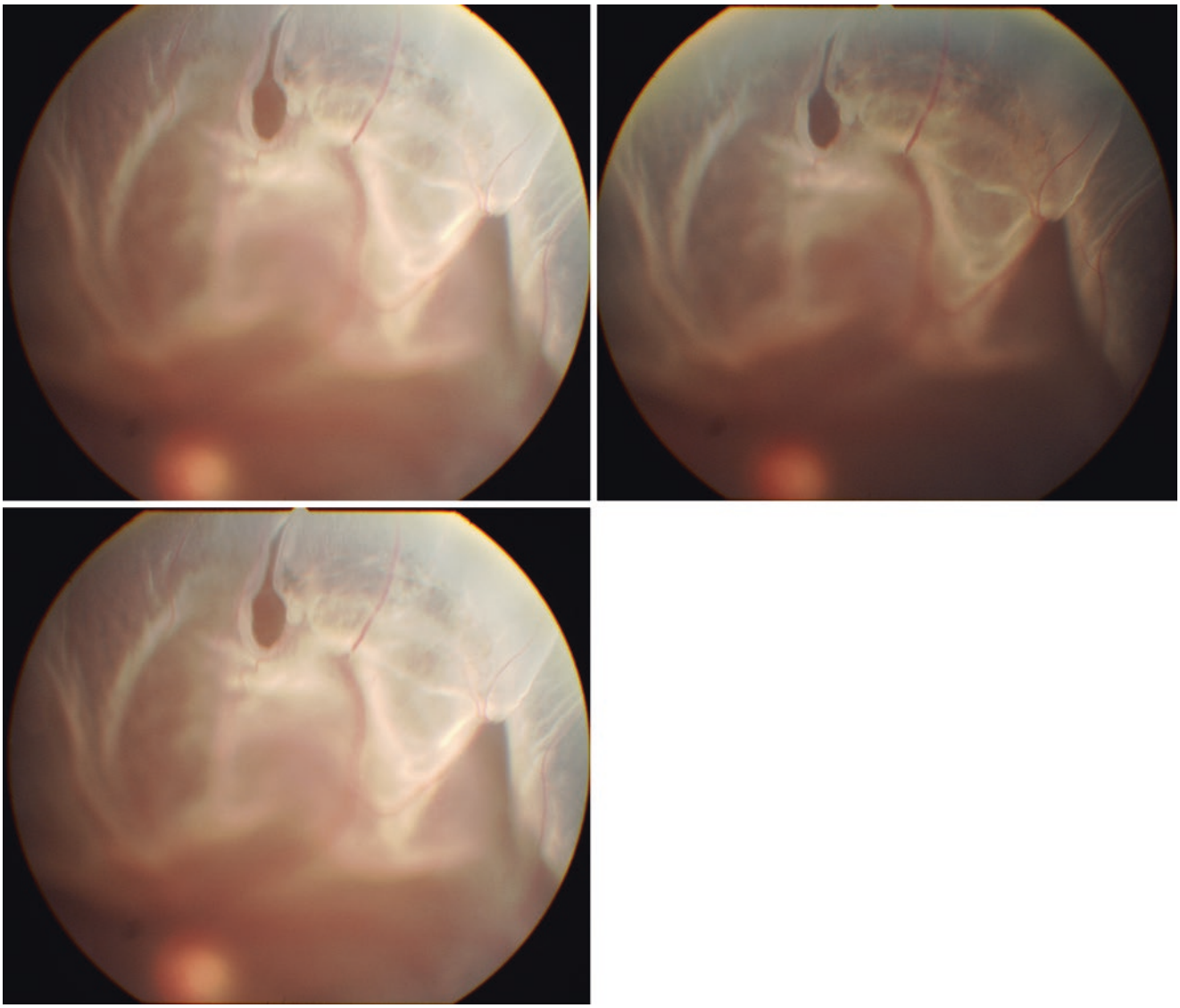

Fig. 2.48 Rhegmatogenous retinal detachment
I. Horse-shoe tear
II. Anterior flap with curly edge
III. Extensive retinal detachment and the lowest area of retinal detachment
IV. Apex of retinal detachment

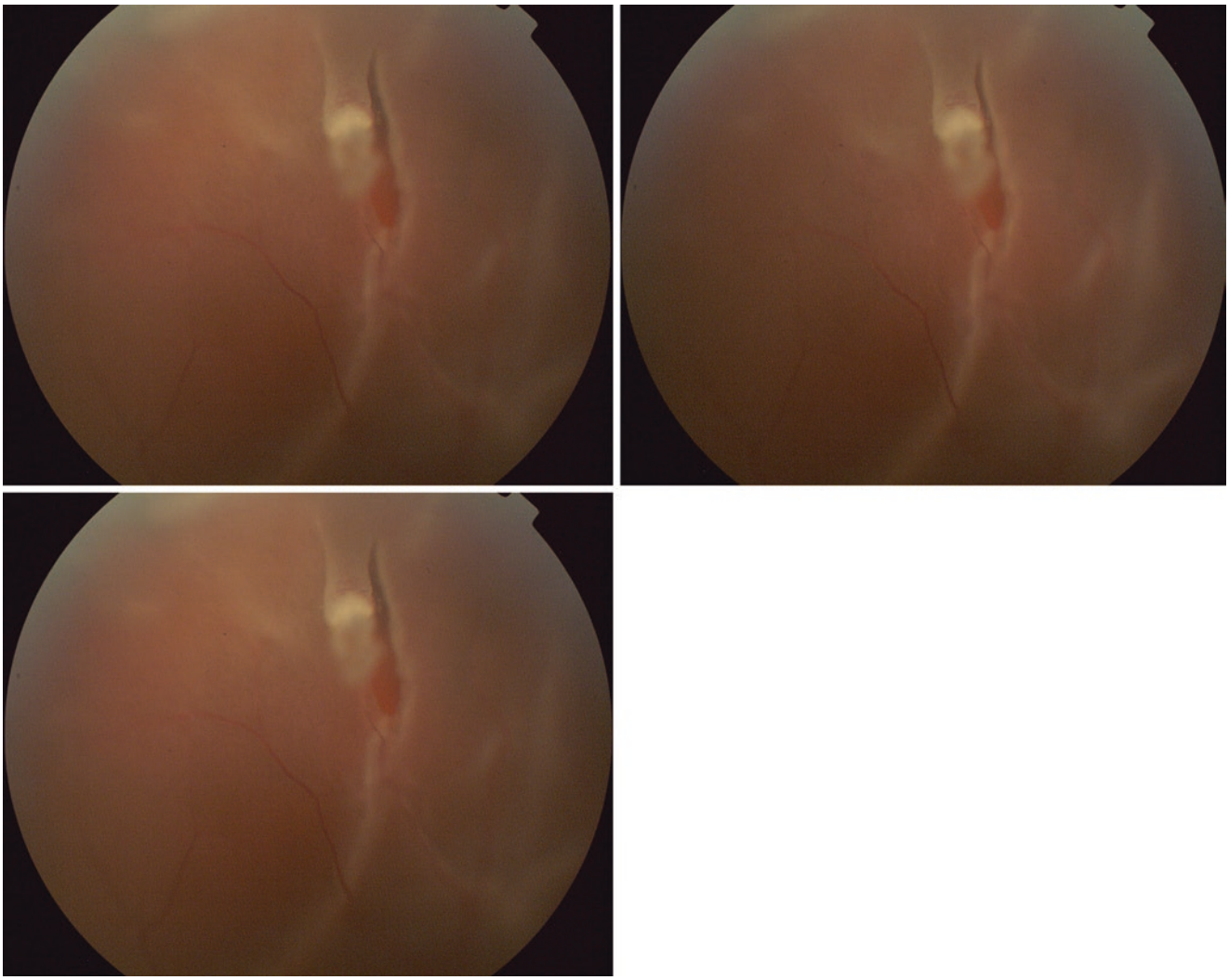

Fig. 2.49 Rhegmatogenous retinal detachment
I. U-tear and the floating flap
II. Strong adhesion with the vitreous
III. Base of the flap
IV. RPE exposed
V. Apex of the detached retina

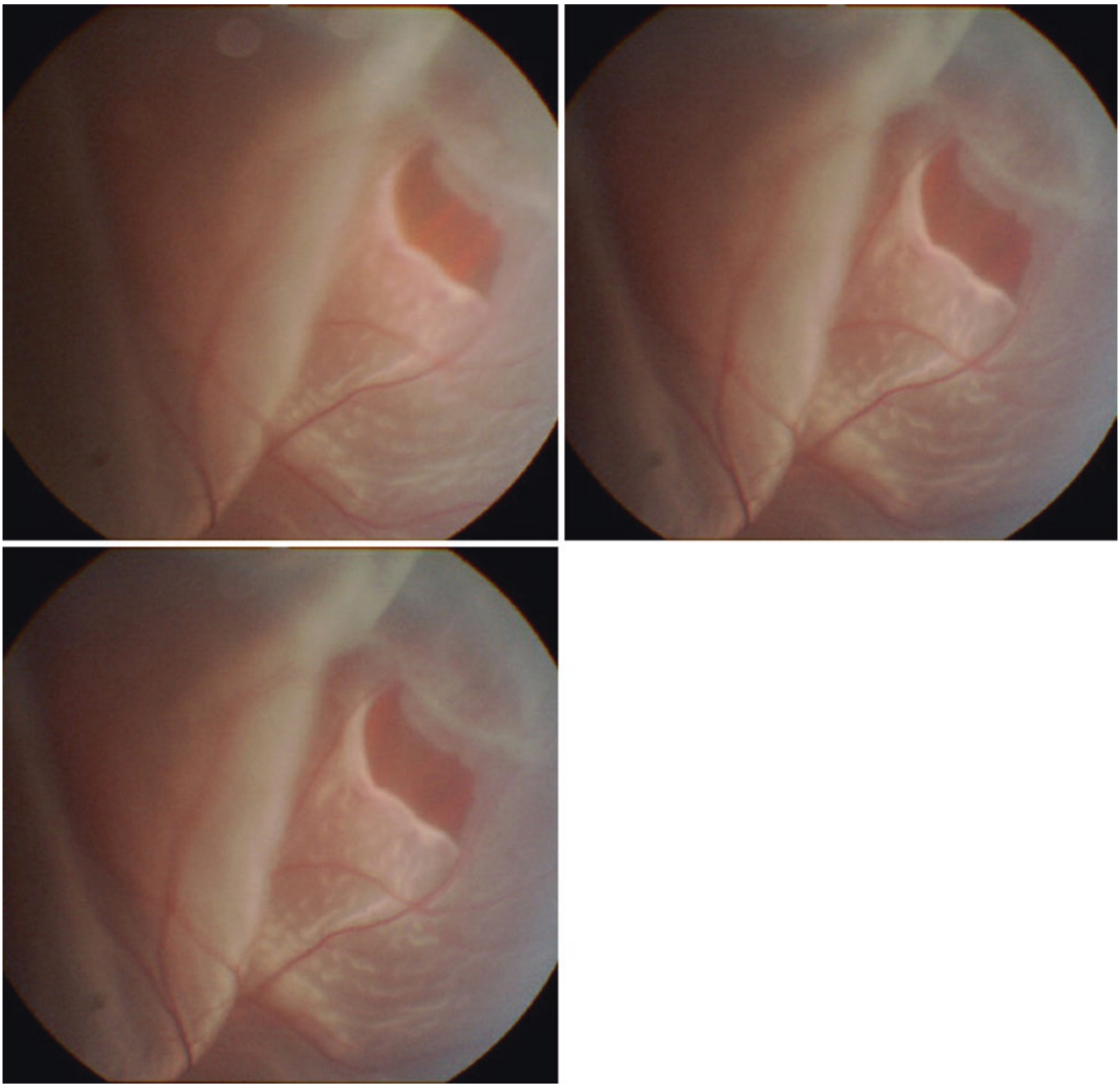

Fig. 2.50 Rhegmatogenous retinal detachment
I. Anterior flap of the retinal tear
II. Retinal tear with exposed underlying choroid
III. Posterior flap of retinal tear
IV. Retinal fold

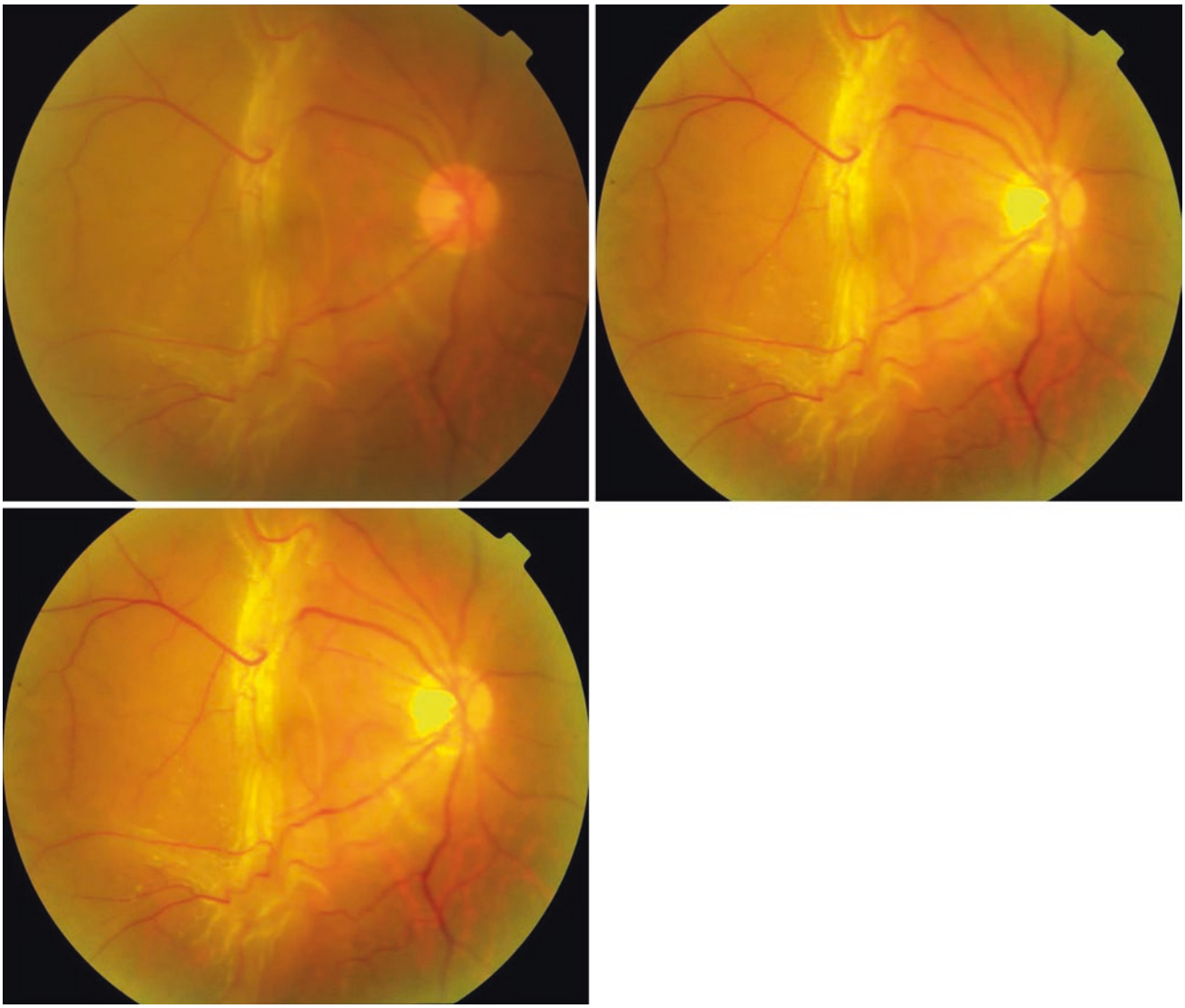

Fig. 2.51 Tractional retinal detachment
I. Embedded and tortuous retina vein
II. Epiretinal membrane
III. Macular detachment duo to fibrous tissue

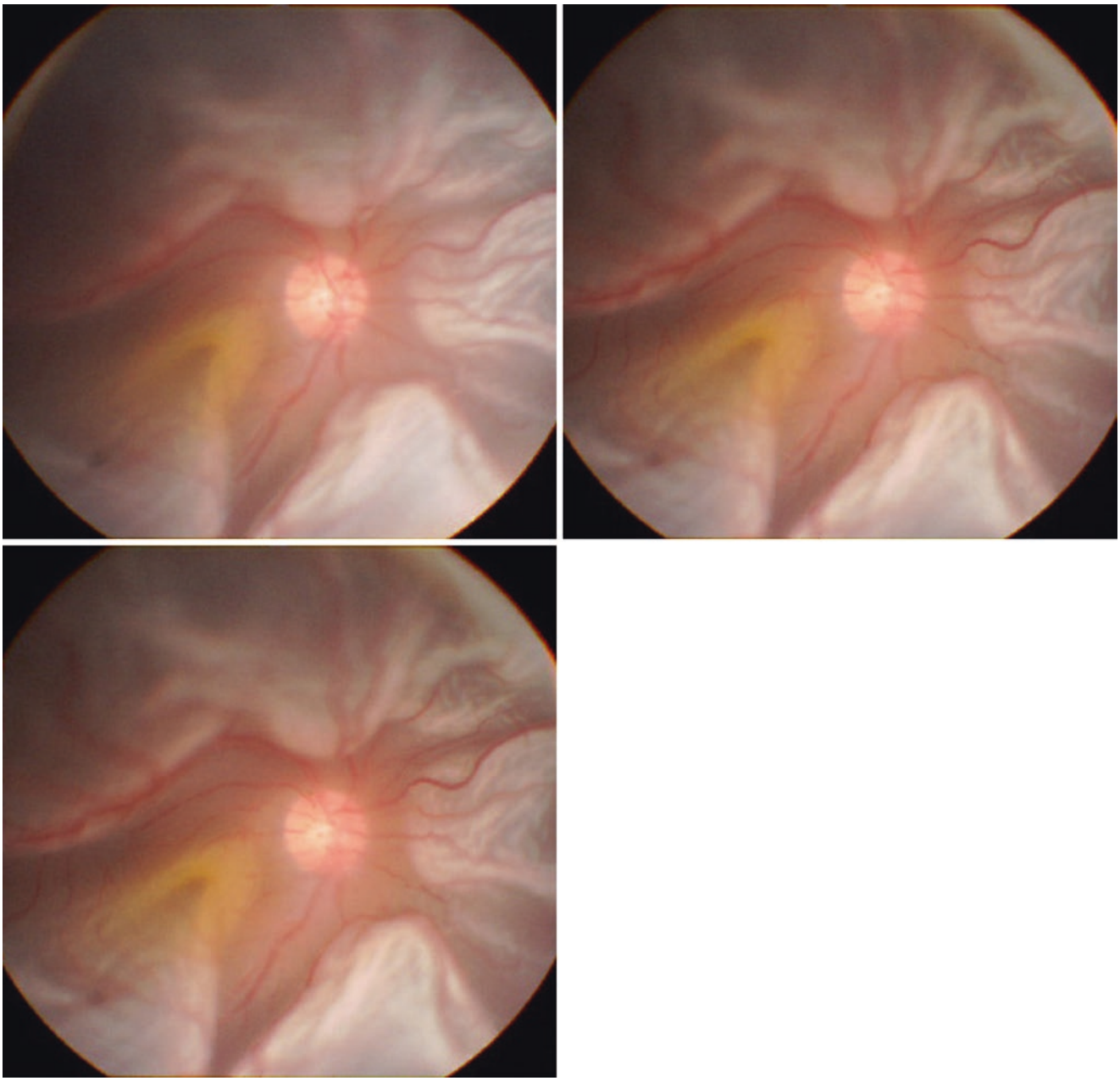

Fig. 2.52 Funnel retinal detachment
I. Optic disc
II. Detached macula
III. Detached retina

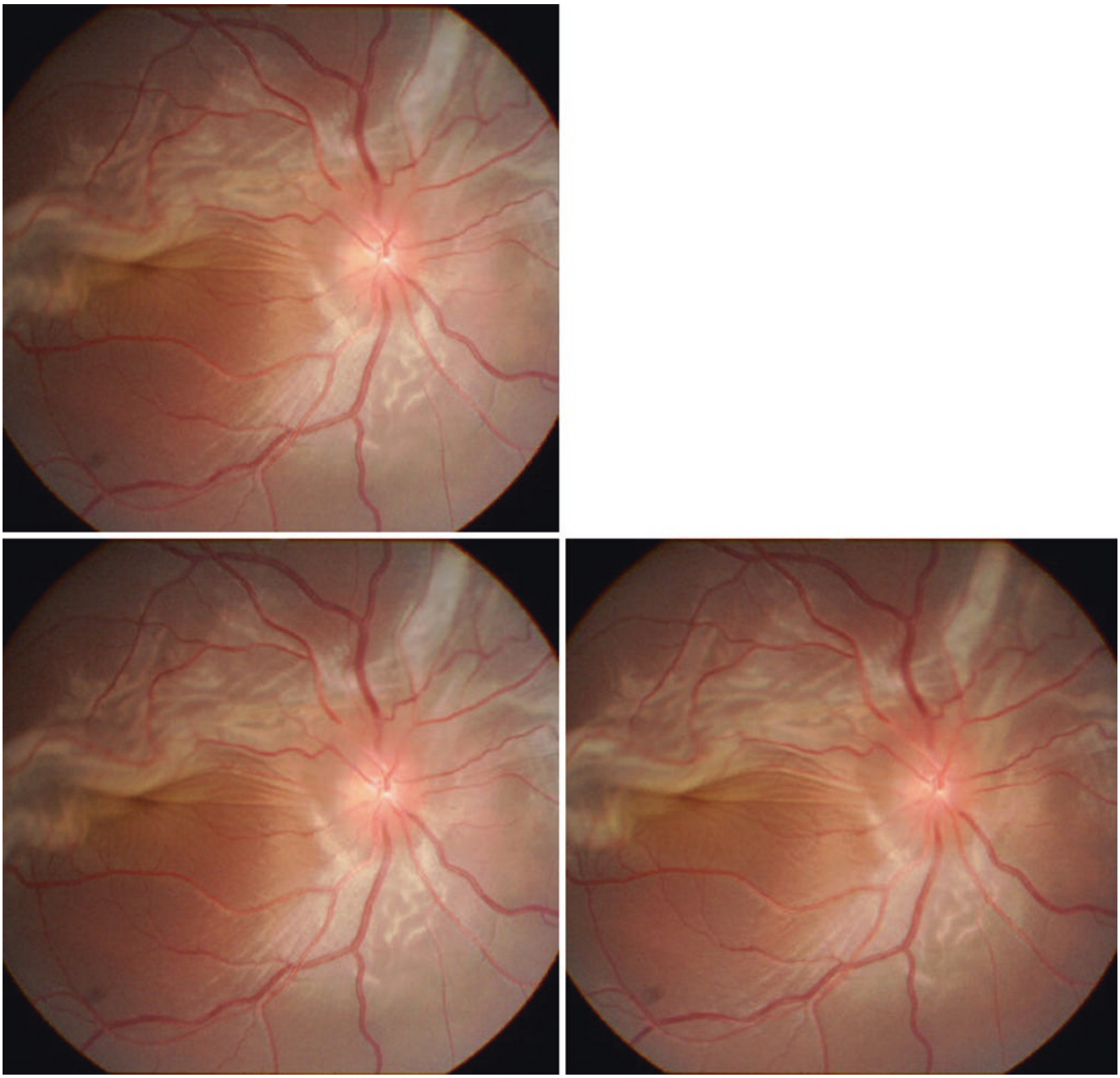

Fig. 2.53 Funnel retinal detachment
I. Extensive subretinal membrane
II. Detached retina in the macula and dislocation of macula

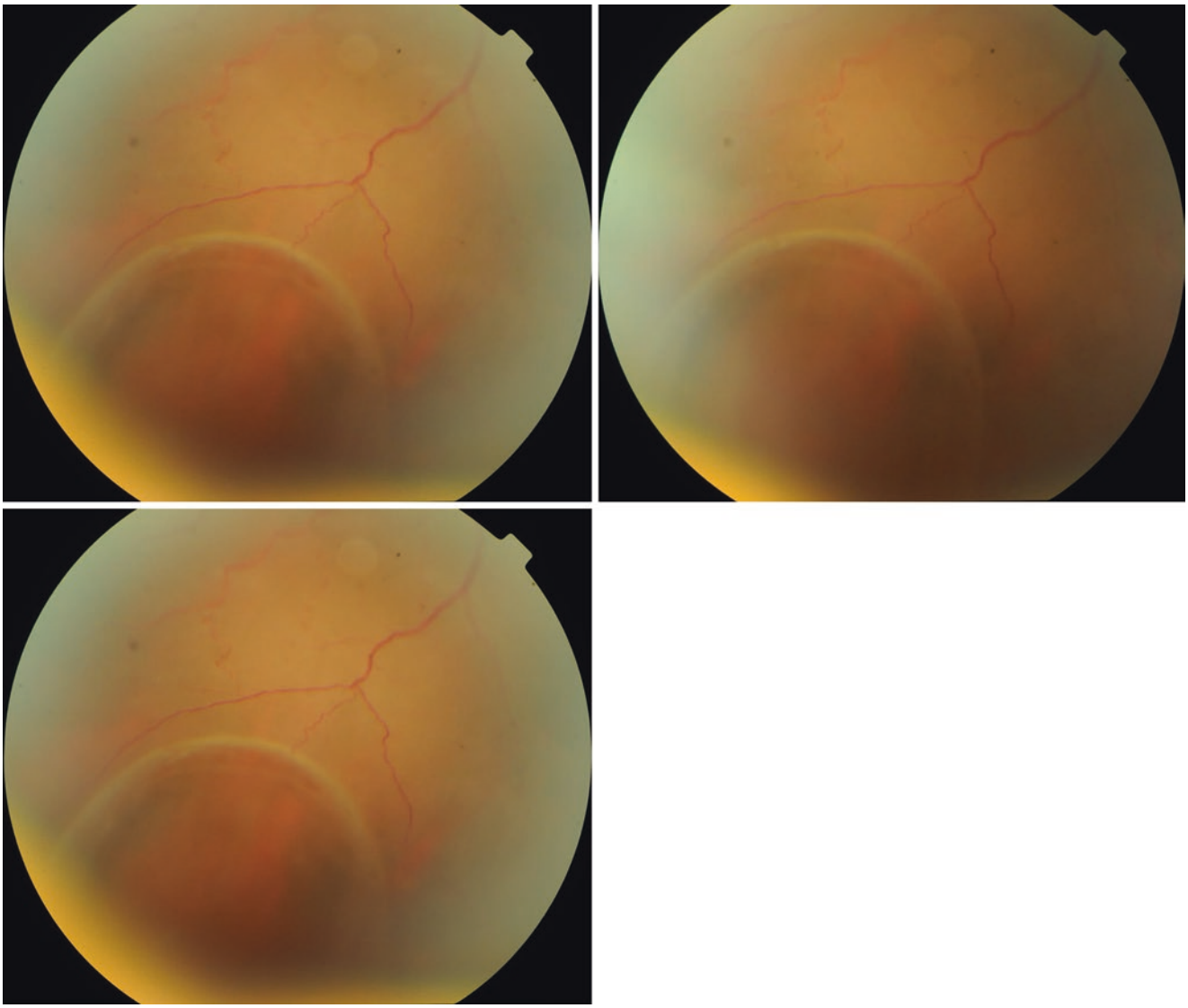

Fig. 2.54 Retinal cyst due to long-term retinal detachment
I. Retinal cyst and its border
II. Retinal tear
III. Retinal detachment

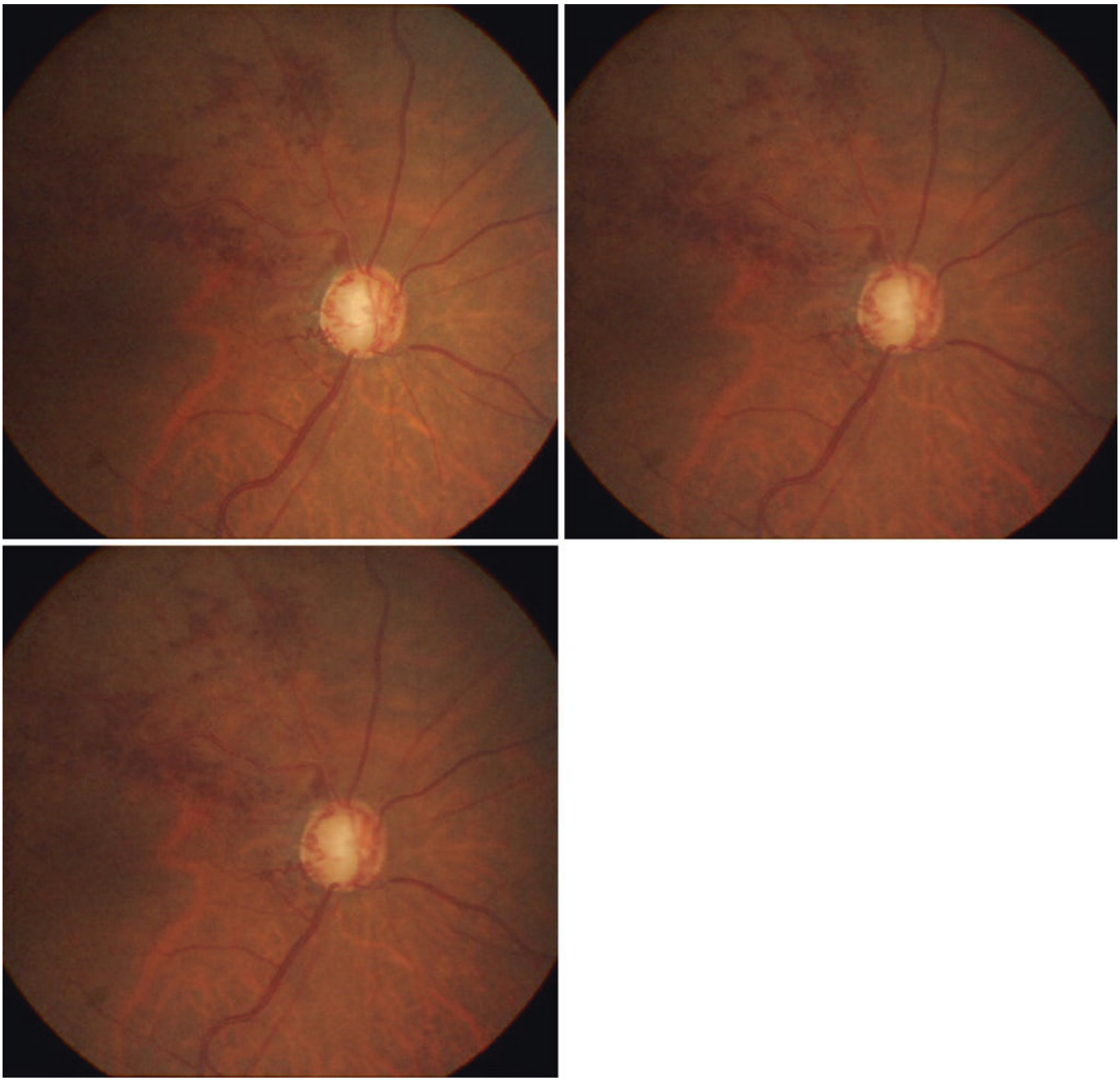

Fig. 2.55 Hypertensive retinopathy complicated with enlarged cup/disc ratio
I. The retinal artery was attenuated and straight
II. Engorged retinal vein, the *A*/*V* ratio was 1:3 to 1:2
III. Deep retinal hemorrhage
IV. *C*/*D* ratio ≈ 0.9
V. The vessel around the optic disc was tortuous and dilated

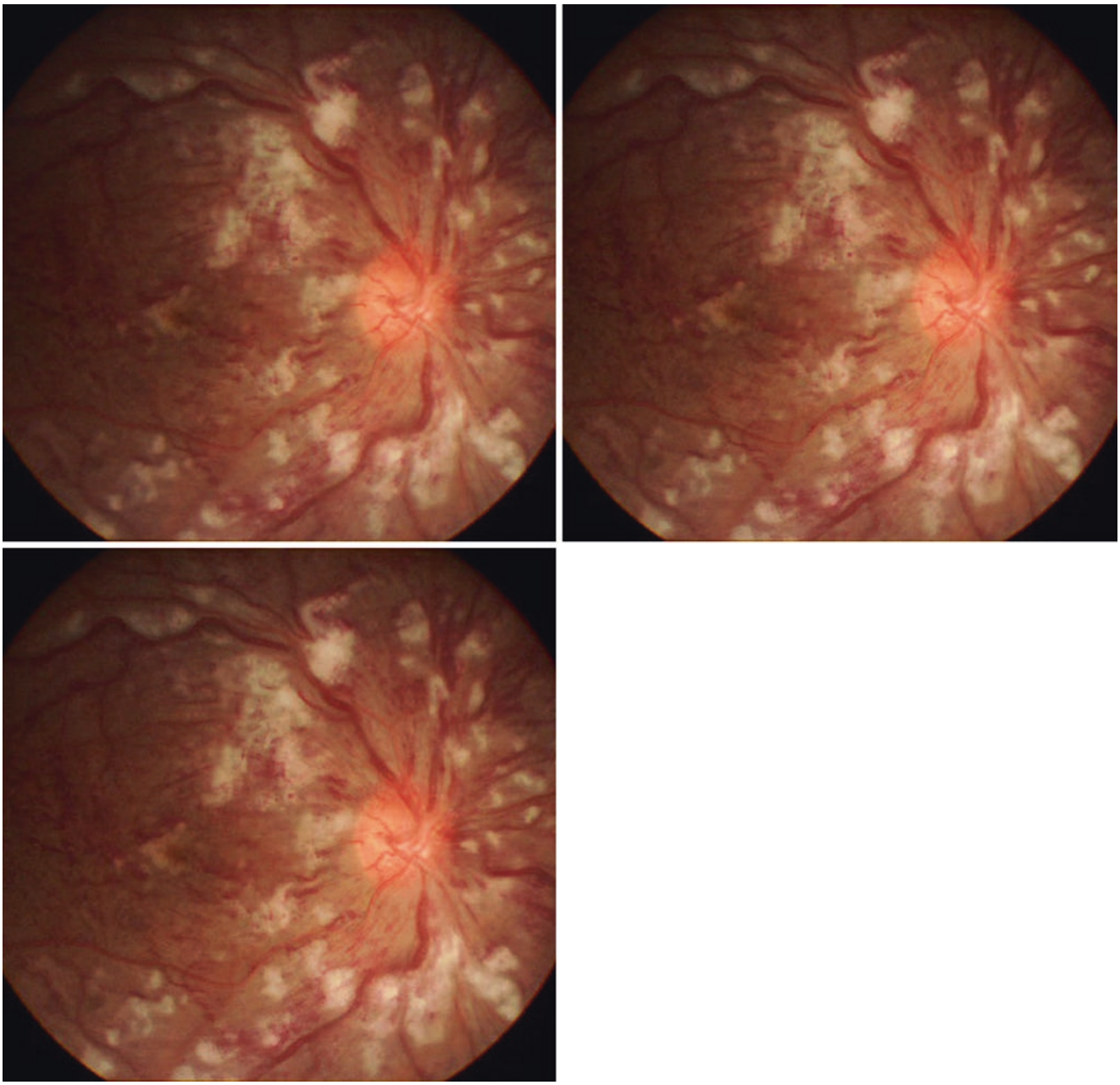

Fig. 2.56 Acute hypertensive retinopathy
I. Superficial hemorrhage and cotton wool spots in the macula
II. The retinal vein is engorged and tortuous, the *A*/*V* ratio is 1:3
III. Superficial retinal cotton wool spot
IV. Deep retinal cotton wool spot

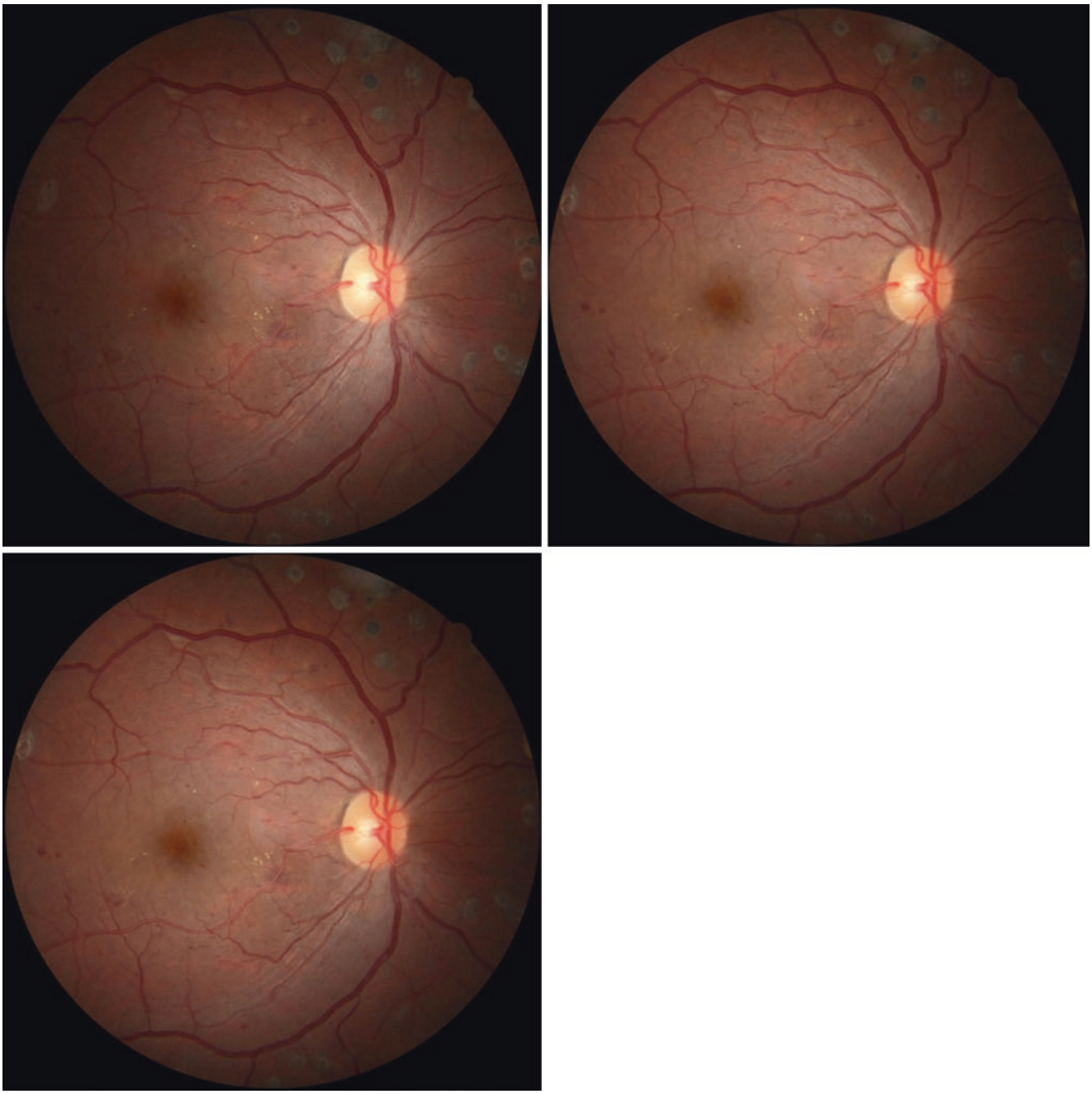

Fig. 2.57 Diabetic retinopathy
I. Deep microaneurysm
II. Superficial exudates
III. Dilated retinal vein
IV. Pigmentation of the laser spot
V. Intra-retinal microvascular abnormality (IRMA)

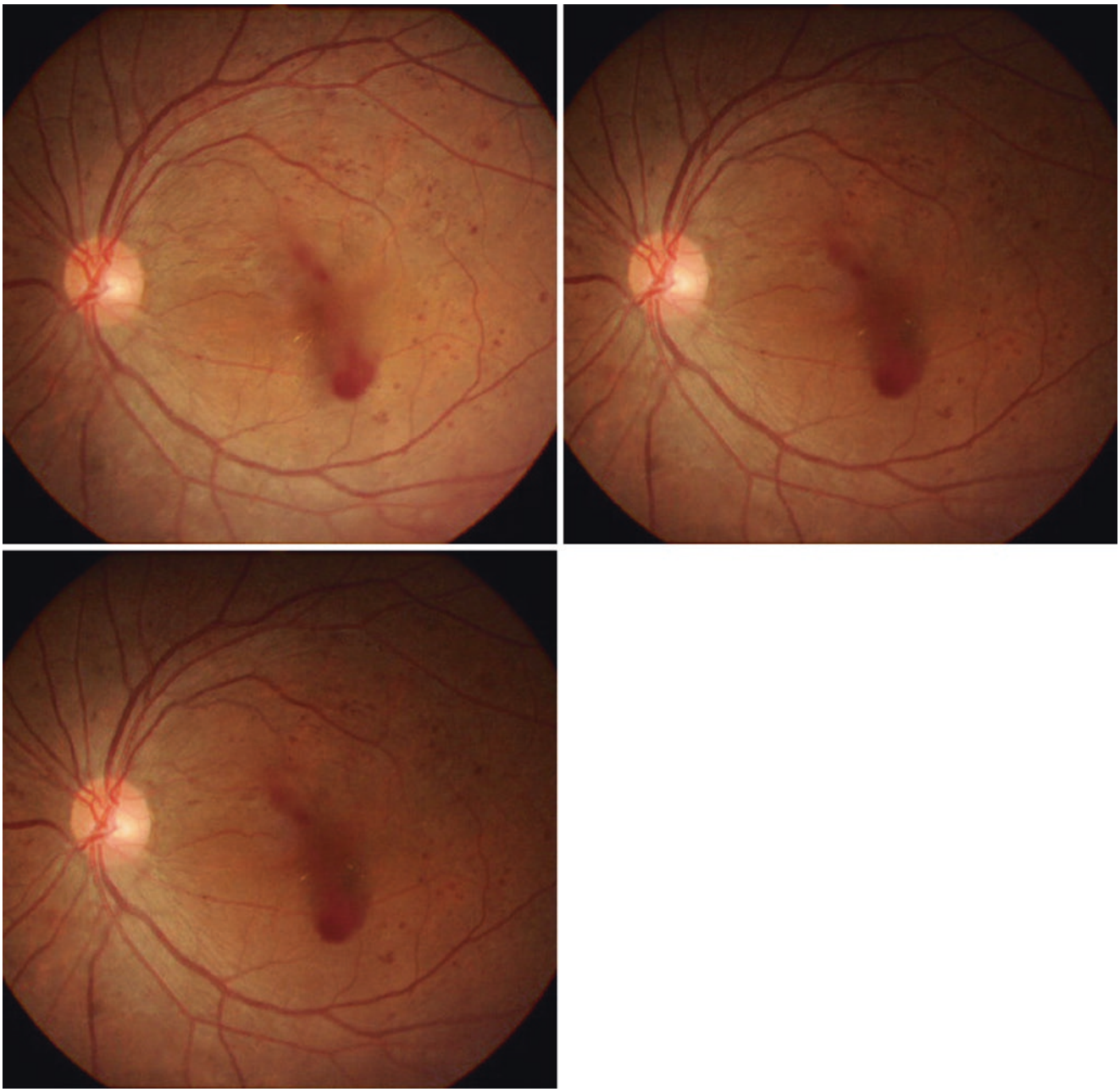

Fig. 2.58 Non-proliferative diabetic retinopathy
I. Vitreous hemorrhage
II. Intra-retinal microaneurysm
III. Hard exudates

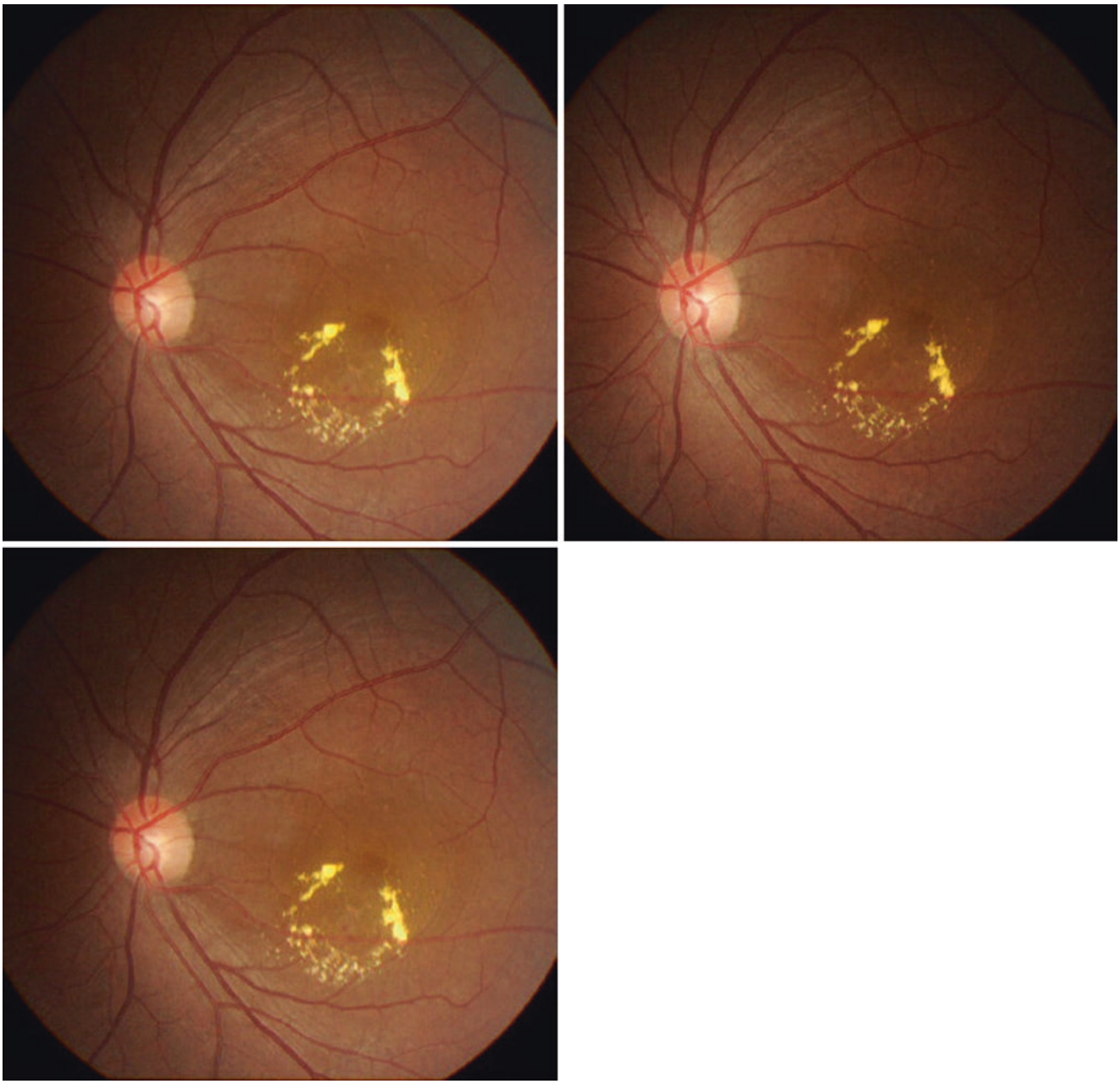

Fig. 2.59 Non-proliferative diabetic retinopathy
I. Microaneurysm
II. Circular exudates
III. Macular edema

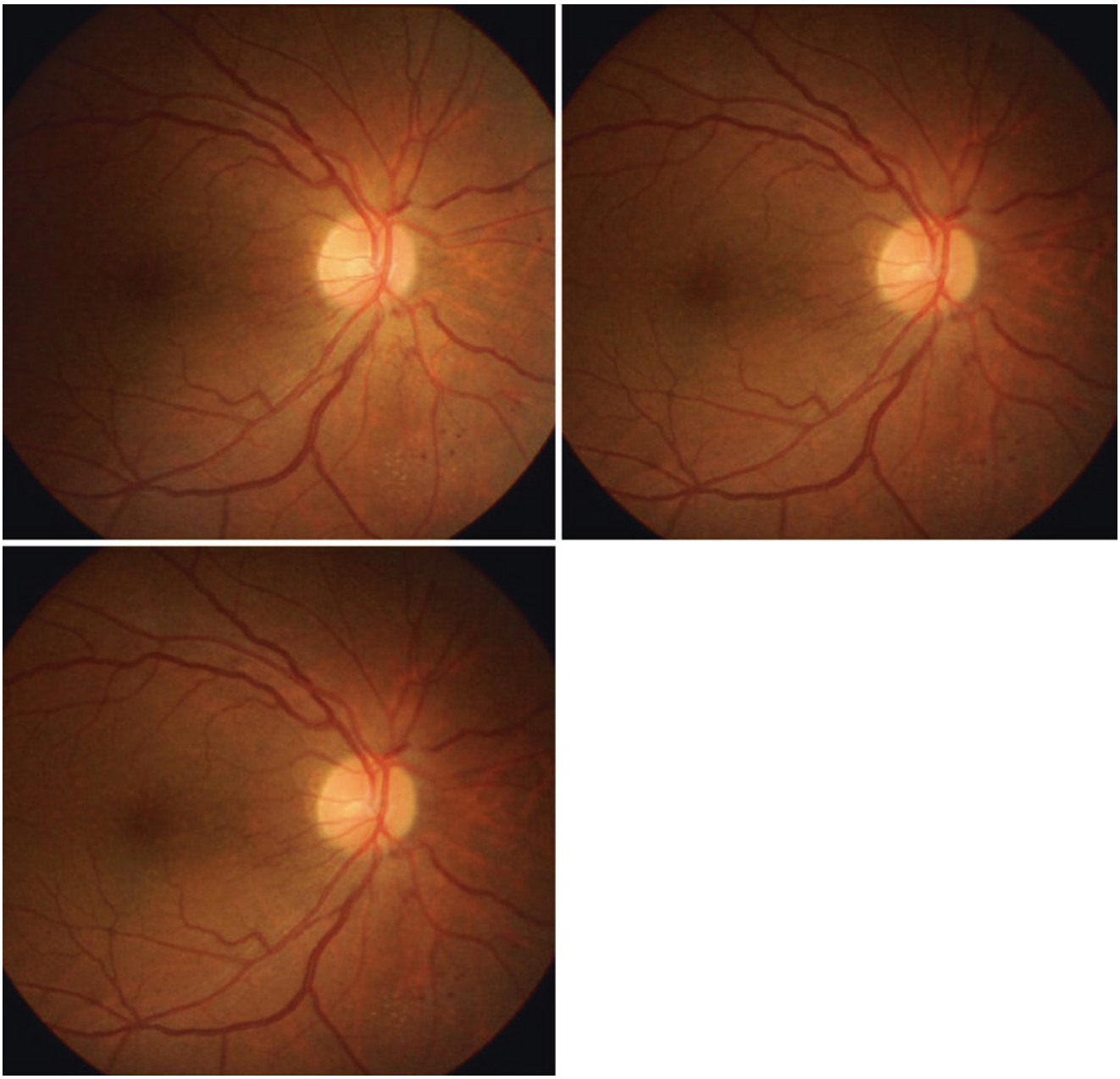

Fig. 2.60 Non-proliferative diabetic retinopathy
I. Retinal microaneurysm
II. Intermediate retinal exudates
III. Multiple drusen

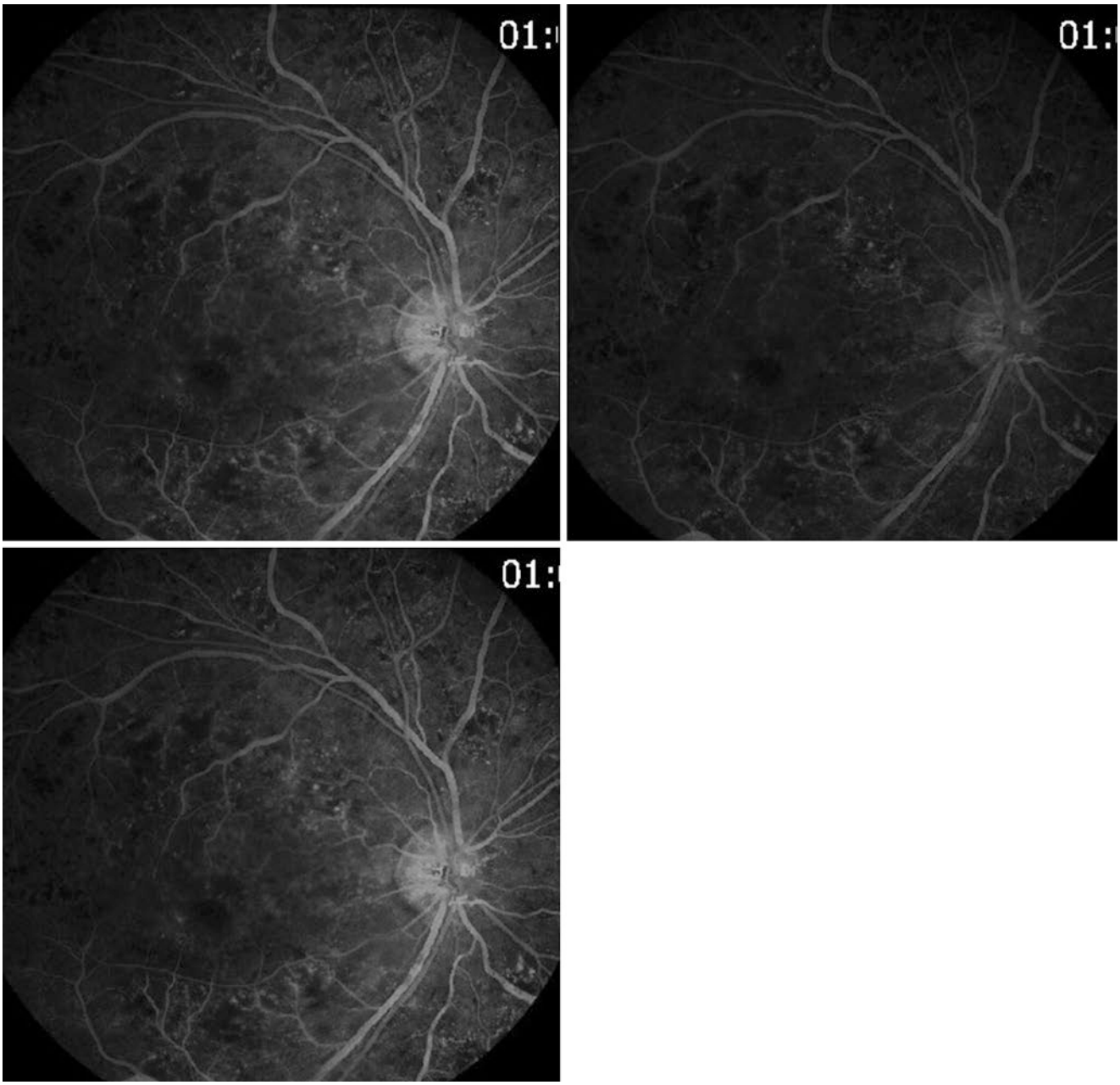

Fig. 2.61 Severe non-proliferative diabetic retinopathy
I. Macular edema
II. Microaneurysm
III. Non-perfusion area (NPA)
IV. Intra-retinal microvascular abnormality (IRMA)
V. Neovascularization of the optic disc (NVD)

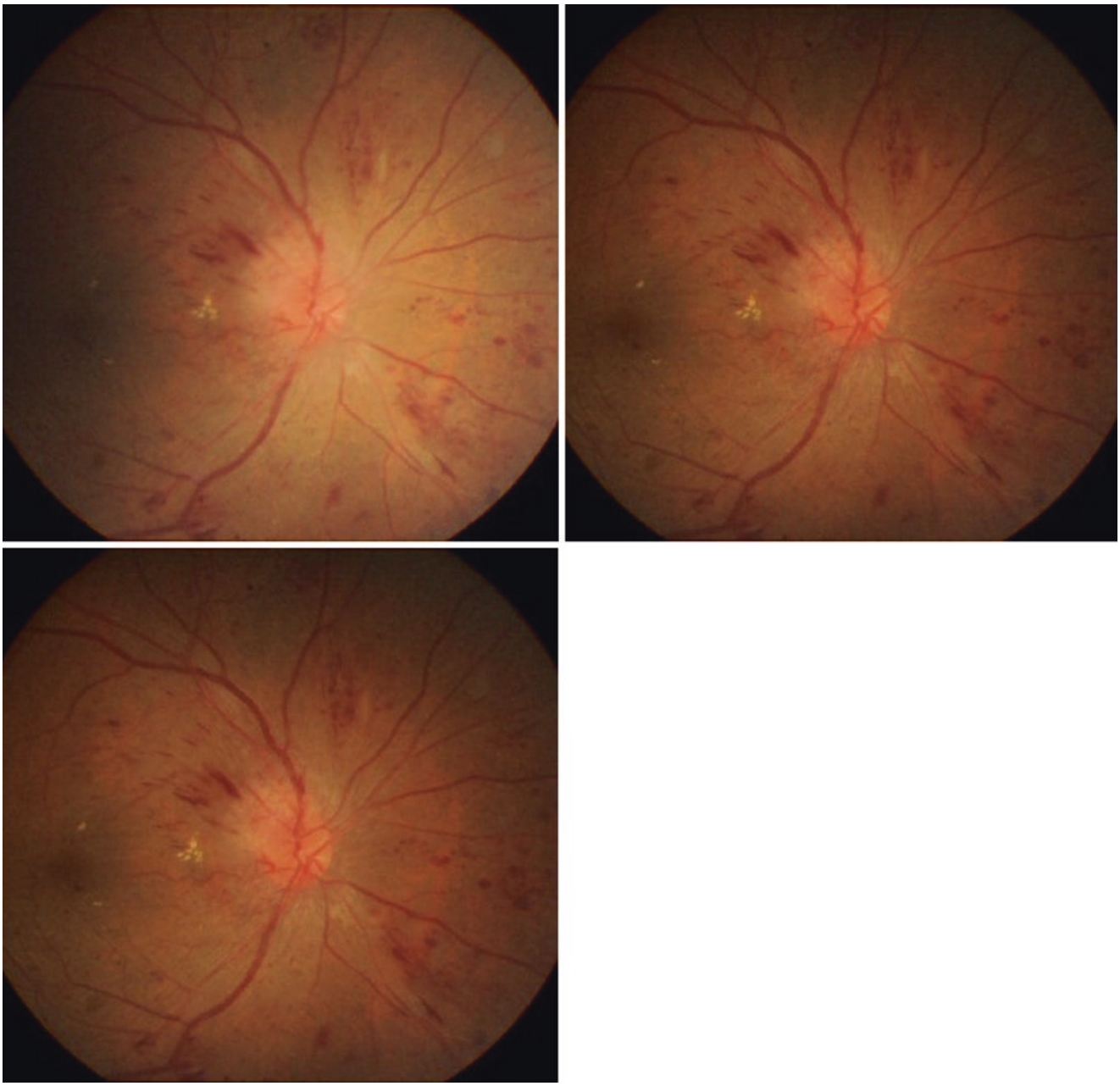

Fig. 2.62 Diabetic retinopathy
I. Localized edema of the optic disc
II. Flame-shaped superficial retinal hemorrhage
III. Freckle deep retinal hemorrhage
IV. Hard exudates
V. Cotton wool spot
VI. Microaneurysm

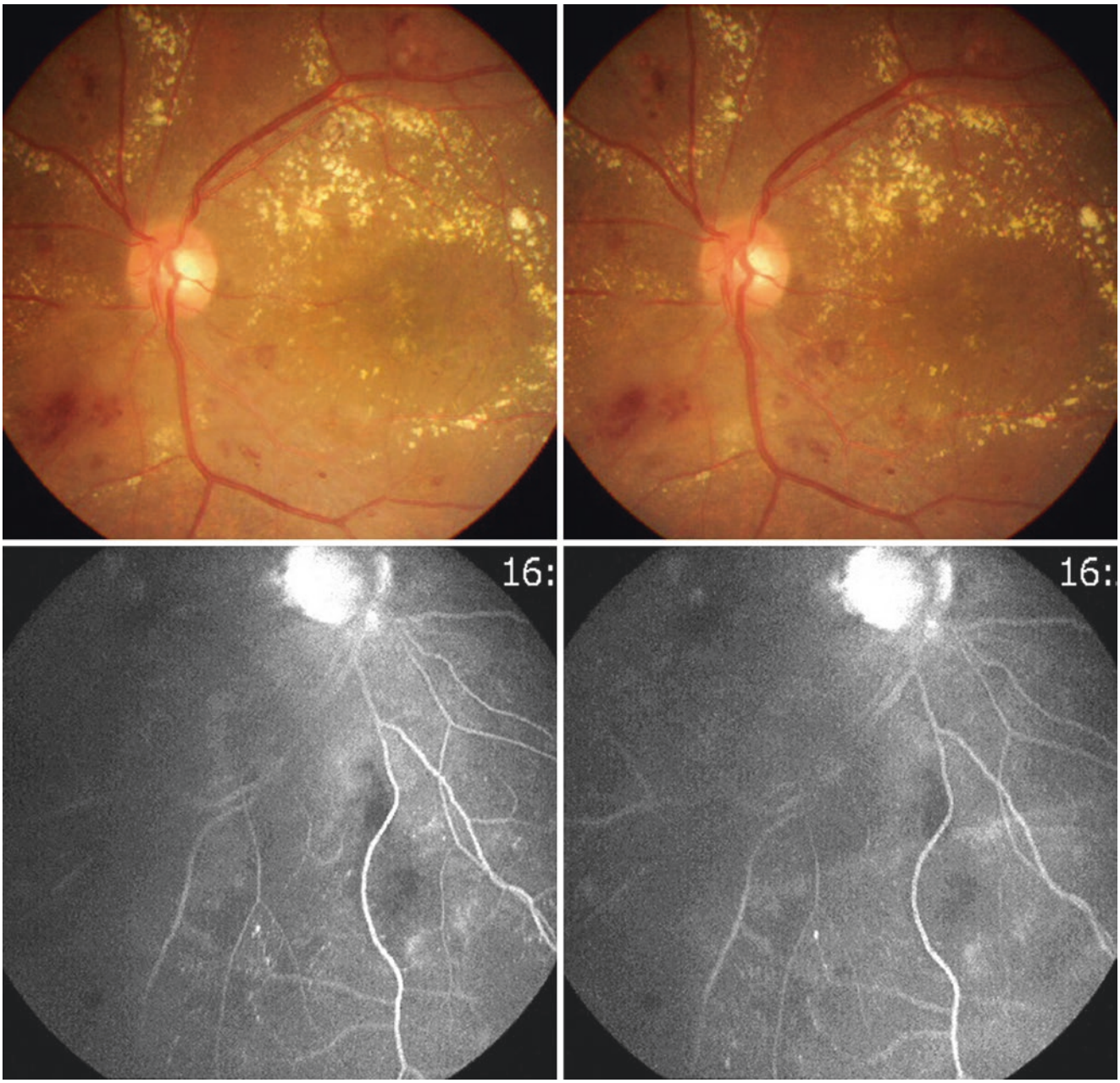

Fig. 2.63 Fluorescein fundus angiography of diabetic retinopathy (early phase)
I. Optic disc
II. Edematous retina and elevated retinal vein
III. Retinal microaneurysm
IV. Intra-retinal microvascular abnormality (IRMA)

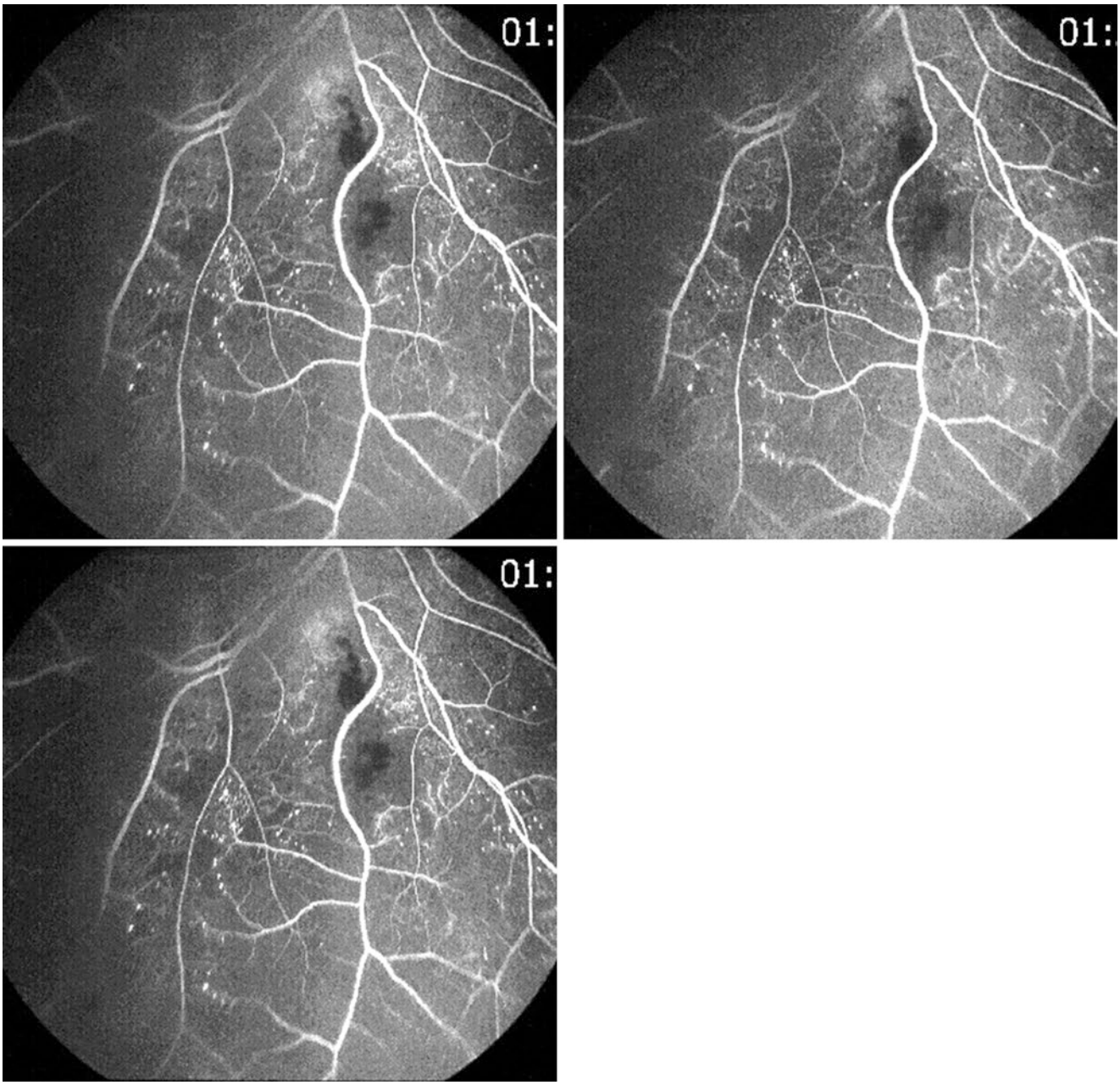

Fig. 2.64 Fluorescein fundus angiography of diabetic retinopathy (middle phase)
I. Blocked fluorescence by the hemorrhage inferior to the optic disc
II. Edematous retina and elevated retinal vein
III. Retinal microaneurysm
IV. Intra-retinal microvascular abnormality (IRMA)
V. Non-perfusion area (NPA)

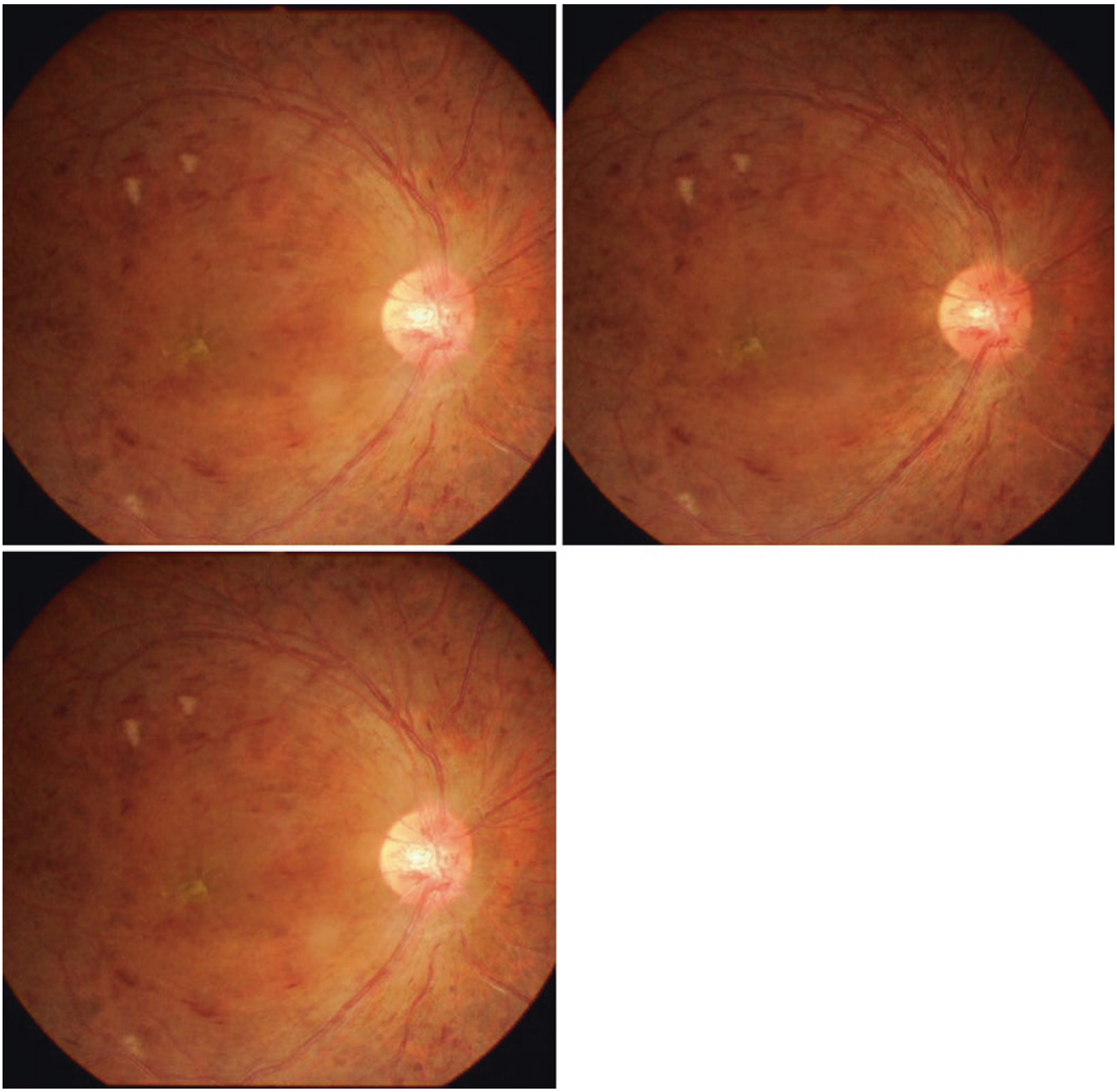

Fig. 2.65 Diabetic retinopathy
I. Thread-like superficial retinal hemorrhage superior to the optic disc
II. Spotted deep retinal hemorrhage
III. Retinal microaneurysm
IV. Soft exudates

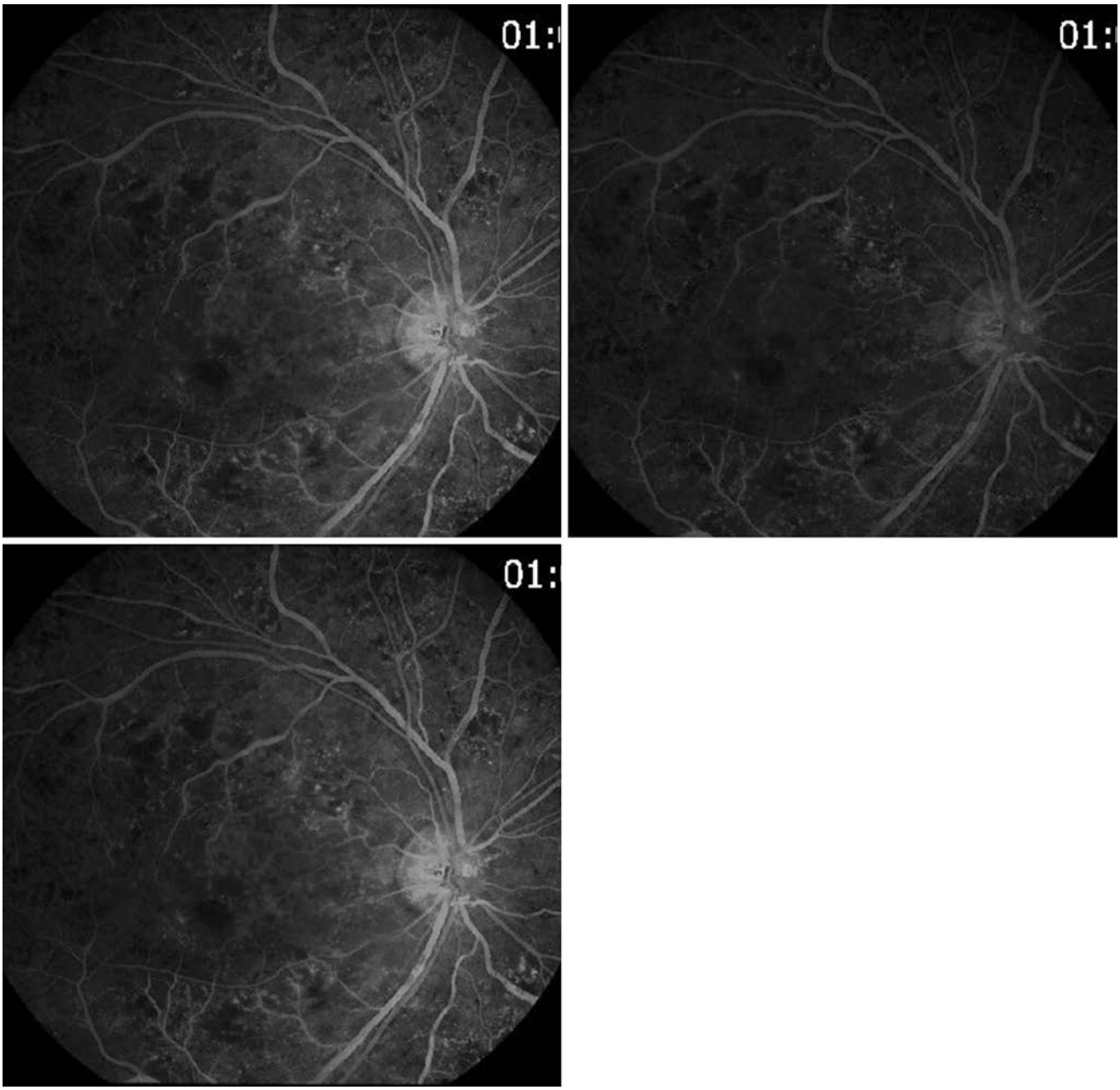

Fig. 2.66 Fluorescein fundus angiography of diabetic retinopathy (middle phase)
I. Thread-like superficial retinal hemorrhage superior to the optic disc and showed blocked fluorescence
II. Deep retinal hemorrhage and blocked fluorescence
III. Retinal microaneurysm
IV. Soft exudates and non-perfusion area

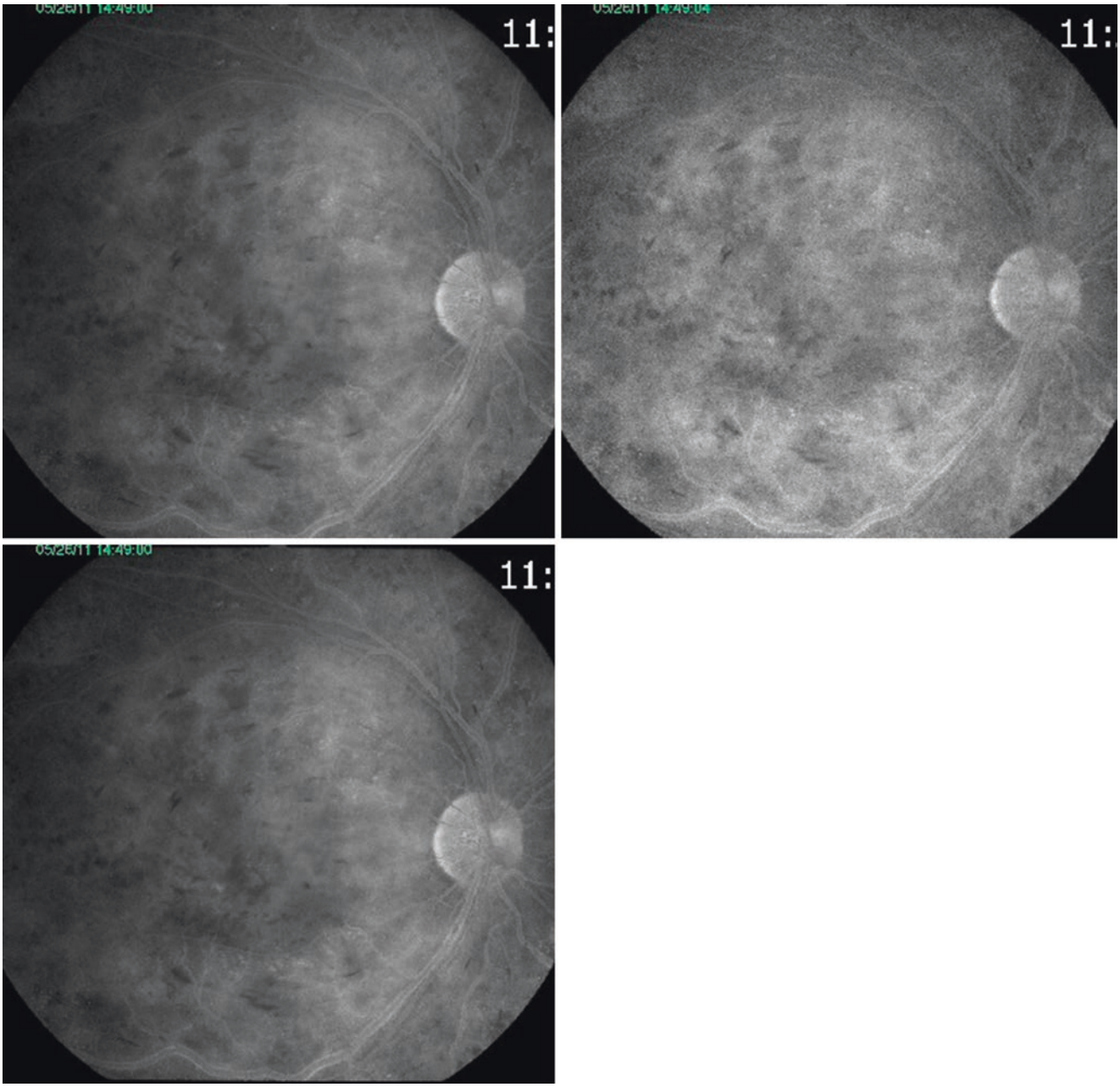

Fig. 2.67 Fluorescein fundus angiography of diabetic retinopathy (late phase)
I. Thread-like superficial retinal hemorrhage superior to the optic disc and showed blocked fluorescence
II. Deep retinal hemorrhage and blocked fluorescence
III. Retinal microaneurysm
IV. Soft exudates and non-perfusion area

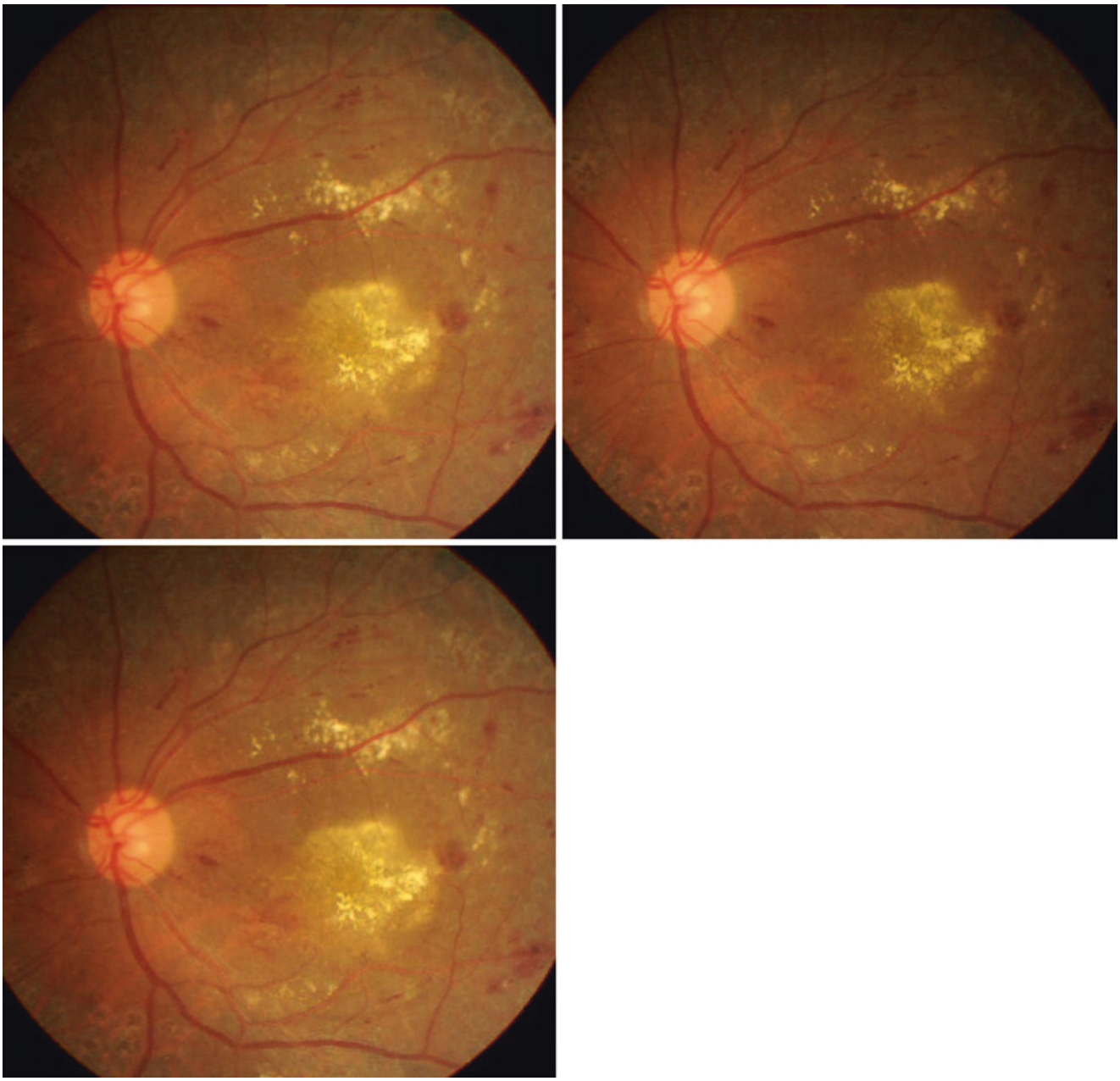

Fig. 2.68 Non-proliferative diabetic retinopathy
I. Macular edema and massive hard exudates
II. Flame-shaped superficial retinal hemorrhage
III. Retinal microaneurysm
IV. Sectional white sheath of retinal artery
V. Deep retinal exudates

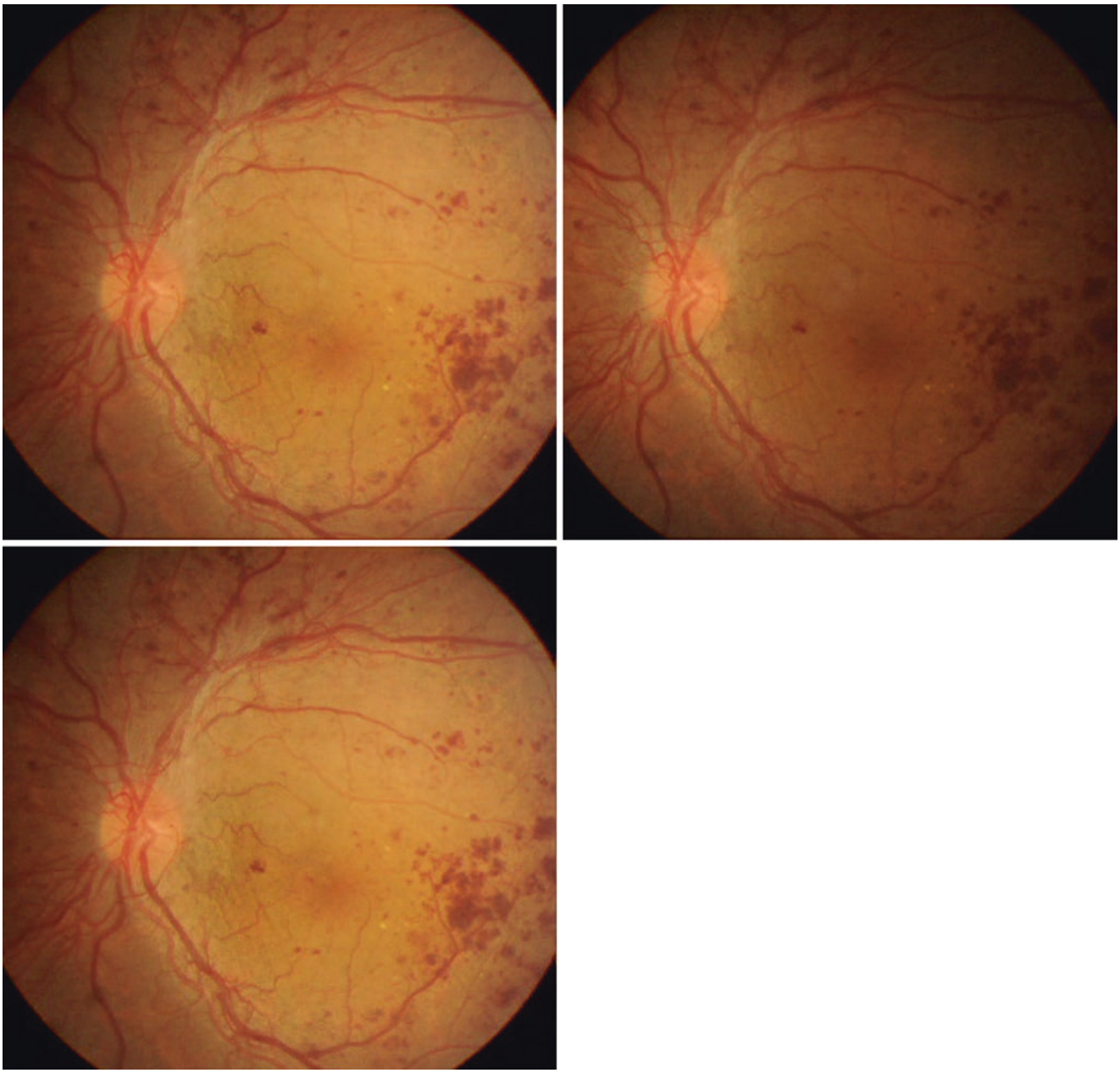

Fig. 2.69 Proliferative diabetic retinopathy
I. Venous beading
II. IRMA
III. NVD
IV. NVE
V. Microaneurysm
VI. Epiretinal membrane

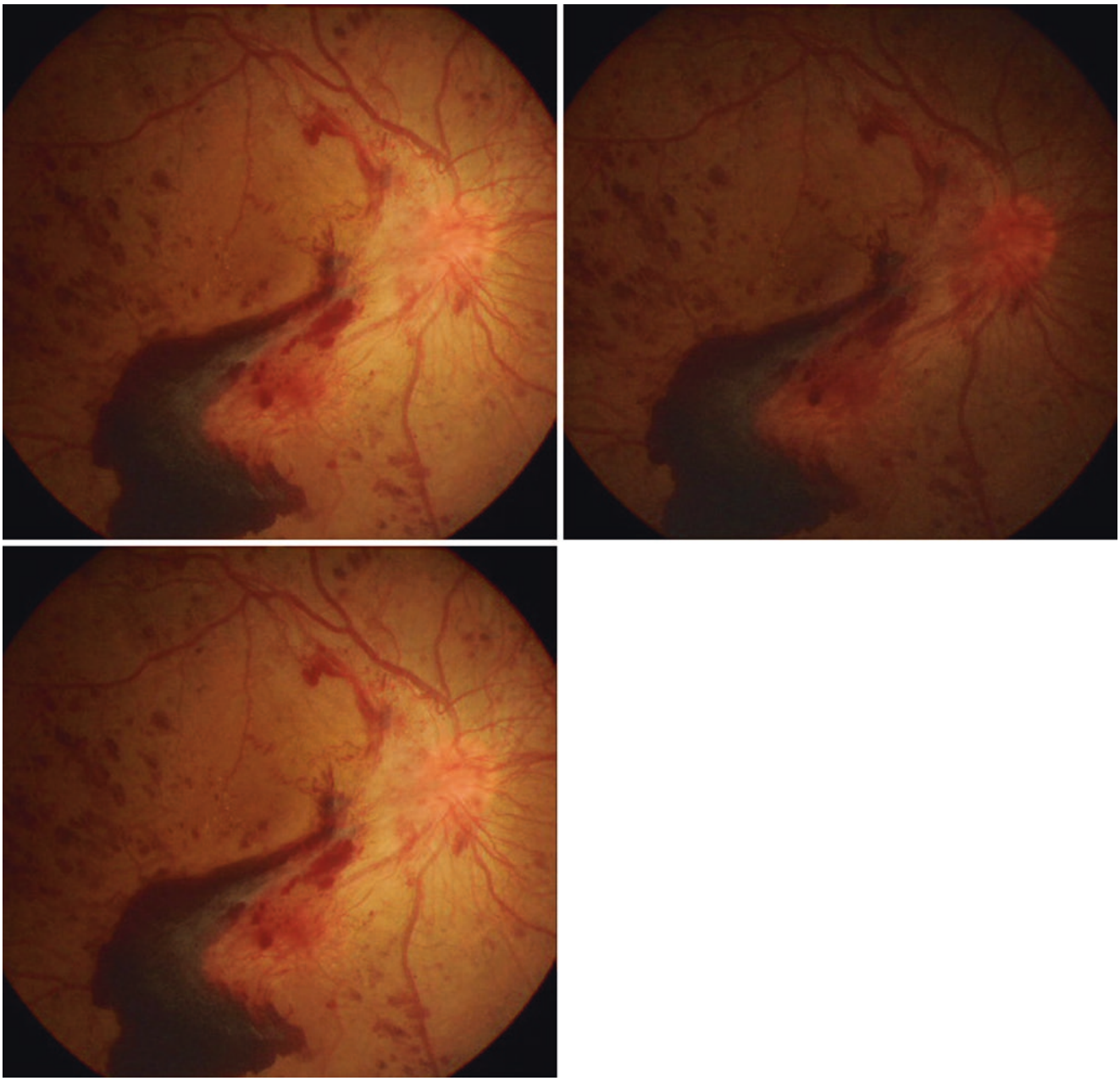

Fig. 2.70 Proliferative diabetic retinopathy
I. NVD
II. NVE
III. Proliferative membrane of the vitreous
IV. IRMA
V. Hemorrhage adhesive to the vitreous filaments
VI. Sub-hyaloid hemorrhage

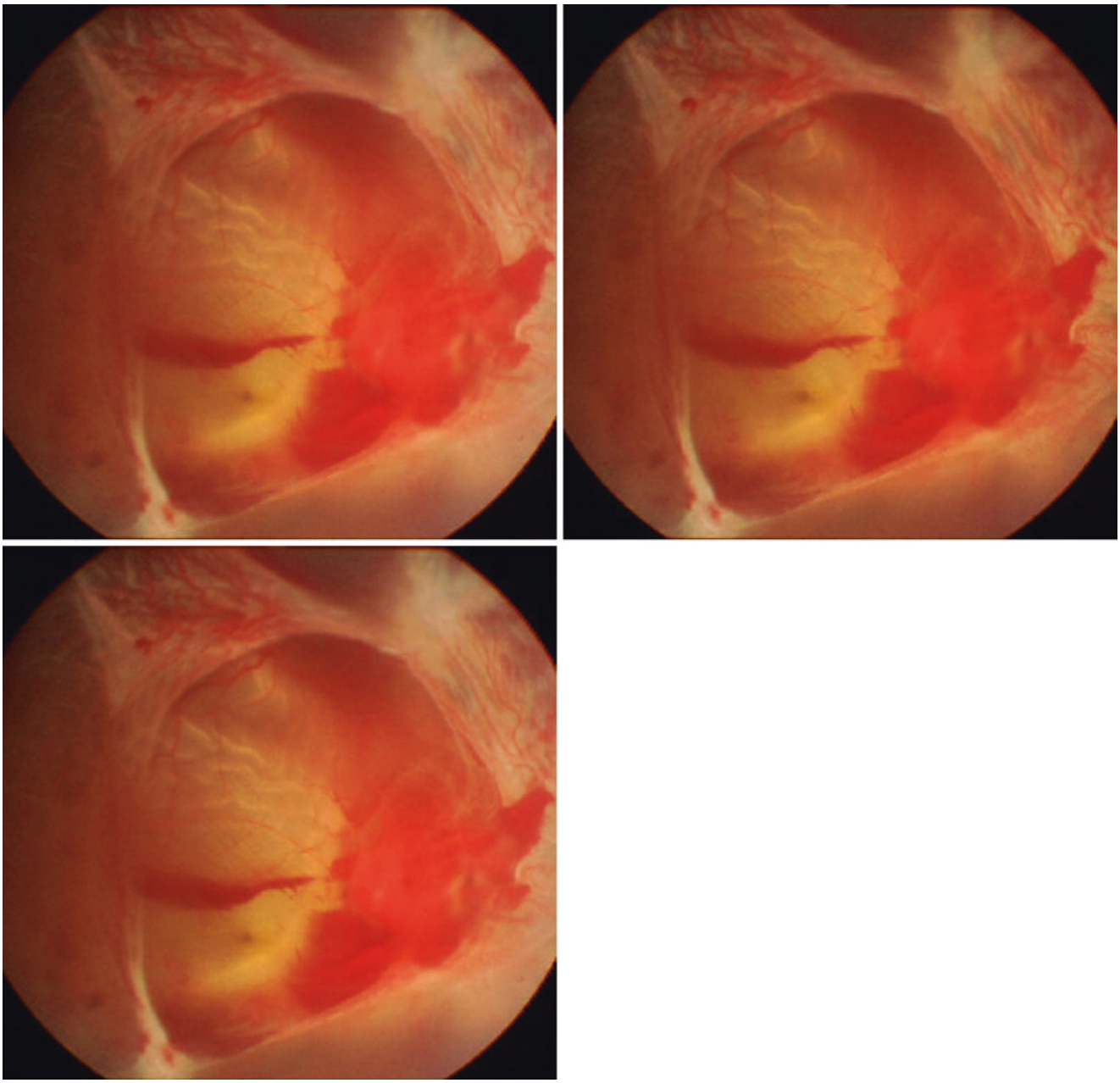

Fig. 2.71 Proliferative diabetic retinopathy
I. NVD
II. NVE
III. Proliferative membrane in the posterior pole along the vascular arc
IV. Retinal detachment
V. Vitreous hemorrhage

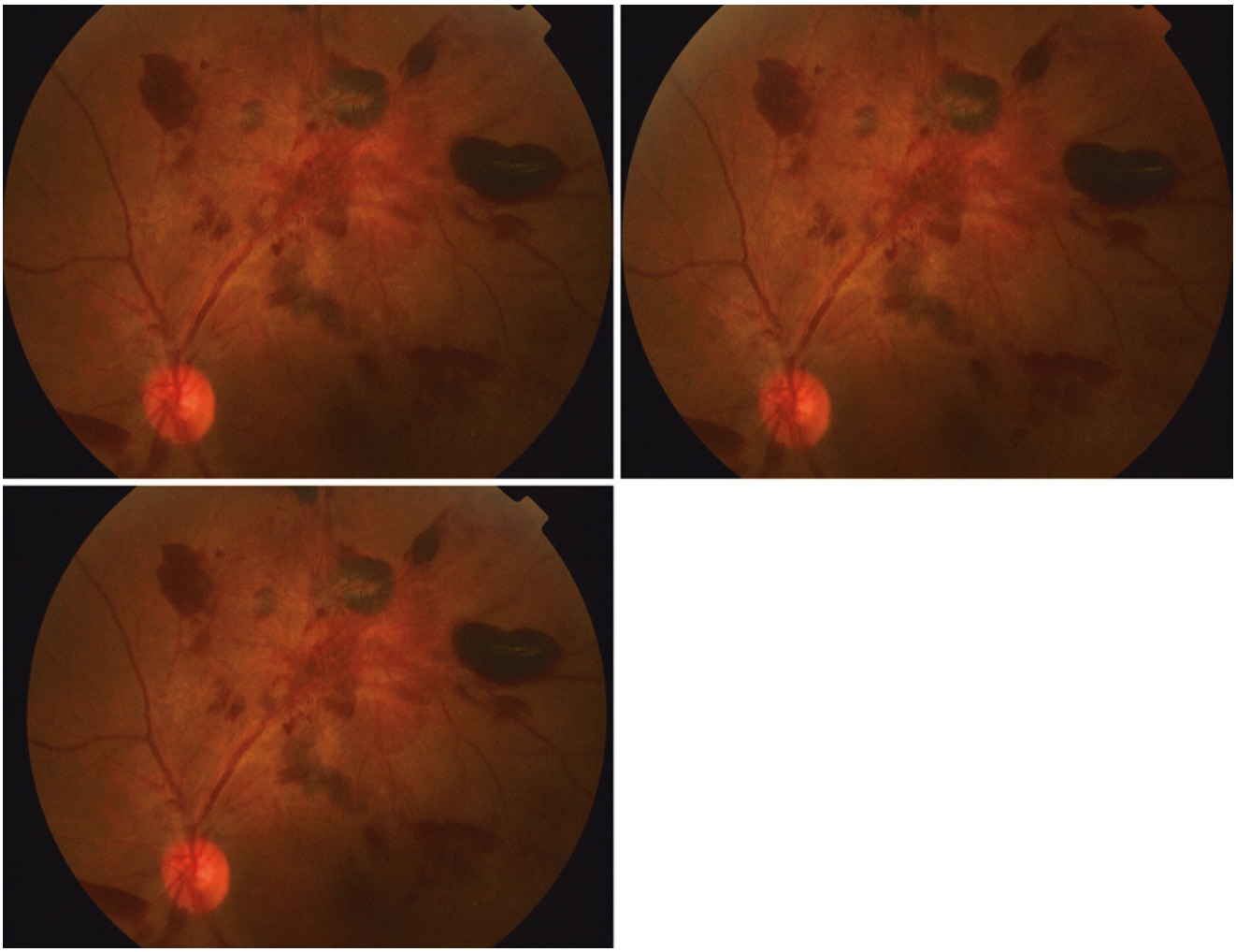

Fig. 2.72 Proliferative diabetic retinopathy
I. Abnormal retinal vessels
II. Superficial retinal hemorrhage
III. Subretinal hemorrhage
IV. Neovascularization showed by FFA
V. Irregular retinal vessels

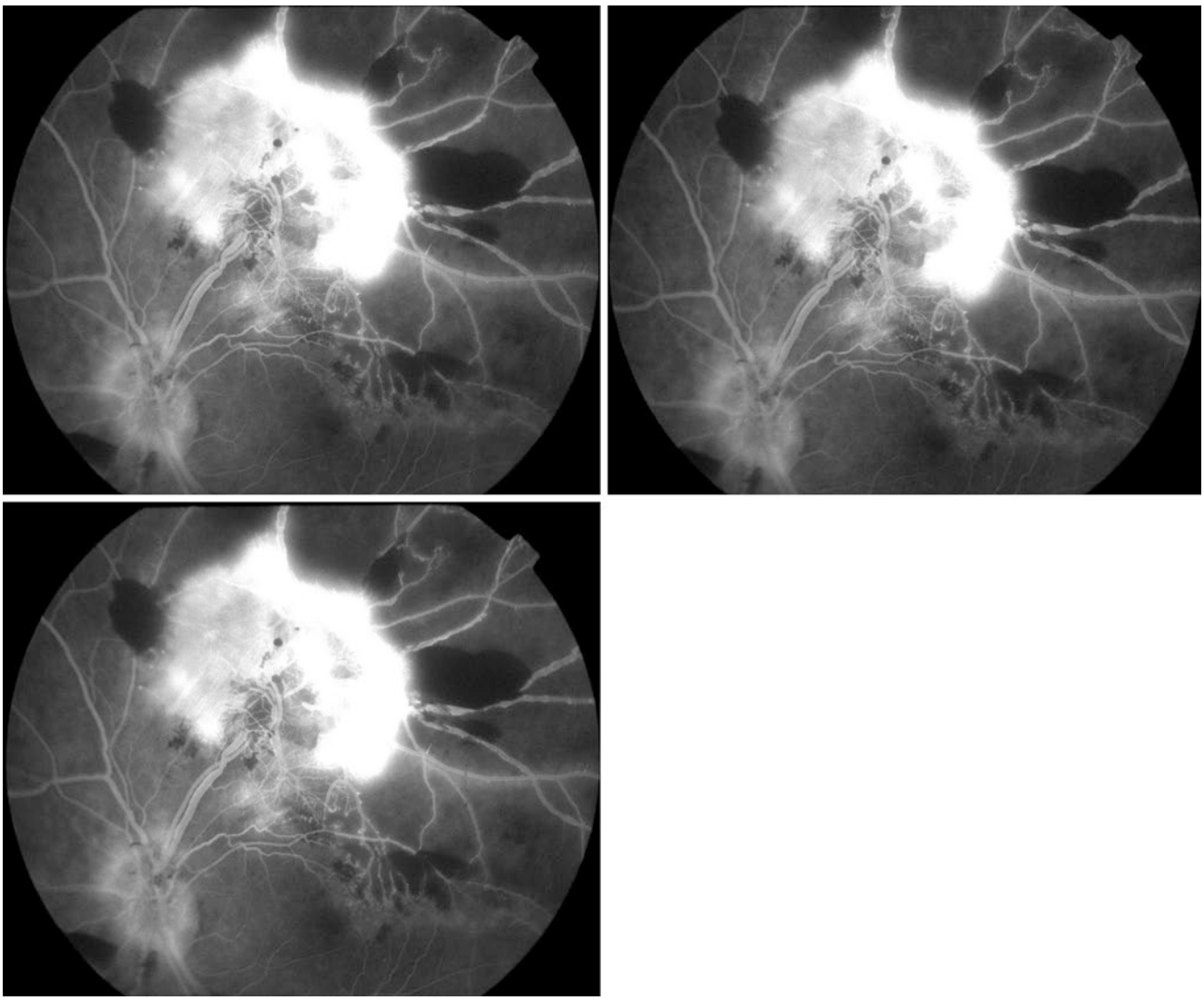

Fig. 2. 72 (continued)

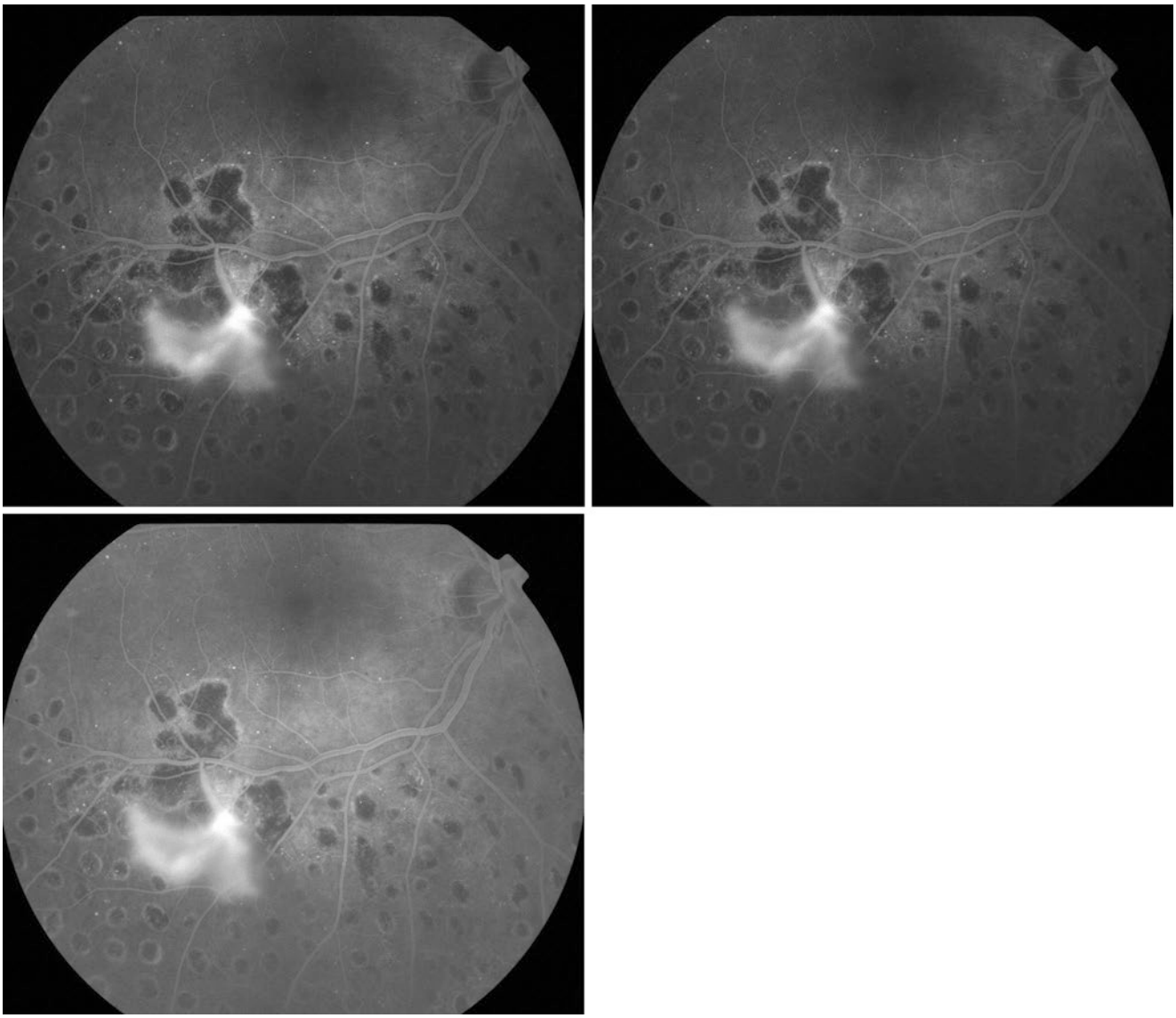

Fig. 2.73 NVE on FFA
I. NVE extending into vitreous cavity
II. Dilated vein
III. Laser spots
IV. Microaneurysm

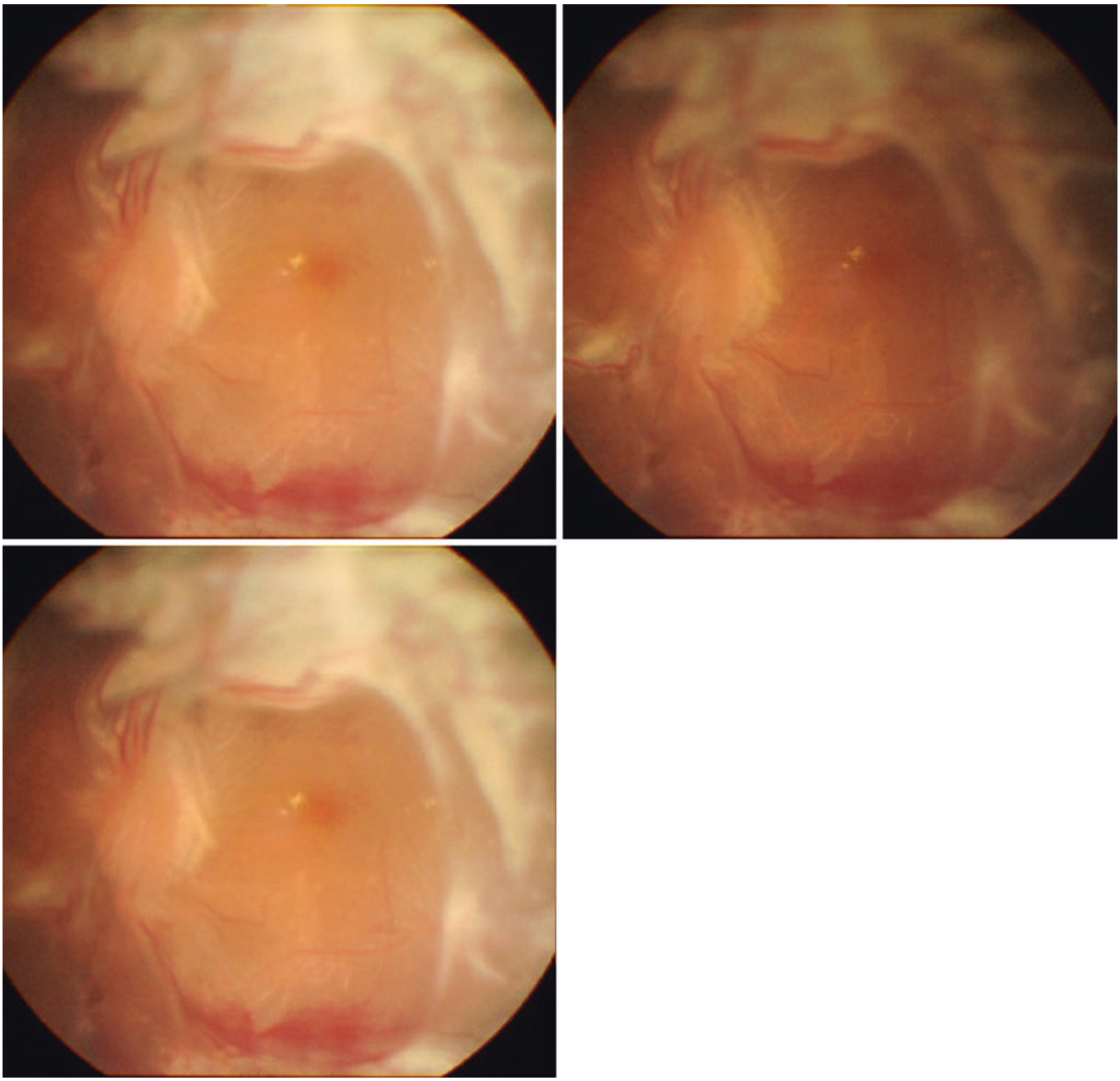

Fig. 2.74 Proliferative diabetic retinopathy
I. NVD
II. Cystoid macular edema
III. NVE
IV. Deep NVD

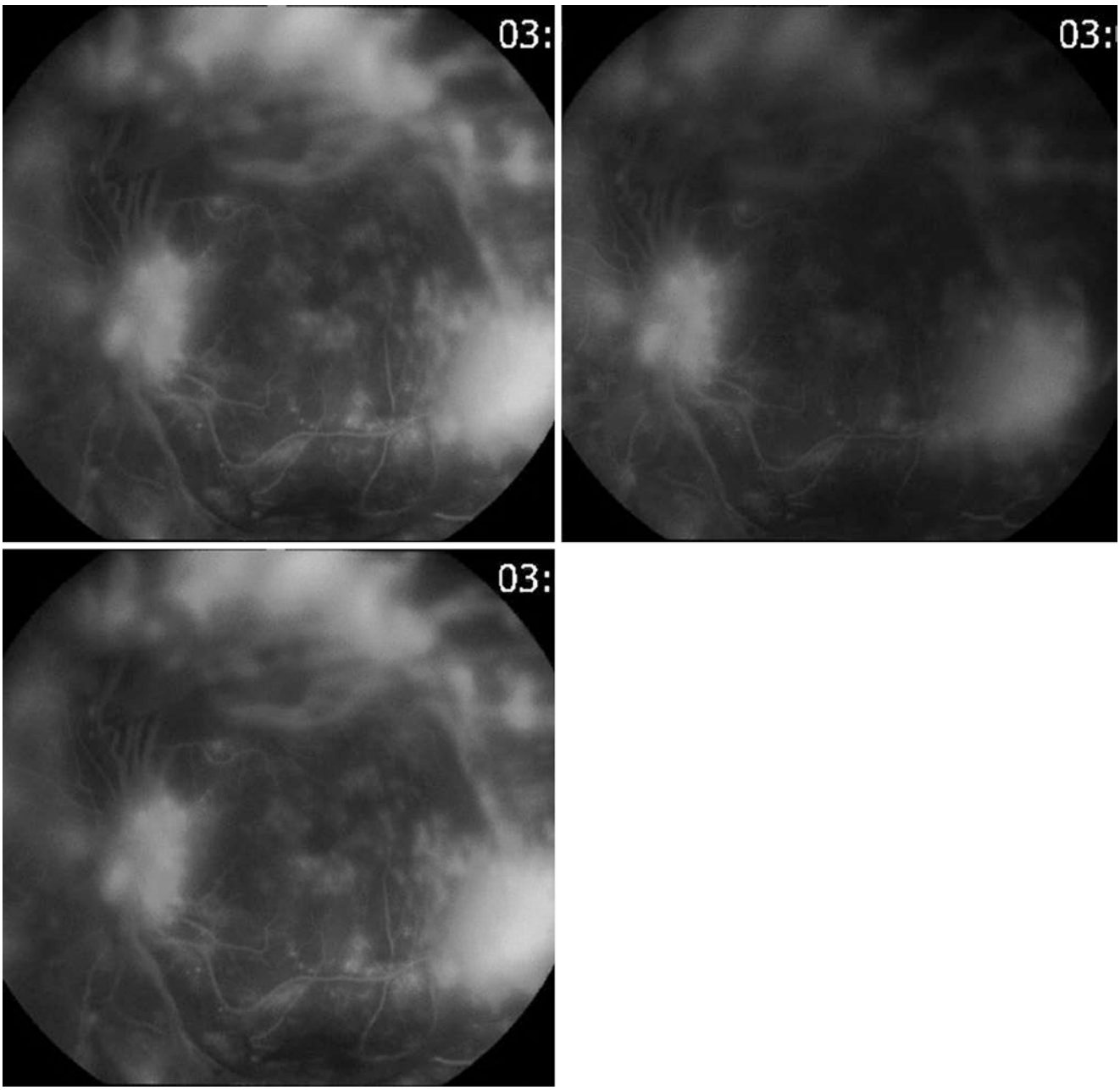

Fig. 2. 74 (continued)

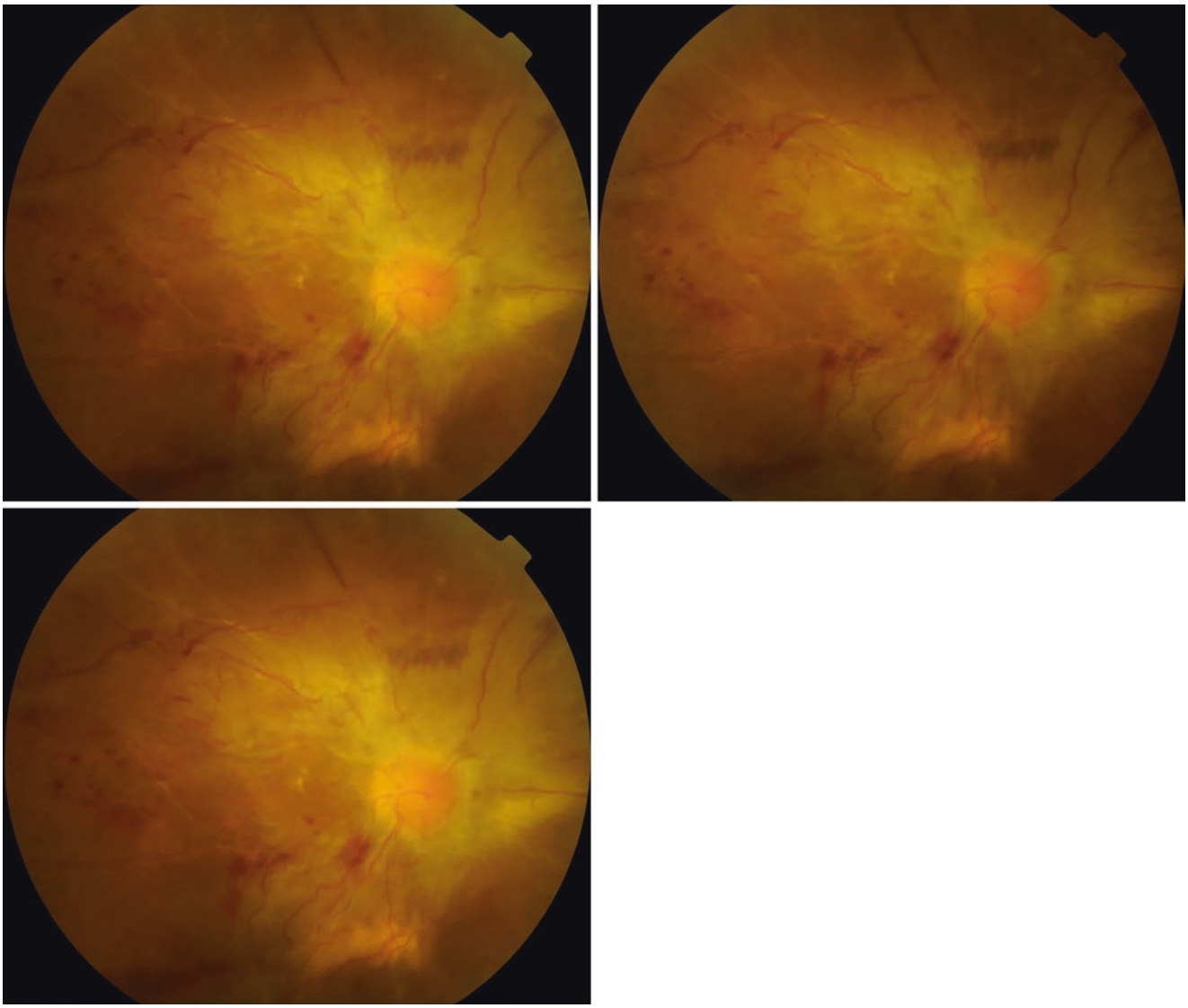

Fig. 2.75 Proliferative diabetic retinopathy after anti-VEGF injection
I. Fibrosis of NVD after VEGF injection
II. Residual NVE
III. Intra-retinal hemorrhage
IV. Bean-like vein

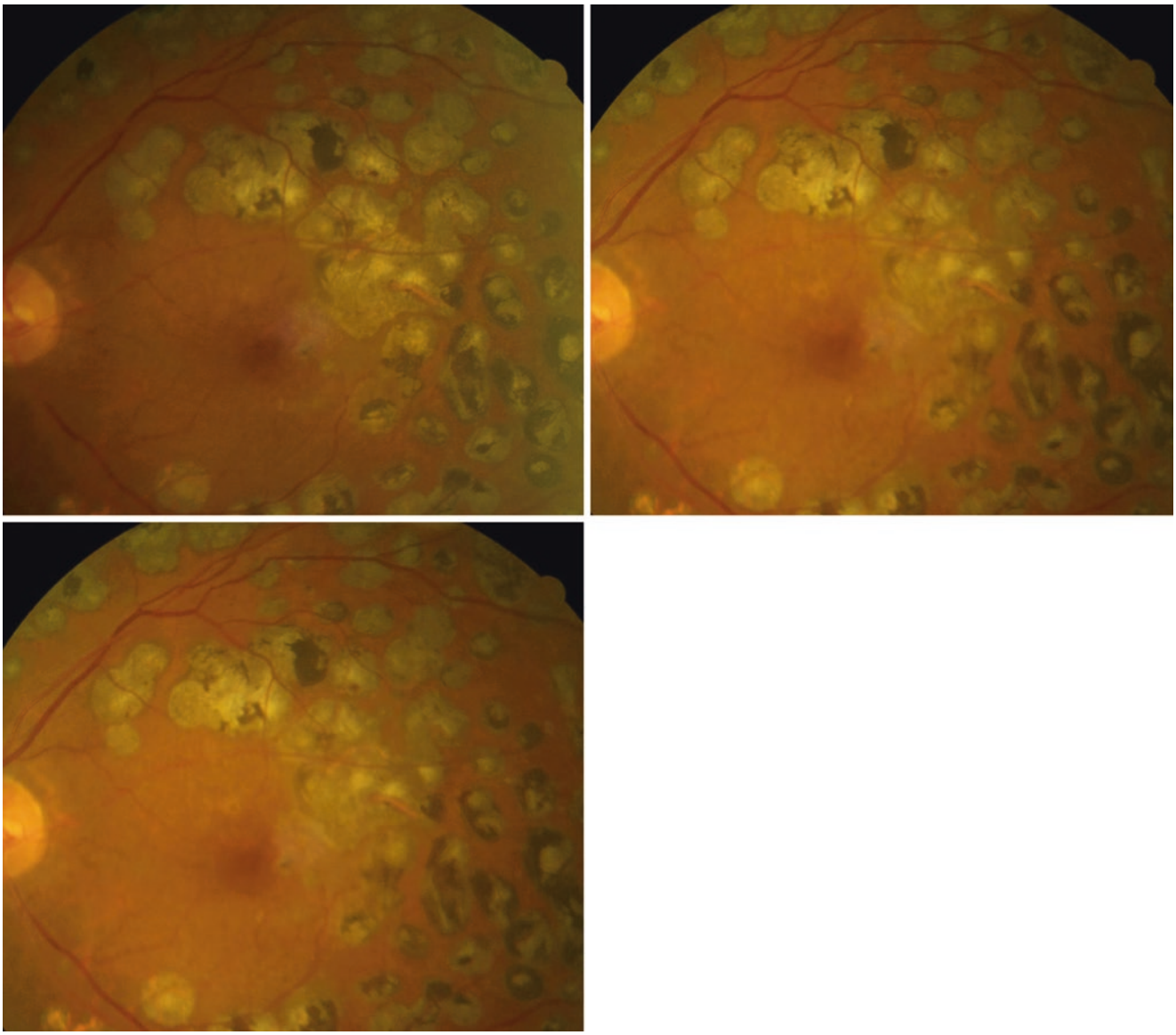

Fig. 2.76 Diabetic retinopathy after pan-retinal photocoagulation
I. Atrophied lesion of retinal pigment epithelium
II. Pigmentation
III. Retinal vessels
IV. Choroidal vessels
V. Vitreous opacities

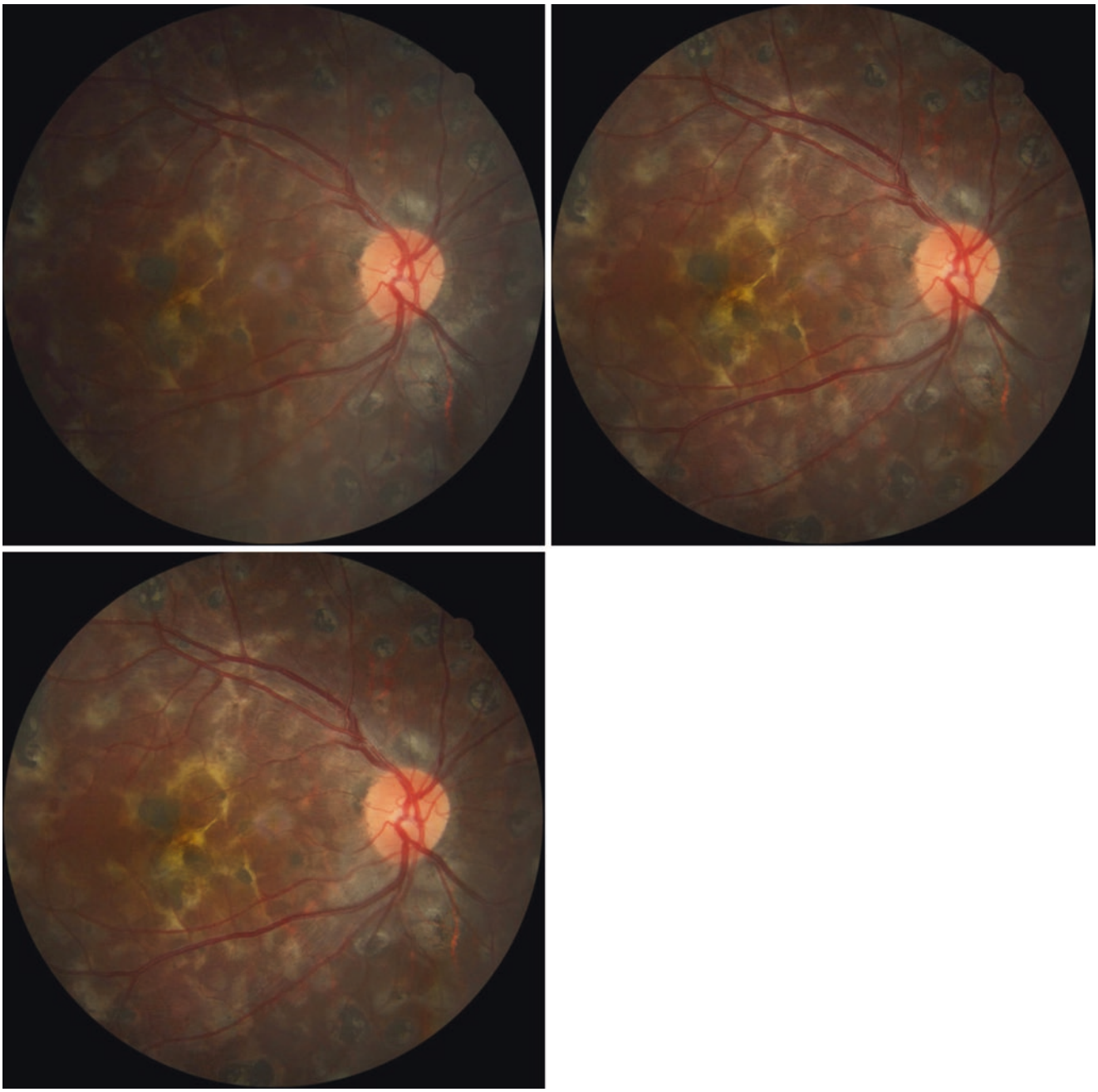

Fig. 2.77 Diabetic retinopathy after pan-retinal photocoagulation
I. Proliferative streak of the vitreous
II. Pigmentation
III. Subretinal membrane
IV. A/V crossing

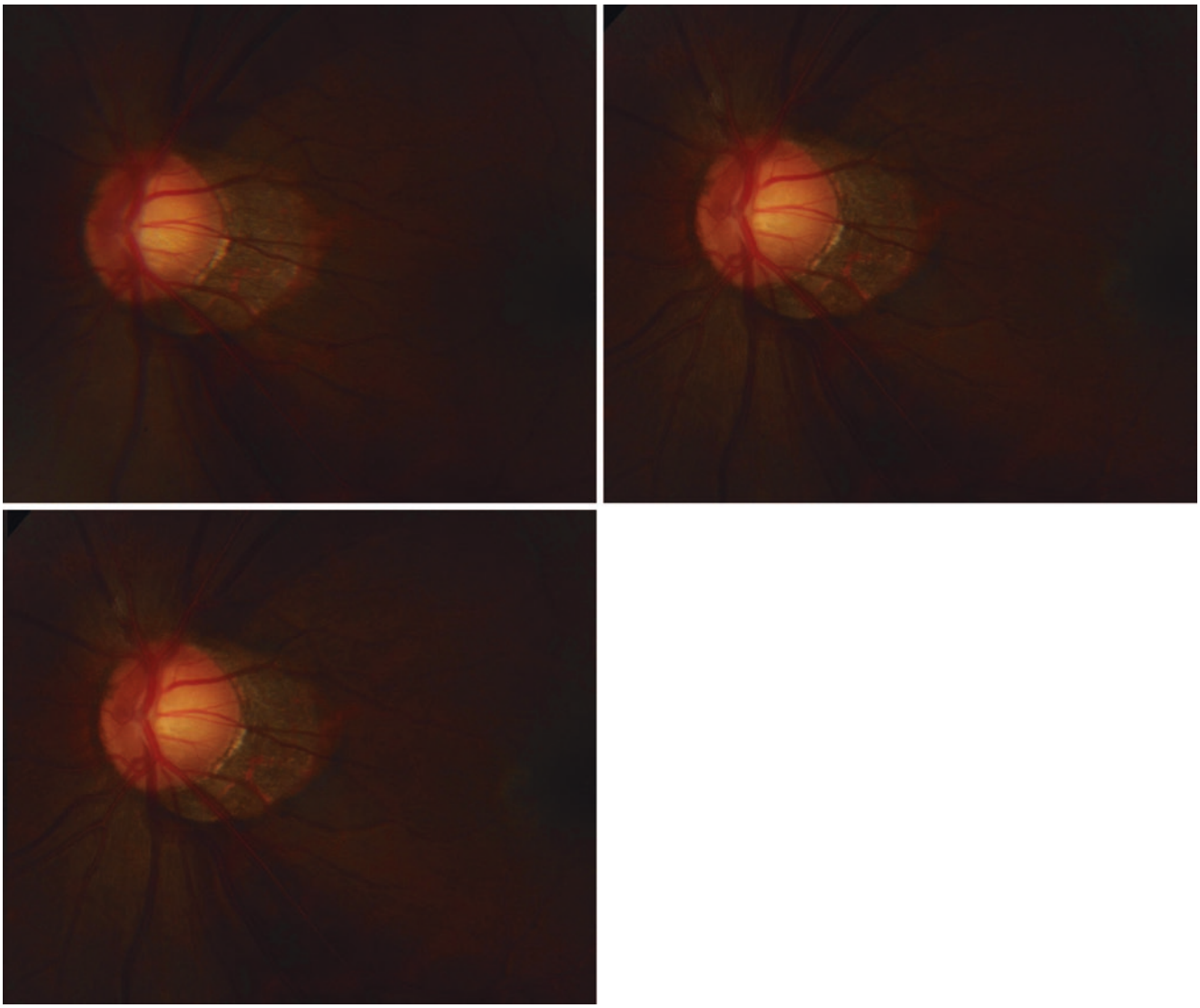

Fig. 2.78 Myopic fundus changes
I. The optic disc artery over the retinal vein
II. Optic cup
III. Choroidal atrophy temporal to the optic disc and exposed large vessels
IV. Pigmentation around the area of choroidal atrophy

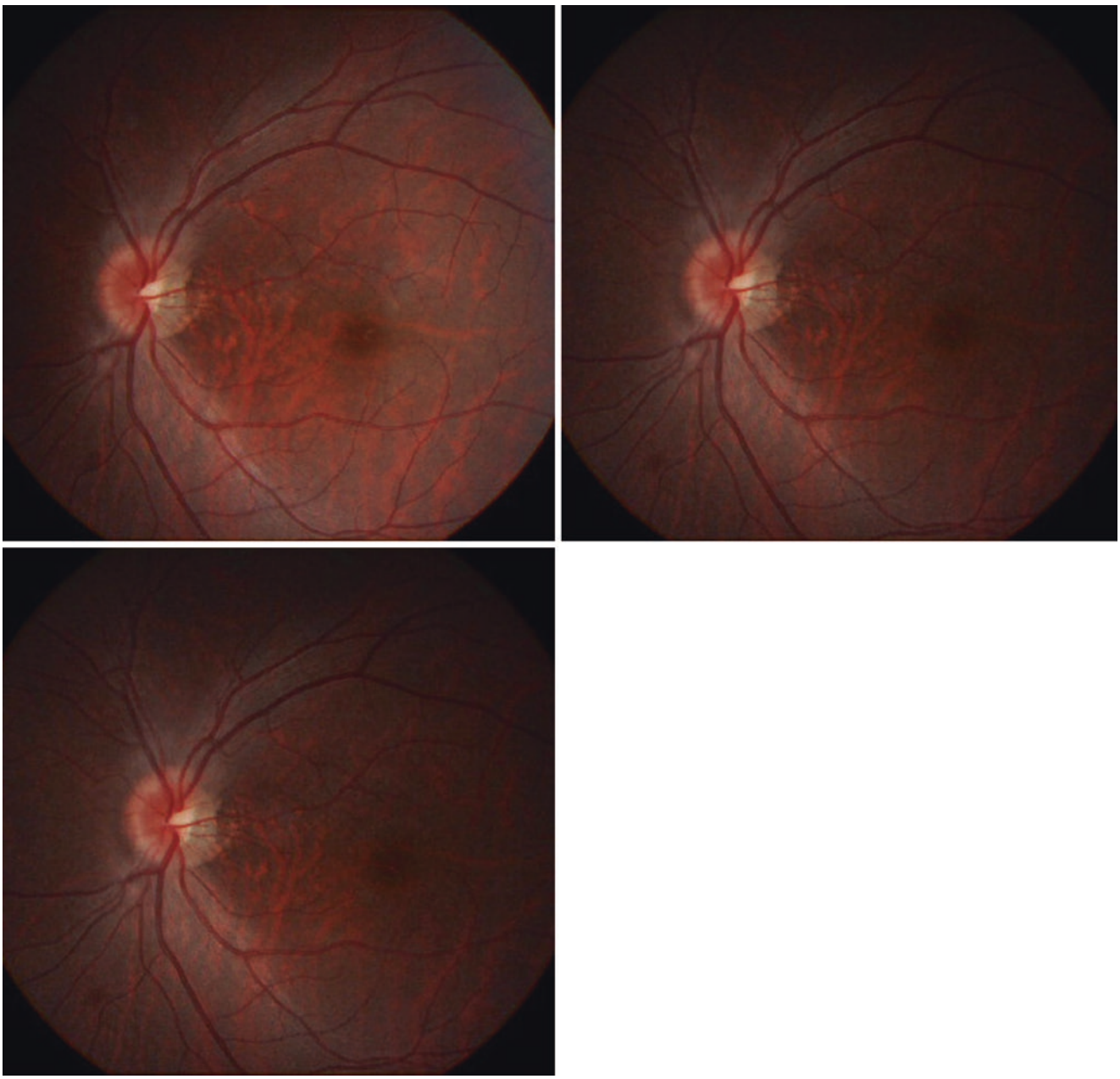

Fig. 2.79 Myopic fundus changes
I. Leopard fundus changes and large choroidal vessels
II. Myopic crescent

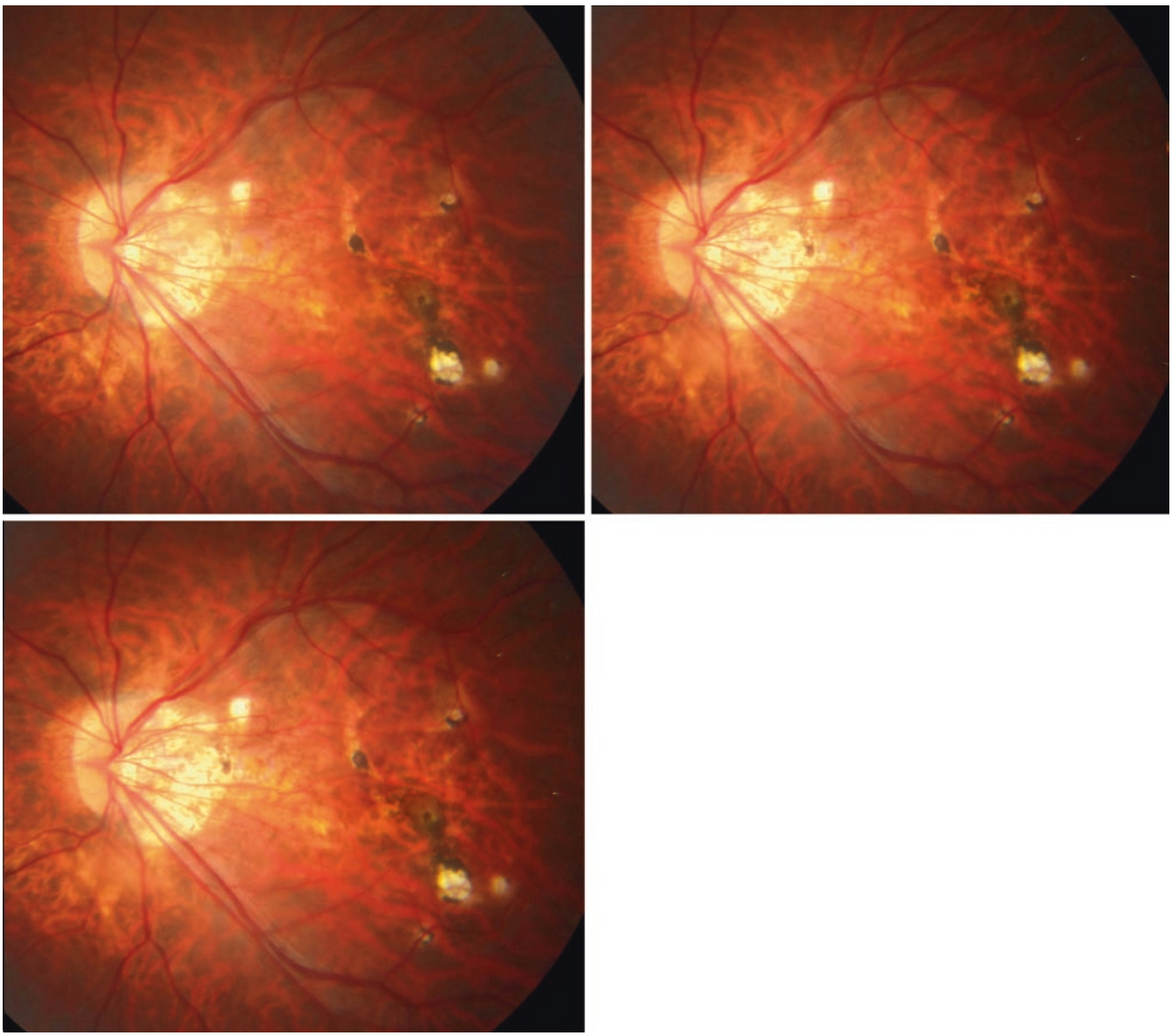

Fig. 2.80 Myopic fundus changes
I. Estimated boundary of the posterior scleral staphyloma
II. Fuchs spot
III. Pigmentation and elevation
IV. Choroidal neovascularization
V. Coloboma of choroid and exposed sclera

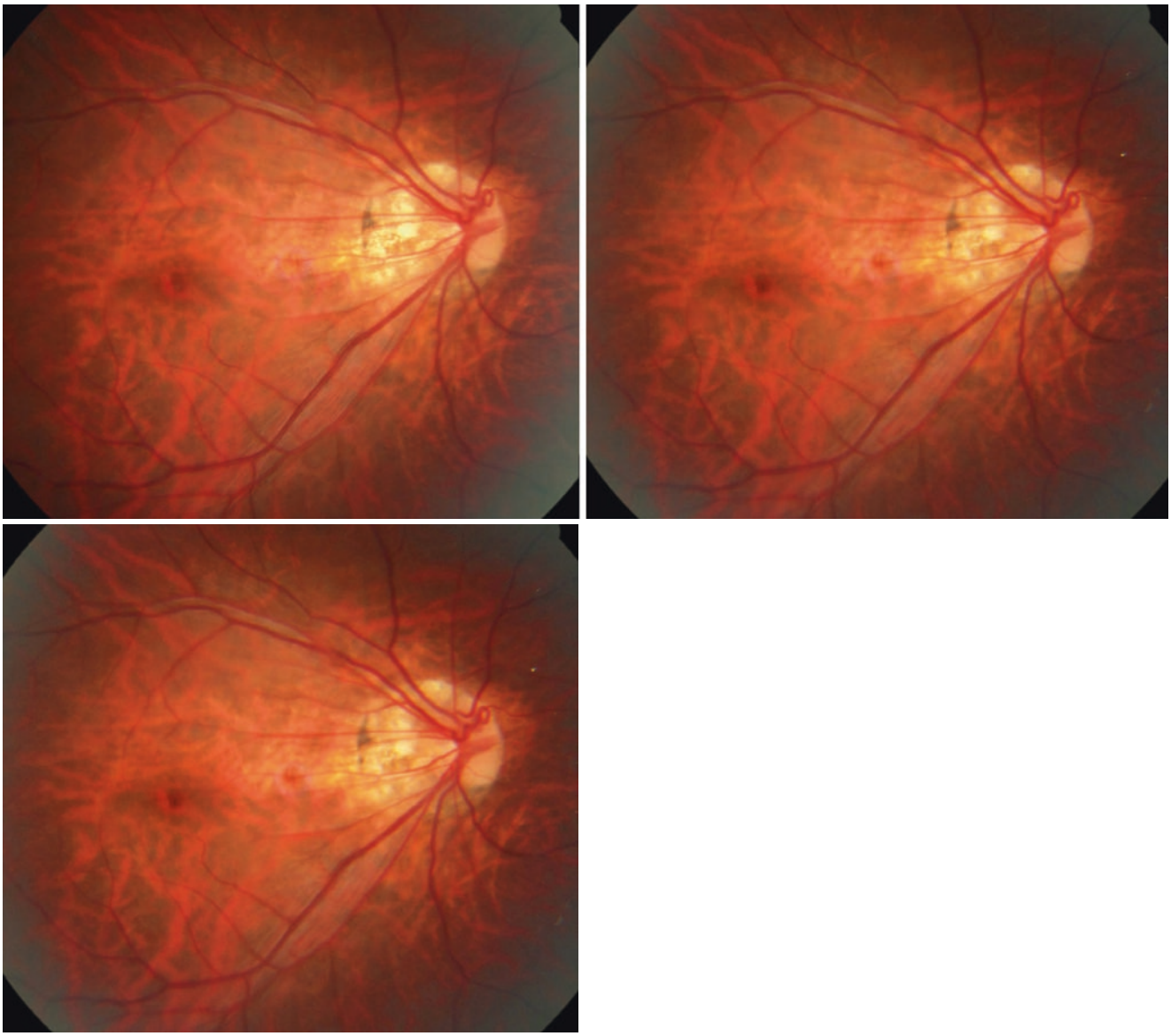

Fig. 2.81 Myopic fundus changes
I. Choroidal atrophy temporal to the optic disc and exposed large vessels
II. Retinal hemorrhage
III. Choroidal neovascularization

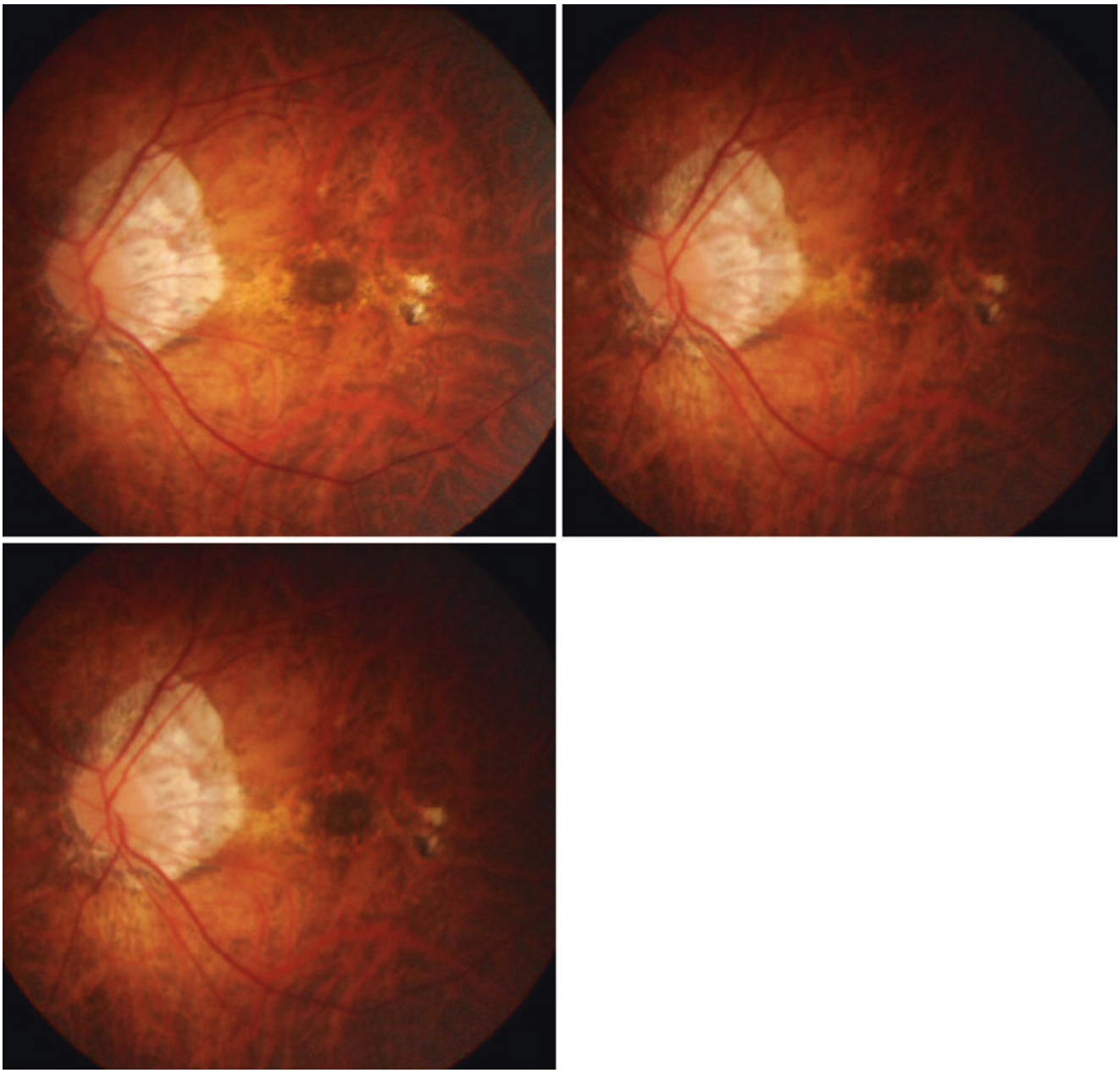

Fig. 2.82 Myopic fundus changes
I. Massive choroidal atrophy around the optic disc
II. Sub-macular choroidal neovascularization
III. Choroidal atrophic area

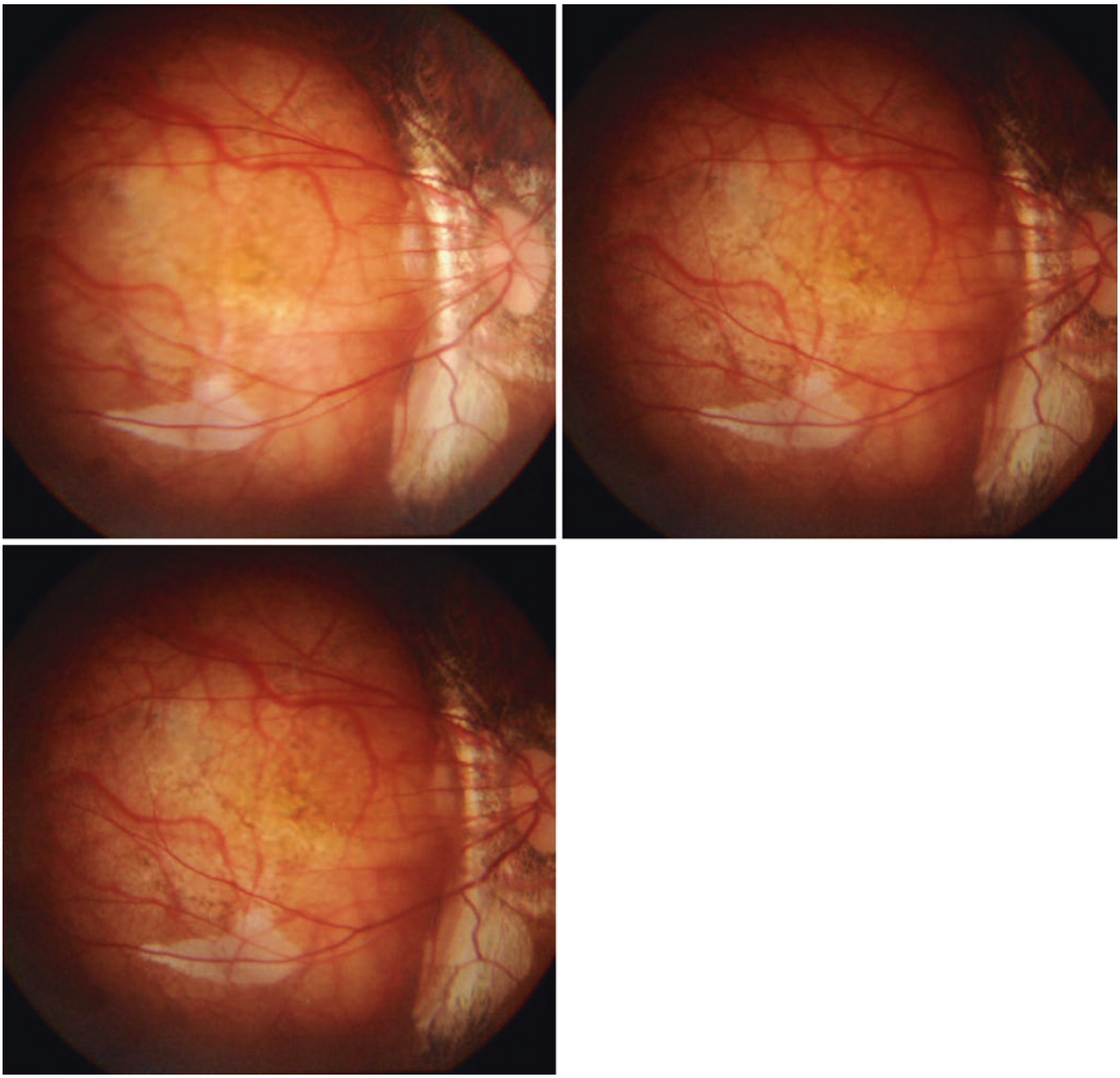

Fig. 2.83 Myopic fundus changes
I. Posterior scleral staphyloma like a basin
II. Exposure of large choroidal vessels
III. Macular atrophy
IV. Disappearance of choroidal vessels

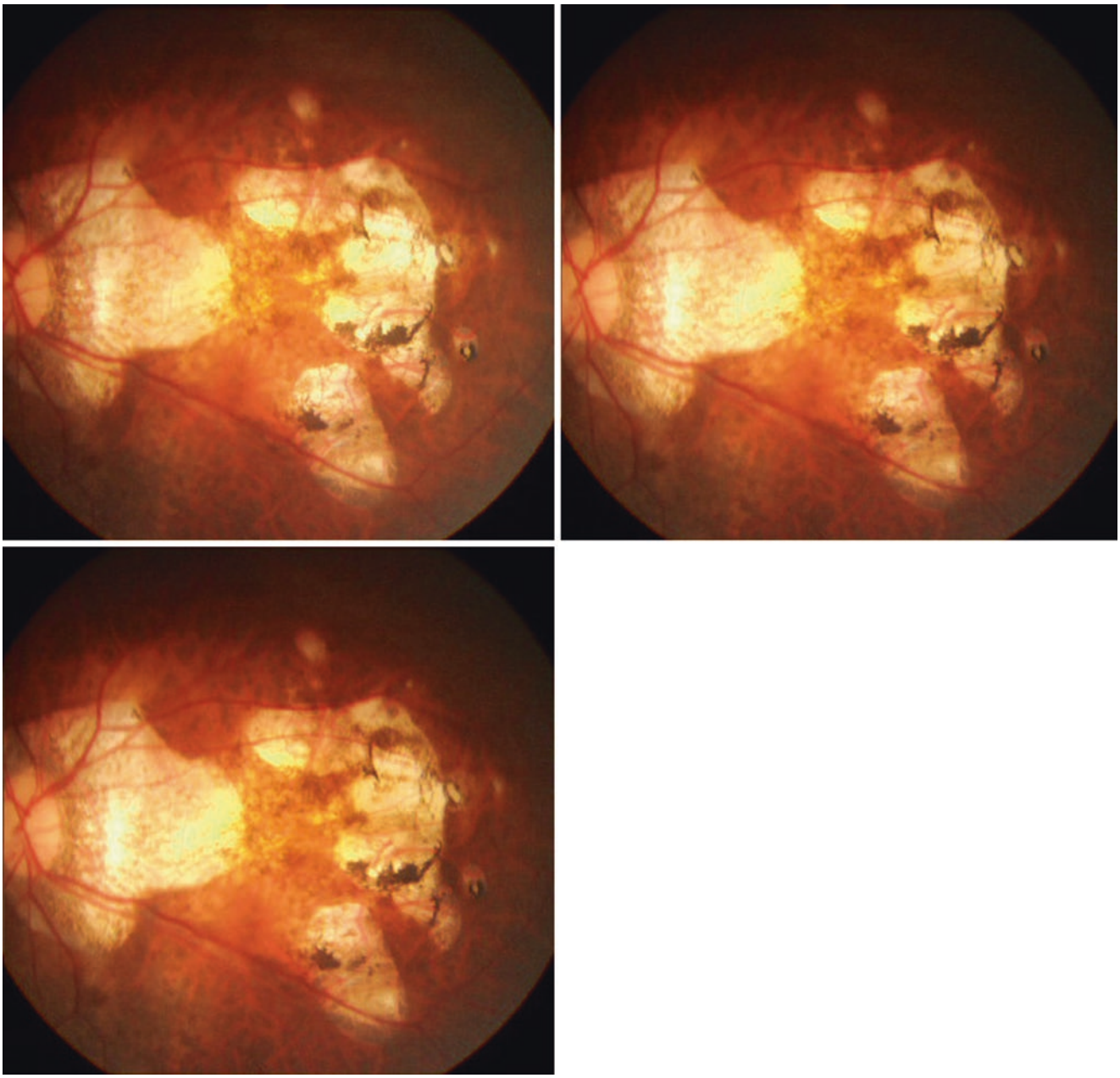

Fig. 2.84 Myopic fundus changes
I. Estimated boundary of the posterior scleral staphyloma
II. Multiple choroidal atrophy
III. Pigmentation in front of the retinal vessels
IV. Pigmentation of retinal pigment epithelium
V. Exposed choroidal vessels

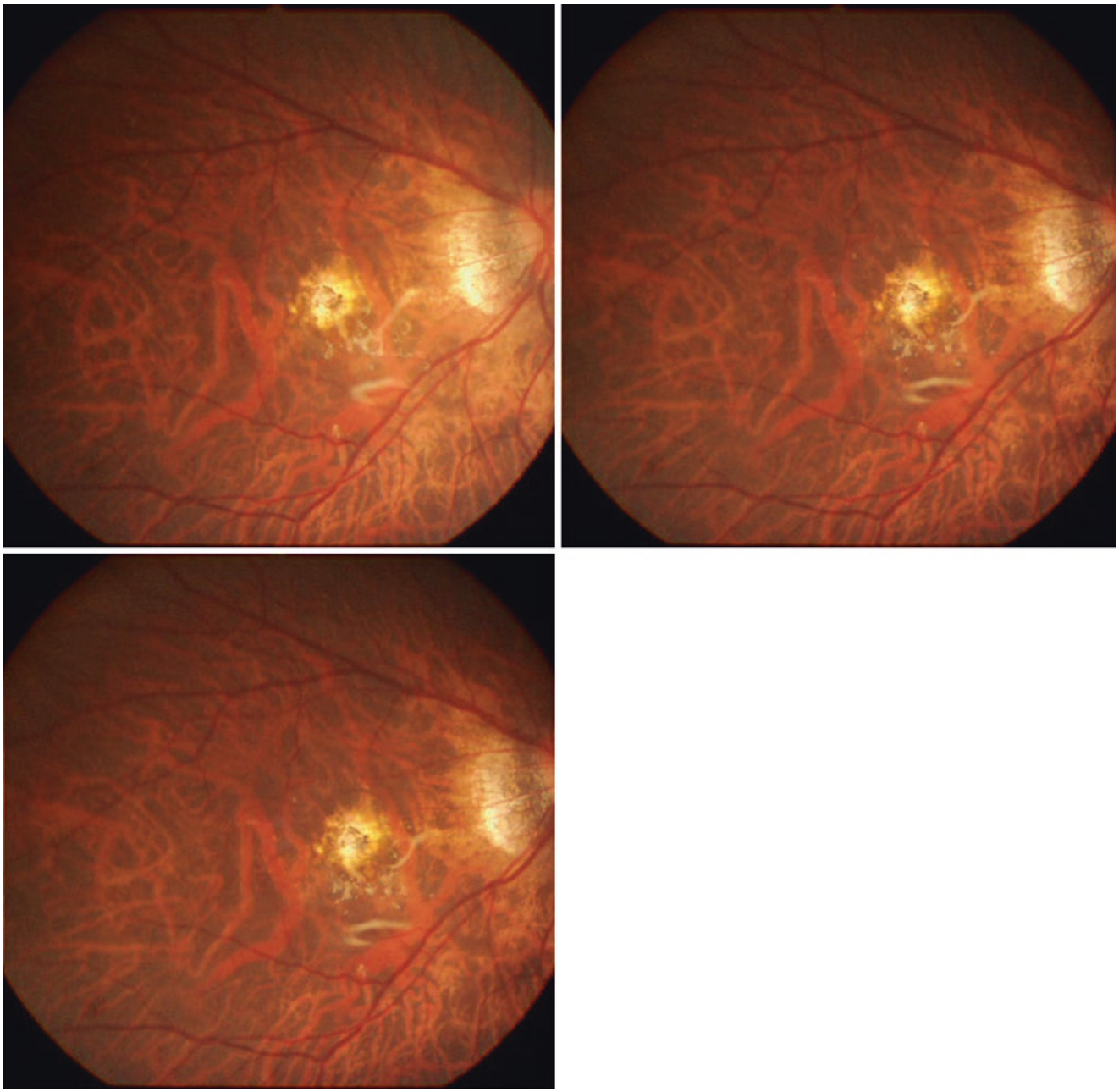

Fig. 2.85 Myopic fundus changes
I. Reflections of silicone oil
II. Pigmentation of retinal pigment epithelium
III. Pigment proliferation and atrophy
IV. Leopard fundus changes

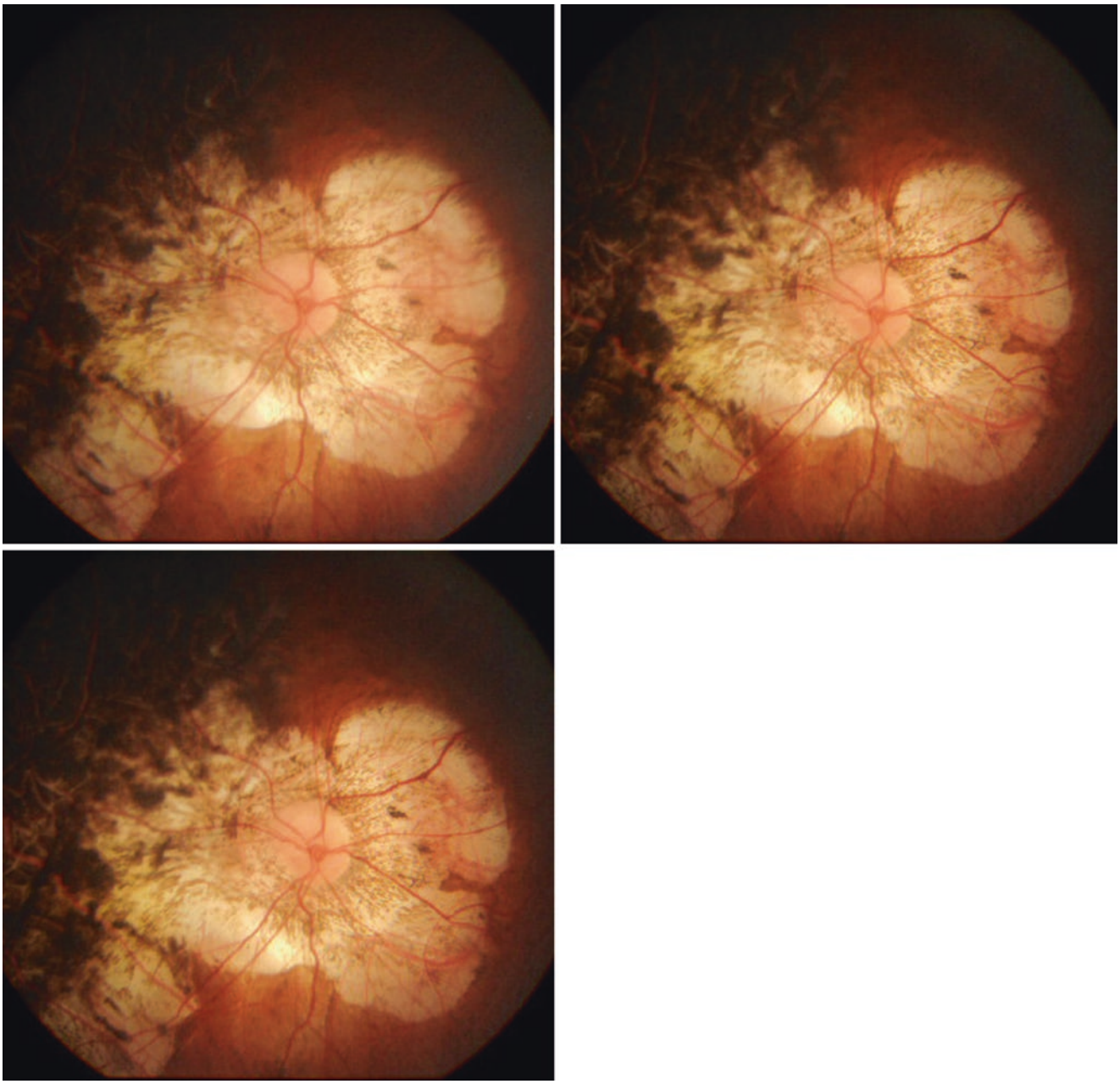

Fig. 2.86 Myopic fundus changes
I. Stair-step shaped staphyloma
II. Boundary of staphyloma
III. Retinal and choroidal atrophy and impending retinal vessels, cavity change underneath and exposed large choroidal vessels

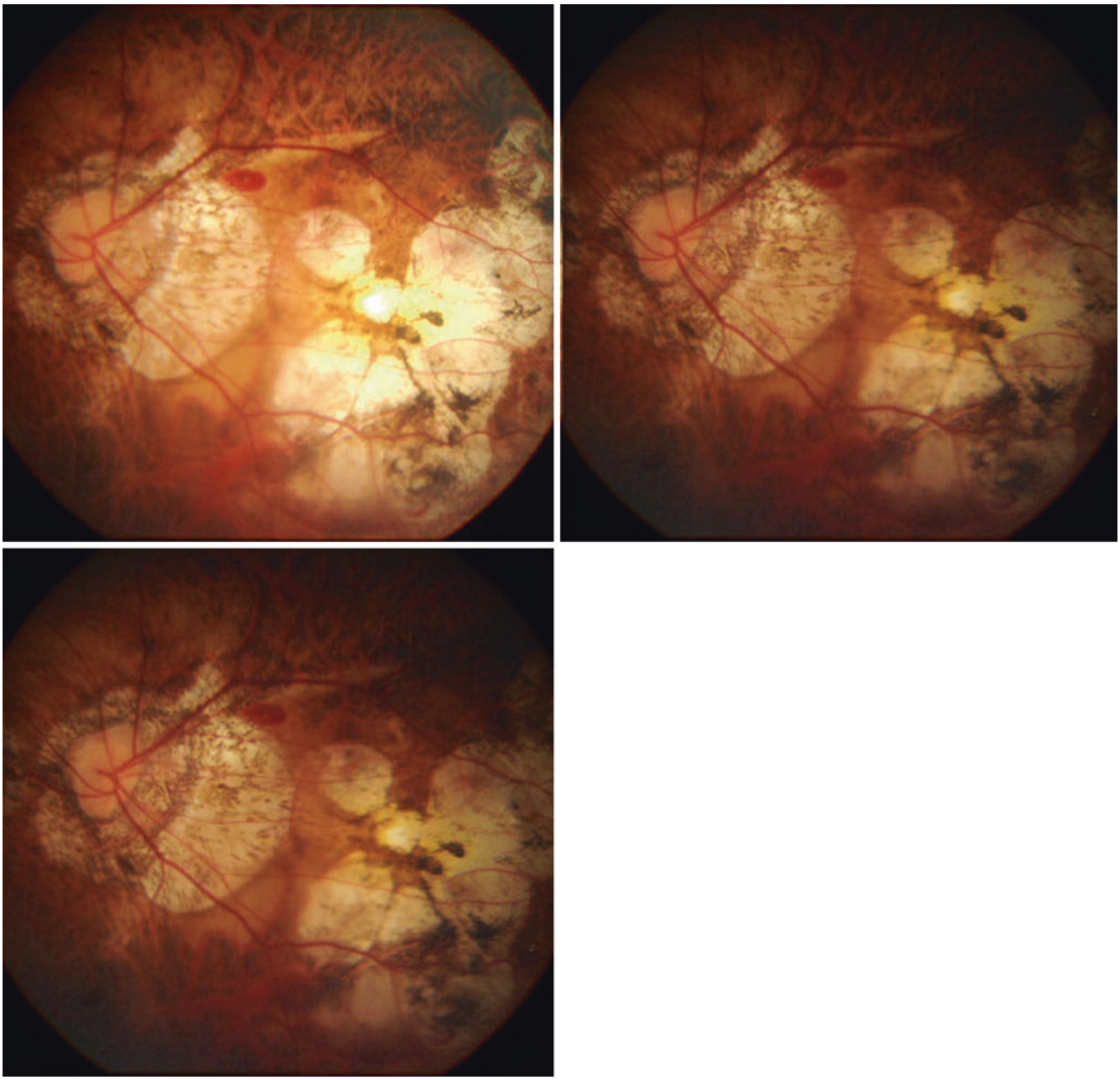

Fig. 2.87 Myopic fundus changes
I. Estimated boundary of the posterior scleral staphyloma
II. Multiple choroidal atrophy and impending retinal vessels
III. Choroidal atrophy temporal to the optic disc and exposed large vessels
IV. Elevated retina
V. Deep retinal hemorrhage (CNV suspected)

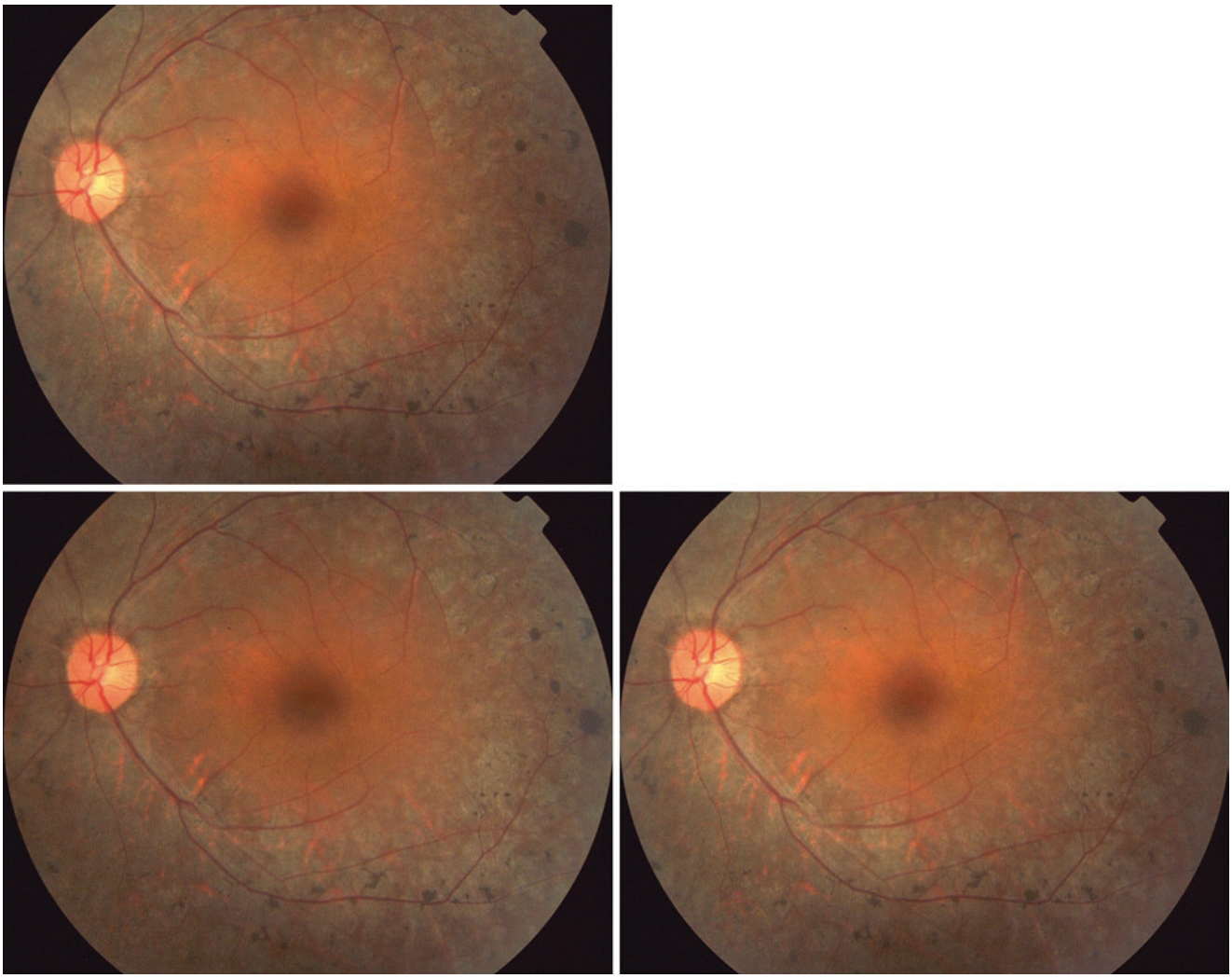

Fig. 2.88 Retinitis pigmentosa
I. The thickness of the macula is within normal range
II. Severe thinning of retina outside the vascular arc
III. Attenuated retinal arteries
IV. Bone spicule formation

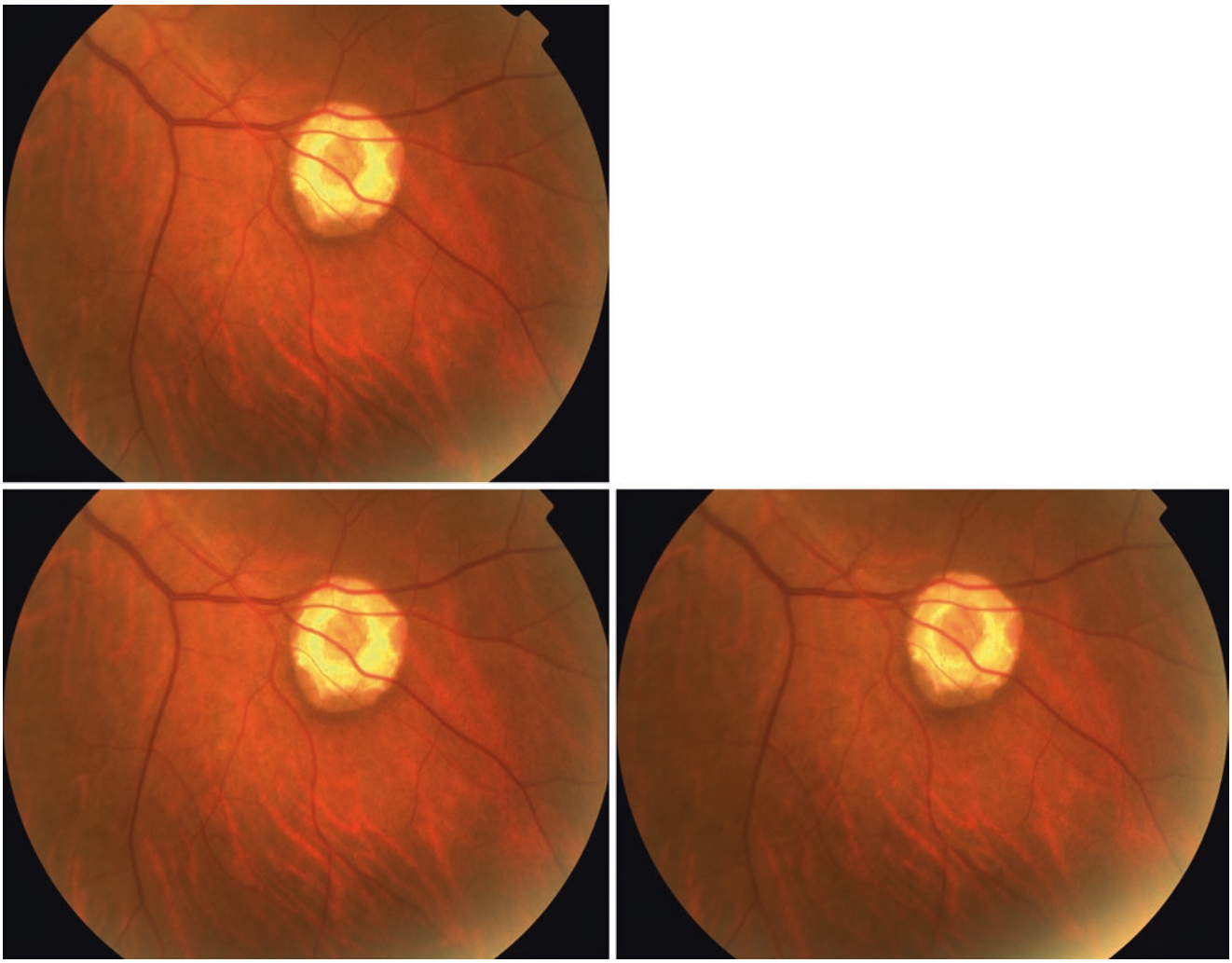

Fig. 2.89 Subretinal yellow-white exudates
I. The lesion locates under the sensory retina and above the RPE

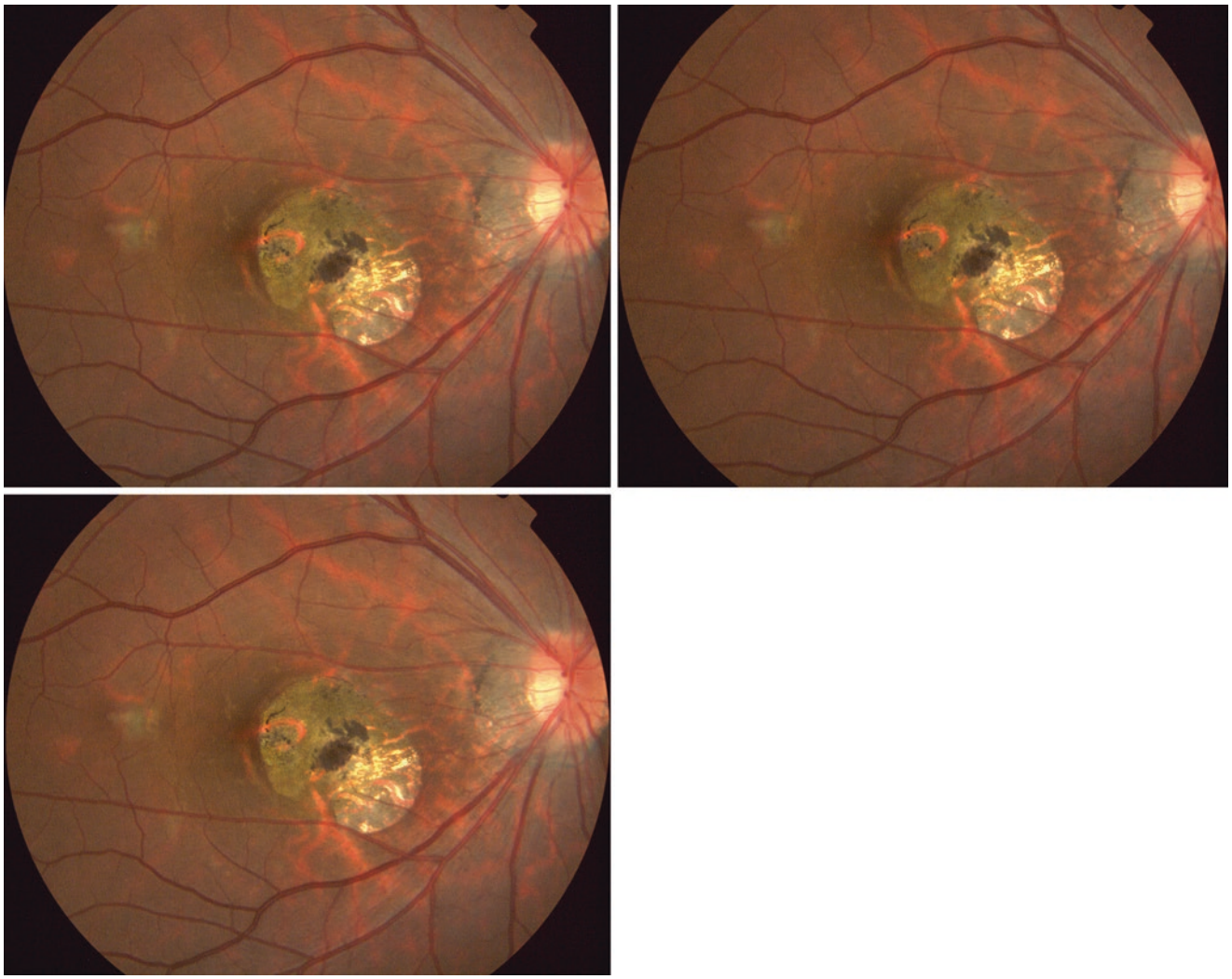

Fig. 2.90 Multiple dotted choroidopathy
I+II. The lesion locates under the retina and different degrees of pigment proliferation
III. Exposure of large choroidal vessels and sclera
IV. Pigment proliferation under the retina showed livid color
V. Subretinal pigment proliferation showed black color

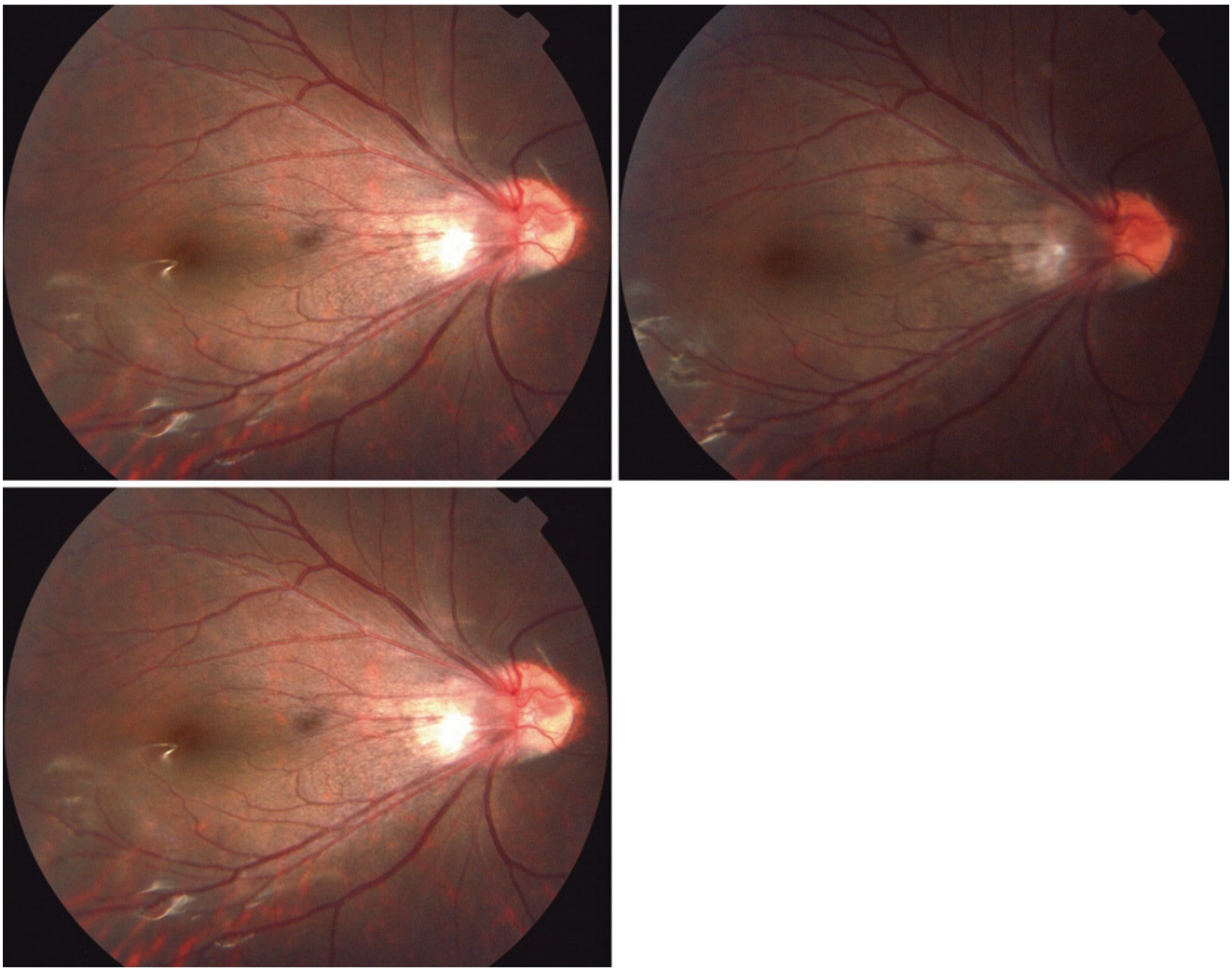

Fig. 2.91 Familial exudates vitreoretinopathy
I+II. The superior and inferior temporal retinal vessels are straight
III. Vitreous opacities and their shadows on the retina
IV. Vessels of different layers
V. Leakage of fluorescence of neovascularization in the peripheral retina

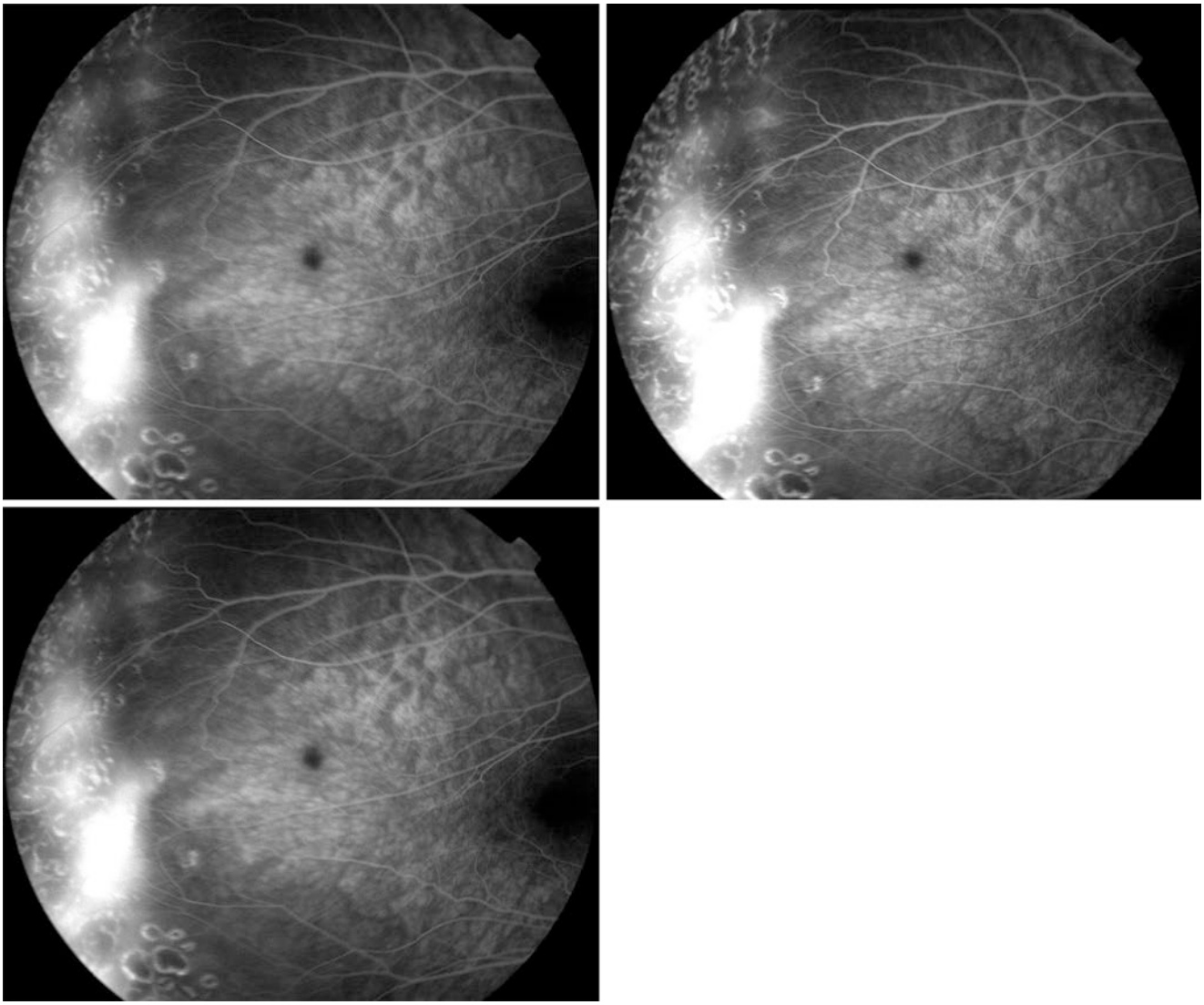

Fig. 2. 91 (continued)

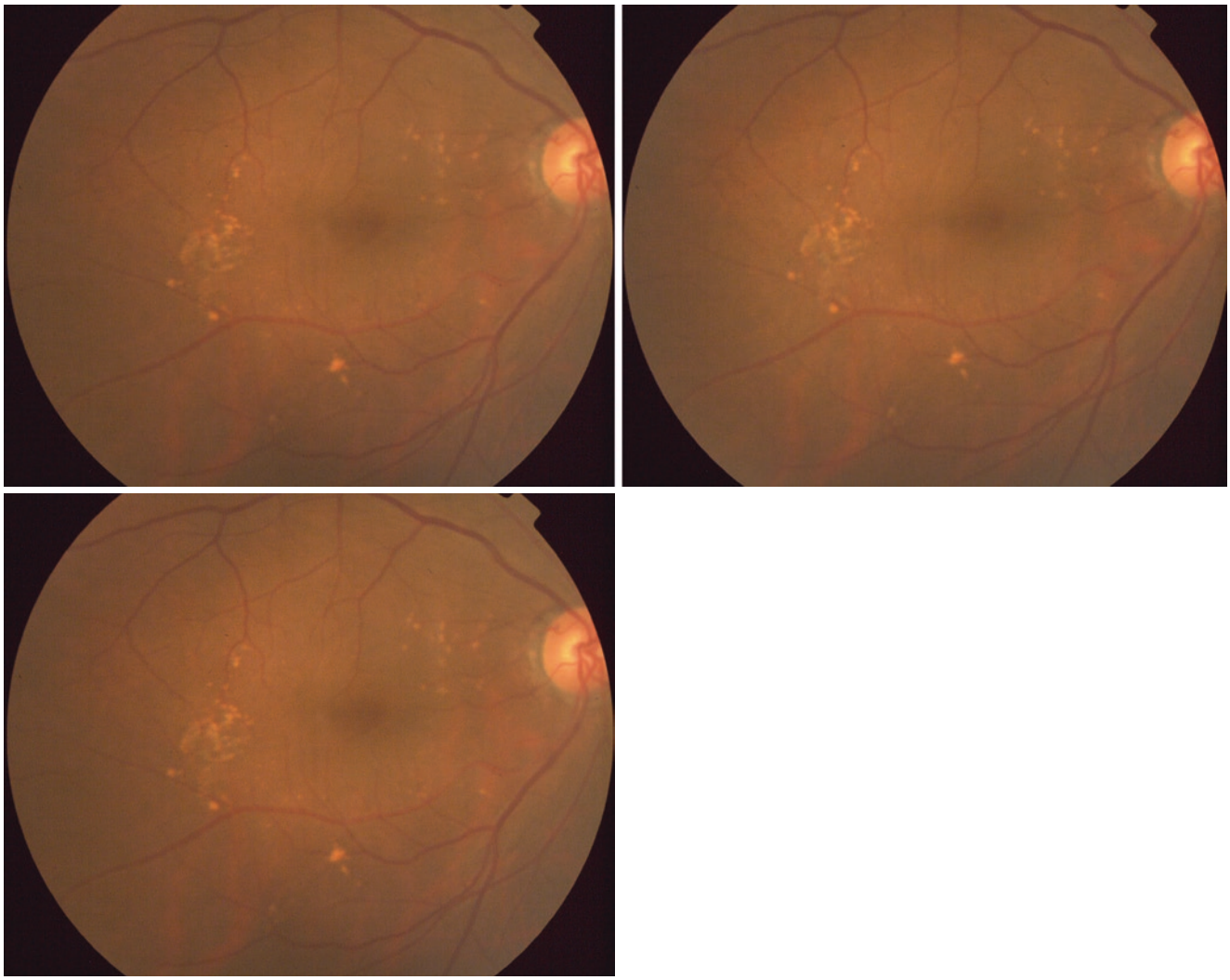

Fig. 2.92 Dry age-related macular degeneration
I. Intermediate retinal exudates
II+III. Confluent drusen under the retina
IV. Confluent drusen between the optic disc and macula
V. Fovea

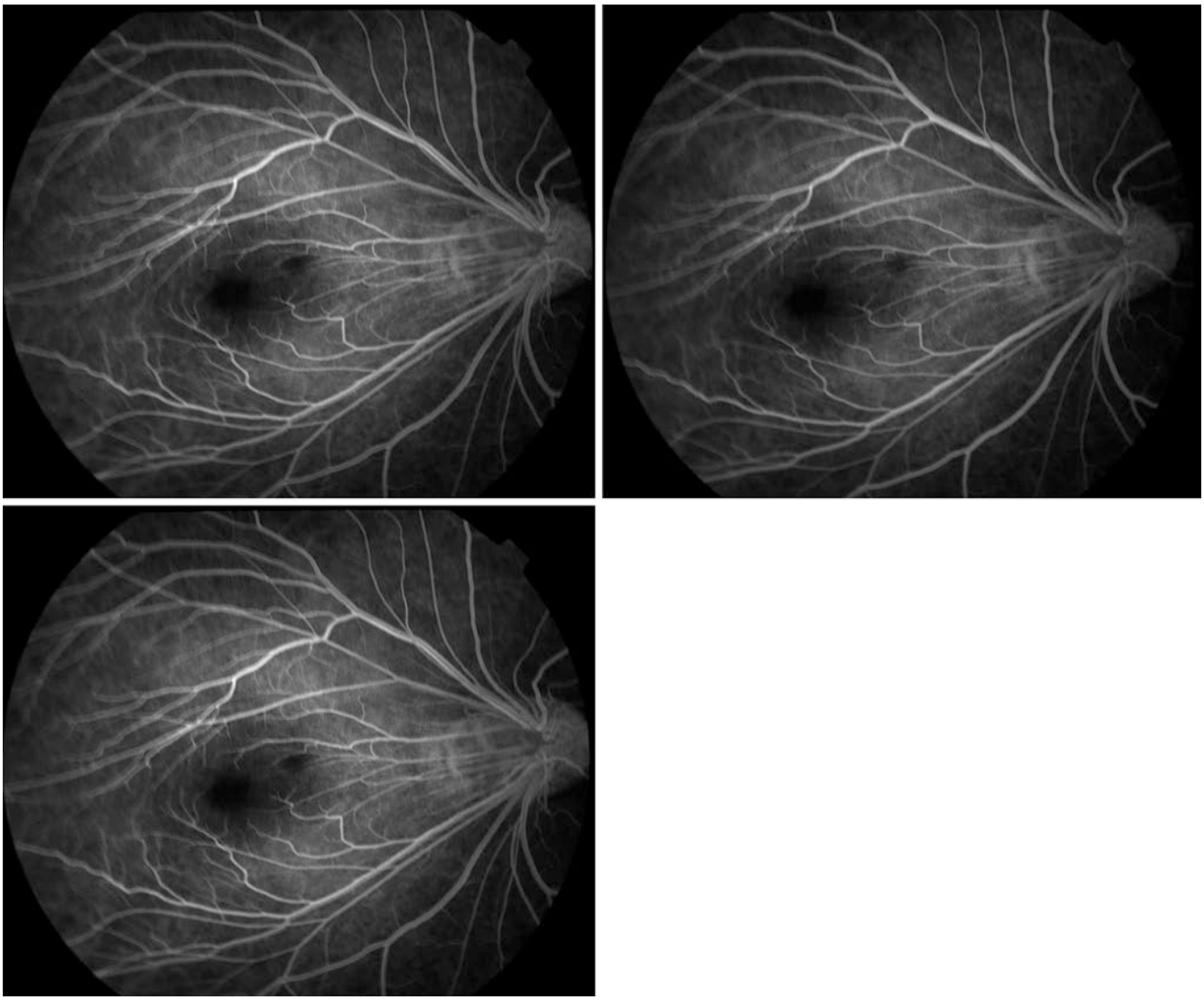

Fig. 2.93 Familial exudates vitreoretinopathy
I+II. The superior and inferior temporal retinal vessels go straightly
III. Macular dislocated far away from the papilla

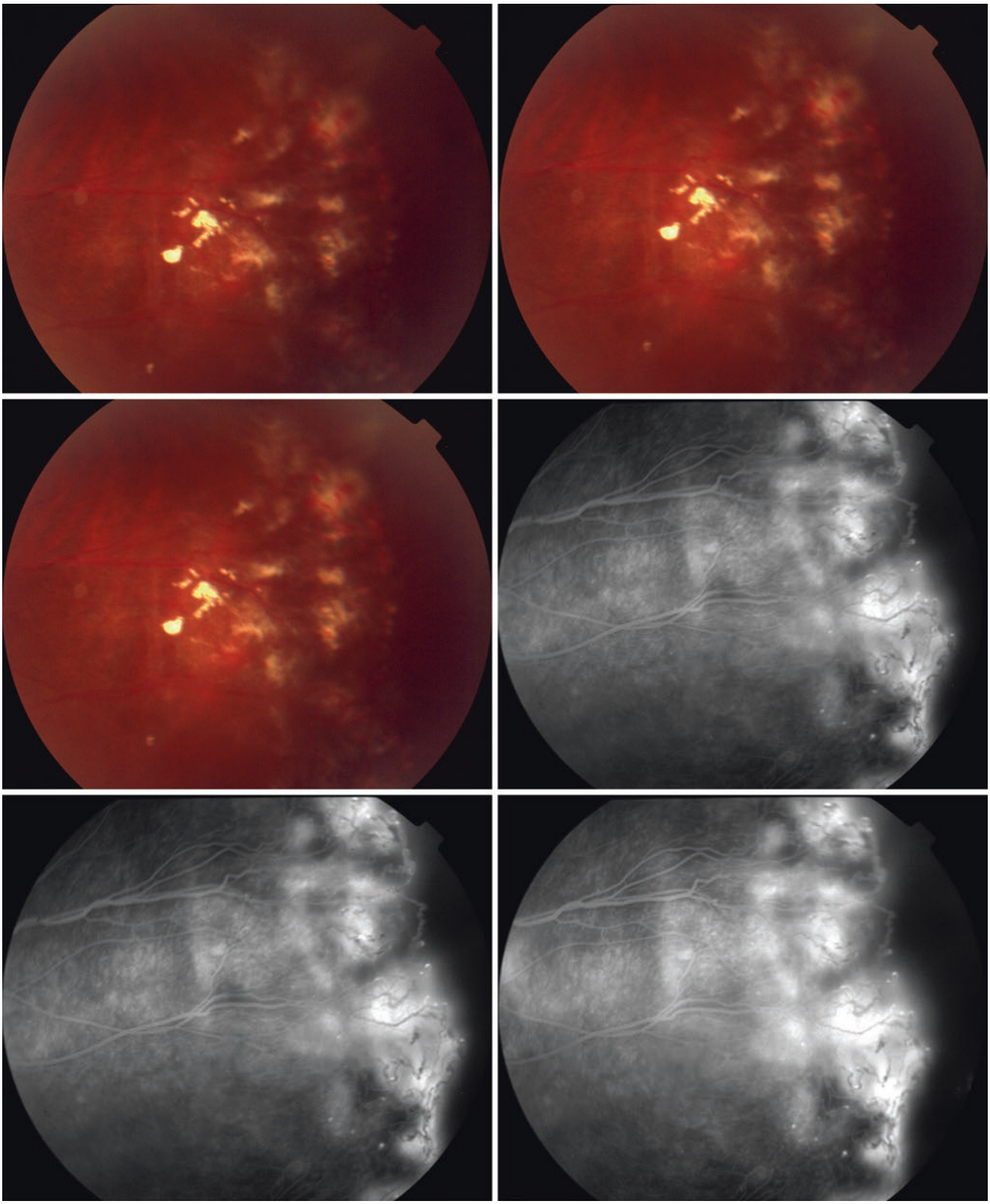

Fig. 2.94 Familial exudates vitreoretinopathy
I+II. Dendritic retinal vascular endings
III. Bulged endings of retinal vessels
IV. Communicative ending among veins/arteries
V. Leakage of fluorescence of neovascularization in the peripheral retina

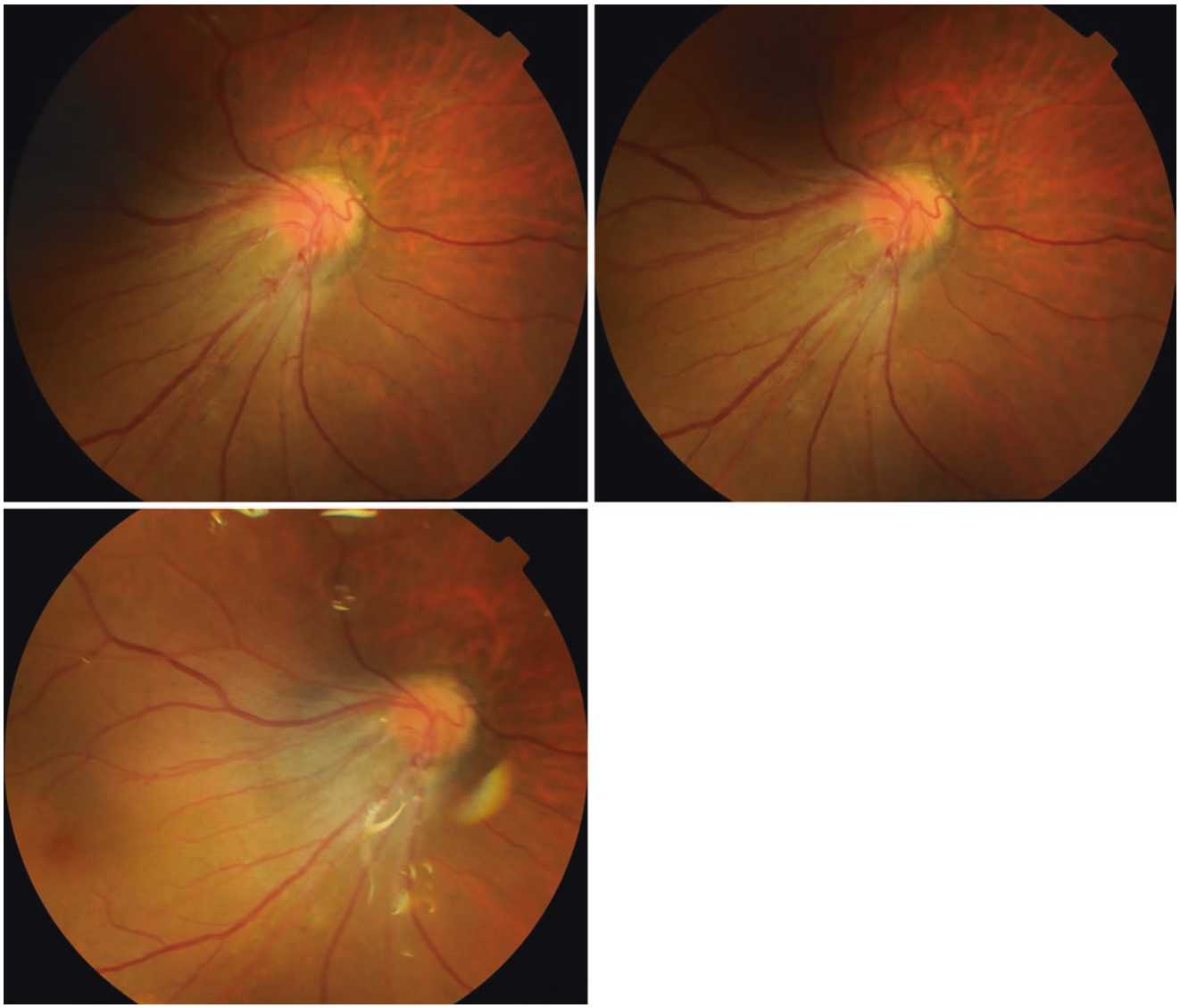

Fig. 2.95 Congenital retinal folds
I. Temporal dislocation of papilla and vessels
II. Macula dislocation
III. Partially dilated veins around papilla

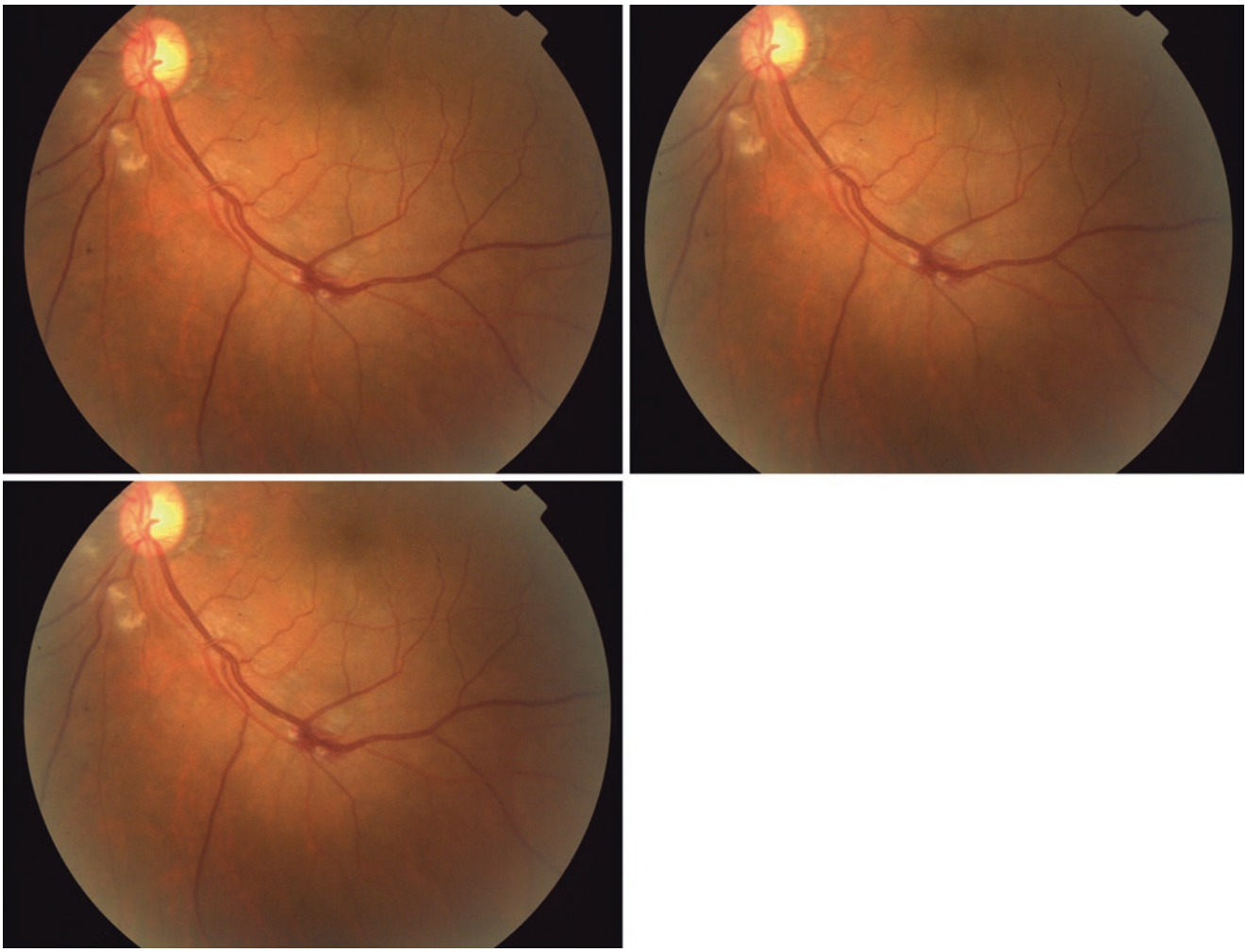

Fig. 2.96 Roth dot
I. White-gray spot due to bacterial accumulation and inflammation
II. Bleeding around the white-gray spot
III. Vitreous exudates

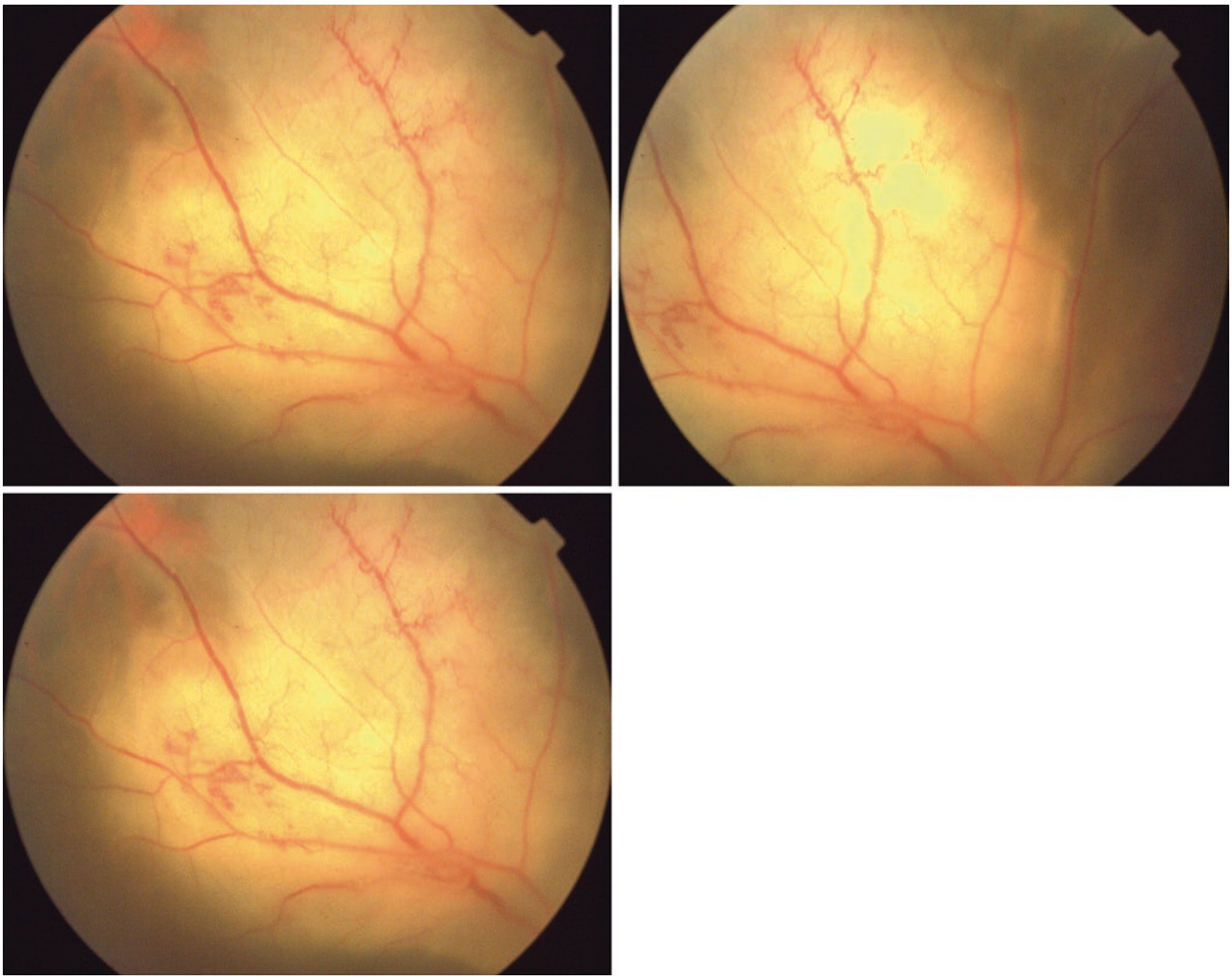

Fig. 2.97 Subretinal abscess
I. Superior-temporal white-gray abscess under retina
II. Retinal bleeding spots
III. Dilated retinal vein

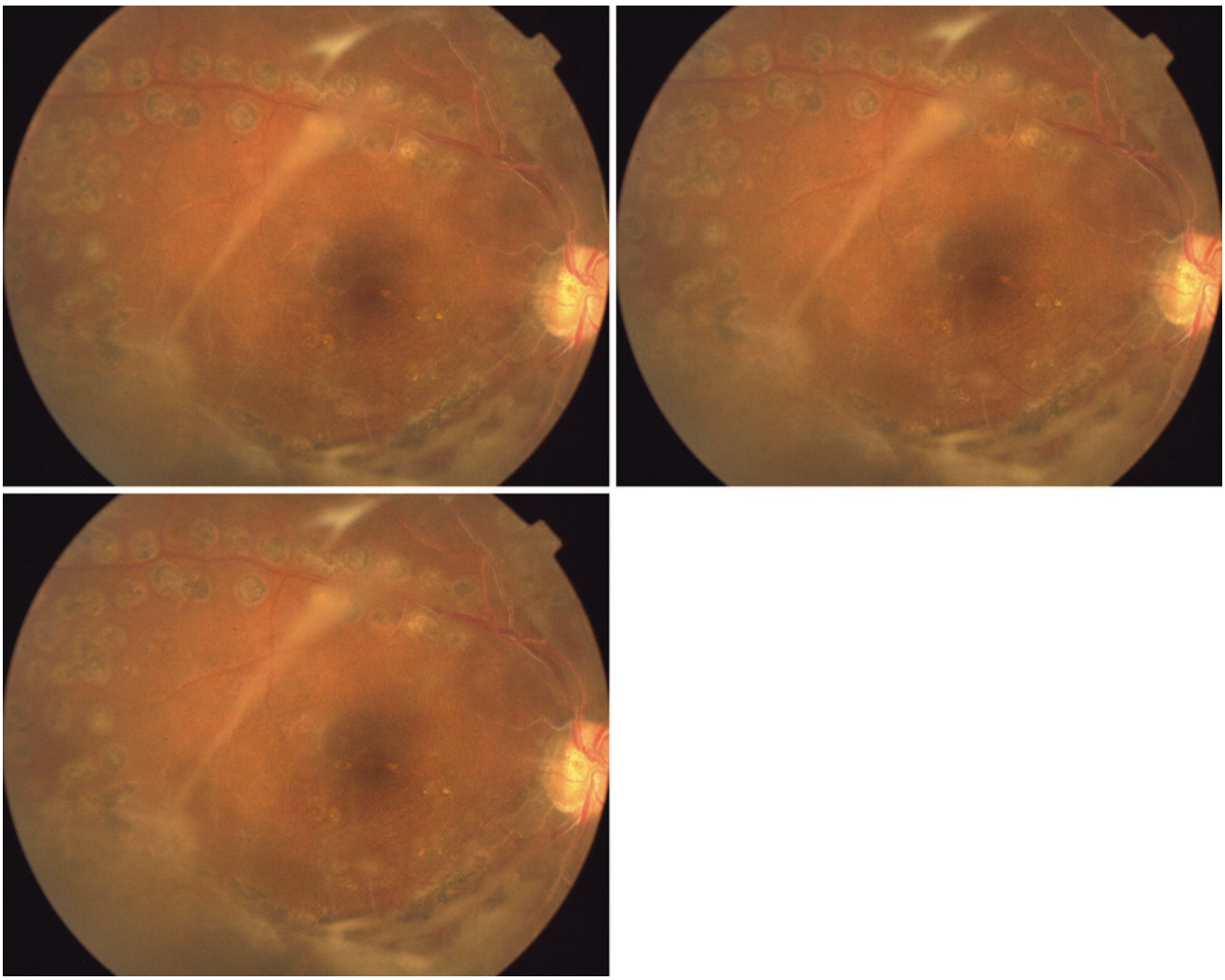

Fig. 2.98 Syphilis masquerade by retinal vasculitis
I. Vitreous opacities or PVR
II. Sheathed retinal arteries and veins
III. Laser spots
IV. Syphilis spot

References

1. Tyleer ME. Stereo fundus photography: principles and techniques. In: Saine PJ, Tyler ME, editors. Ophthalmic photography: retinal photography, angiography, and electronic imaging. 2nd ed. Boston: Butterworth-Heinemann; 2002. p. 118–35.
2. Allen L. Ocular fundus photography: suggestions for achieving consistently good pictures and instructions for stereoscopic photography. Am J Ophthalmol. 1964;57:13–28.
3. Early Treatment Diabetic Retinopathy Study Research Group. Grading diabetic retinopathy from stereoscopic color fundus photographs: an extension of the modified Airlie House classification. ETDRS report 10. Ophthalmology. 1991;98:786–806.
4. The Age-Related Eye Disease Study Research Group. The age-related eye disease study system for classifying age-related macular degeneration from stereoscopic color fudus photography: the age-related eye disease study report number 6. Arch Ophthalmol. 2001;31:167–75.
5. Li HK, Hubbard LD, Danis RP, et al. Monoscopic versus stereoscopic retinal photography for grading diabetic retinopathy severity. Retina. 2010;51:3184–92.
6. Lawrence MG. The accuracy of digital-video retinal imaging to screen for diabetic retinopathy: an analysis of two digital-video retinal imaging systems using standard stereoscopic seven-field photography and dilated clinical examination as reference standards. Trans Am Ophthalmol Soc. 2004;102:321–40.
7. Hubbard LD, Danis RP, Neider MW. Brightness, contrast, and color balance of digital versus film retinal images in the age-related eye disease study 2. Invest Ophthalmol Vis Sci. 2008;49:3269–82.
8. Rudnisky CJ, Hinz BJ, Tennat MTS, et al. High-resolution stereoscopic digital fundus photography versus contact lens biomicroscopy for the detection of clinically significant macular edema. Am J Ophthalmol. 2002;109:267–74.
9. Haug S, Arthur DF, Robert NJ, et al. Fulorescein angiography: basic principles and interpretation. In: Schachat AP, editor. Ryan's retina. 6th ed. Edinburgh: Elsevier; 2018. p. 1–45.